WBS: 1.2.1.10
QA: N/A

Civilian Radioactive Waste Management System
Management & Operating Contractor

REPORT ON EXTERNAL CRITICALITY OF PLUTONIUM WASTE FORMS IN A GEOLOGIC REPOSITORY

Document Identifier: BBA000000-01717-5705-00018 REV 01

January 28, 1998

Prepared for:

U.S. Department of Energy
Office of Civilian Radioactive Waste Management
1000 Independence Avenue S.W.
Washington, DC 20585

Prepared By:

Civilian Radioactive Waste Management System
Management & Operating Contractor
1180 Town Center Drive
Las Vegas, NV 89134

Under Contract Number
DE-AC01-91RW00134

Civilian Radioactive Waste Management System
Management & Operating Contractor

REPORT ON EXTERNAL CRITICALITY OF PLUTONIUM WASTE FORMS IN A GEOLOGIC REPOSITORY

Document Identifier: BBA000000-01717-5705-00018 REV 01

January 28, 1998

Prepared By:

Peter Gottlieb — Date: 1/28/98

J. W. Davis — Date: 1/28/98

Paul Cloke (Peter Gottlieb FOR PAUL CLOKE) — Date: 1/28/98

Darren Jolley — Date: 1/28/98

John A. McClure — Date: 1/28/98

Reviewed By:

Jerry A. McNeish — Date: 1·28·98

Martin Haas — Date: 1/28/98

Approved By:

Hugh A. Benton, Manager
Waste Package Operations — Date: 1-28-98

EXECUTIVE SUMMARY

This report presents the analyses and results for the potential occurrence of external criticality events which could result from plutonium waste forms emplaced in a geologic repository similar to the one being developed at Yucca Mountain. The analyses evaluate both the MOX spent fuel and the immobilized plutonium waste forms in a repository if the waste package has degraded and if the fissile material has migrated to the invert and out into the far-field. Previous analyses have already examined the potential for criticality in an intact waste package configuration (Reference 1), and the degraded waste package configuration (Reference 2) for these waste forms.

To ensure commonality in analysis, the methodology for the development of scenarios that affect flow and transport of the plutonium wastes into the external repository environment is the same as that being used for the commercial SNF and HLW. The mechanisms for release of the fissile material from the matrix are, however, a function of the waste form characteristic. A systems approach for development of the scenario trees that could result in the accumulation of fissile material, was used in which all applicable features, events, and processes that can cause material to flow, transport, and accumulate were considered. Specific threads for the occurrence of each event were constructed, geochemical analyses conducted to determine the possibility of fissile material/neutron absorber partitioning, absorption/adsorption of fissile materials on clays estimated, natural analogs analyzed to provide insight into the possible long term behavior of these configurations, geometric configurations defined, and neutronic analyses conducted to determine the circumstances under which criticality events can occur. Further, analyses were performed to determine the consequences of any the criticality event which comes the closest to possibility.

The potential for criticality events were evaluated in the invert, the bulk of the unsaturated and saturated zones, and from studying natural analogs. Because of the chemical reactions involved in the degradation process of the waste forms and the canisters, the solution pH varies between an alkaline regime and an acidic regime. The solution pH is an important factor in determining the solubility of the fissile materials and hence the potential for precipitation under different environmental conditions. The major findings from these analyses are presented below:

Deposition Mechanisms

The mechanisms for the accumulation of fissile material in the Yucca Mountain geologic environment can be most conveniently classified as follows: (1) adsorption on clays or zeolites, (2) reduction of the +6 or +5 valence states of the U or Pu ions to the +4 valence state, (3) general chemical reaction between the chemically active species in the solution and the rock material of the invert or the host rock just below the waste package. The potential for each of these deposition mechanisms to achieve a critical accumulation of fissile material is discussed in detail in the body of the report, and summarized in the following paragraphs of this executive summary.

Considerations of solution chemistry, pH

Previous analyses of the waste package (Ref. 2) degrading under wetted conditions have shown that the alkaline metal degradation products of the HLW glass tend to make the solution

alkaline (ph > 10) while the possible chromate product of degrading stainless steel tends to make the solution acidic (pH near 5). The present study used the geochemistry code (EQ6) to determine the range of balance between the alkaline tendency of the degrading glass and the acidic tendency of the corroding stainless steel, in order to determine the likely composition of the source term, the fluid flowing out of the waste package, as a function of time, and for the range of likely infiltration rates, with the following conclusions:

- The low pH condition will result in a low concentration of uranium and even lower concentration of plutonium in the source term, but will have a rather high concentration of the neutron absorber, gadolinium. This confirms the earlier preliminary calculations (Ref. 2) which showed the scenarios leading to a low pH to have the greatest potential for internal criticality because of the loss of gadolinium while uranium and plutonium are retained.
- The neutral pH condition will produce a source term with very little uranium, plutonium, or gadolinium. This condition will have no potential for criticality, either internal or external.
- The high pH condition will cause a very high solubility of uranium (and fairly high for plutonium) which may lead to a high concentration of fissile material in the source term, but only if the fissile material has been released from the waste form during the high pH phase of the degradation scenario.

Potential for criticality in the invert and host rock immediately below a single waste package

The basic geochemistry code used for these analyses, EQ6, has been used in a flow-centered mode to simulate the interaction of a fluid element as it moves through a host rock medium, so that precipitation can be modeled as a function of movement distance. In this manner the accumulation of U and Pu has been estimated as a function of distance beneath the waste package: into the invert, drift liner, and the first 10 meters of host rock. The most likely area of contact of the source term will be beneath the footprint of the waste package, and the most likely direction of flow will be downward. As successive parcels of solution flow through a given drift/rock stratum the precipitated solids will accumulate in the voidspace/fractures until they become plugged, after which much of the flow will be diverted to nearby rock, to start the deposition profile over again. The calculated cases covered the likely range of source terms and the likely range of flow rates, with the following significant results:

- The neutral pH source term will have very little deposition of solids of any sort because there is little reaction with the tuff, and virtually no deposition of fissile material because of its low concentration.
- The low pH source term will have significant deposition of solids (completely filling the voidspace at some levels), but very little of that will be fissile because of the low concentration of fissile in the source term. For example, the deposits will plug the flow path to about a 2.2 meter depth in the tuff invert and adjacent rock after approximately 400 years. Since the concentration of fissile in the solution is very small, the 4700 kg of solids which can deposit in the limited fracture and voidspace (10%) of the rock beneath the footprint of a single waste package will contain only 0.0006 g of fissile material. Such a low accumulation of fissile material and will, obviously, not result in any criticality. Even lower accumulations of fissile material were calculated for the case when concrete is used an invert material.
- The high pH source term has both the necessary high concentration of fissile material and the reaction with the tuff to produce an accumulation of fissile material in the

voidspace of the invert and the fractures of the rock immediately below the waste package. Even in this case, however, the geochemistry code shows that the maximum amount of fissile material which can be deposited in the zone of highest concentration (nearest the waste package) is more than an order of magnitude less than that necessary for criticality.

Potential for criticality in the far-field

The possibility of accumulating a critical mass in highly adsorbing zeolites, which are present in abundance in Yucca Mountain was considered in Ref. 2, where it was concluded that a critical mass was barely possible, based on an experimental study which claimed a maximum adsorbing of U in zeolite of 1% by weight (Ref. 36). Re-evaluation of that paper suggests that the maximum adsorbed uranium should be less than 0.166%, which would make criticality impossible.

Potential for critical mass accumulations inferred from natural analogs

One concern of the far-field problem is that the waste placed in a repository, over geologic time, will act as a source of transportable uranium, thus enabling one of the conditions needed for uranium mineral deposition. Natural analogs were evaluated to determine conditions under which epigenetic (i.e., mineralization deposited much later than the host rock) uranium deposits were formed. This analysis showed that even though epigenetic uranium mineral deposits vary in size and grade, a reducing environment is required to cause the precipitation of a uranium mineral (reducing the uranium valence from the soluble +6 to the insoluble +4). An extensive search of the literature shows six possible types of reducing media: upwelling hydrothermal fluids, methane, hydrogen sulfide, organic logs, petroleum, and partially oxidized vanadium.

Site characterization activities to-date at Yucca Mountain have not shown the presence of more than trace amounts of these media, especially over the flow and transport paths that lead to the accessible environment. In fact, the geologic formations which have been identified by the Yucca Mountain site characterization process are all inconsistent with the existence of more than trace amounts of these reducing media. Thus the precipitation of uranium minerals by any reduction mechanisms is estimated to have an extremely low probability.

Because site characterization activities are still on-going, new data will be evaluated as it becomes available to determine if any of these necessary conditions are observed.

Consequence Analysis

In the extremely unlikely case that a criticality does occur external to the waste package the principal consequence will be the increased radionuclide inventory due to the actinides and fission products built up during the reaction. For the immobilized plutonium waste form 6 kg of plutonium-239 accumulating in fractures in a 1 meter cube beneath the waste package has been estimated to be capable of only 500 Watts power level, lasting only 4000 years, which would produce a 14% increase of radioactivity, with respect to the radioactivity already present in the amount of plutonium (< 480 curies).

Recommendations

Because these analyses were scoping in nature, an exhaustive set of risk and sensitivity analyses were not conducted. It is recommended that these be performed as part of the Safety Analysis report of the License Application when the waste form characteristics and canister designs are more mature and the data have been qualified. The effort associated with the License Application is currently scheduled to start in FY99.

Table of Contents

1. BACKGROUND AND INTRODUCTION

This report is concerned with the possibility of criticality external to a waste package (WP) that contains a waste form from the Plutonium Disposition Program, either plutonium (Pu) immobilized in glass or ceramic or mixed oxide (MOX) spent nuclear fuel (SNF). There have been several previous studies of Plutonium Disposition criticality internal to the WP; the current status of the internal criticality issue is reflected in the following reports:

(1) *Report on Evaluation of Plutonium Waste Forms for Repository Disposal* (Ref. 1), which concluded that the intact, or as-fabricated, immobilized plutonium waste form had sufficient built-in criticality control material to satisfy U.S. Nuclear Regulatory Commission (NRC) requirements;

(2) *Degraded Mode Criticality Analysis of Immobilized Plutonium Waste Forms in a Geologic Repository* (Ref. 2), which concluded that dissolution of the immobilized plutonium waste form would still result in the retention of sufficient criticality control material to prevent criticality, provided that the loading is limited to approximately 50 kg of Pu per waste package; and

(3) *Report on Evaluation of MOX Spent Fuel from Existing Reactors for Repository Disposal* (Ref. 3), which, for the given assumptions, concluded that the MOX criticality problem can be treated with using the same criticality control techniques as commercial SNF.

This report extends the methodology used in the previous studies. In particular, this report extends the external sequences of the degradation scenarios initially considered in Ref. 2, in order to identify configurations external to the waste package which might support such critical accumulations. If it is *possible* for fissile material to accumulate outside the waste package, it is *possible* for fissile material released from several waste packages to accumulate in one location, thereby enhancing the probability of criticality. Since, however, any waste packages containing highly enriched uranium or fissile plutonium will be widely separated in the repository, the probability of such an accumulation in either the near- or the far-field is very small. Therefore, in this analysis, the probability of accumulating a critical mass will be considered and shown to be so low as to warrant no further consideration. This conclusion will eventually have to be demonstrated to the USNRC as part of the license application.

The potential accumulation of a critical mass external to a waste package is controlled by the fissile bearing flow from that package, and is not, necessarily, a strong function of the waste form itself. For this study the glass waste form was used to estimate the fissile content and other characteristics of the flow from the waste package, partly because the glass waste form is currently better defined (considered a more mature process), and because there was more data on dissolution rates than for the ceramic waste form. After these external criticality studies were completed, and as this document was being prepared, there was a selection process completed between the glass and ceramic waste forms, resulting in the choice of the ceramic waste form. The chosen ceramic waste form is of a different composition from those analyzed previously (Refs. 1 and 2). Experimental programs presently under way are expected to provide the necessary input parameters (particularly degradation rates) for the re-evaluation of

this study and the two previous studies (Refs. 1 and 2) during the coming year. In the meantime, the results of this study may be considered a very conservative approximation of the possibility of criticality, because the chosen ceramic waste form will have a much lower dissolution rate than was used for this study employing the glass waste form dissolution characteristics.

The content of this report is organized as follows:

- Section 2 provides brief descriptions of the waste package and both the glass and MOX waste forms. Detailed descriptions of the waste package and the glass waste form are given in Reference 2. A detailed description of the MOX waste form is given in Reference 3.

- Section 3 discusses the general approach and identifies the analysis strategy used in the methodology.

- Section 4 describes the repository release scenarios considered.

- Section 5 describes the estimation of the waste package fissile bearing source terms which could result from these scenarios.

- Section 6.1 describes the worst case accumulations of fissile material by identified natural processes acting in the near-field which can be removed from the source term. Section 6.2 describes the mechanisms for far field accumulation which can be inferred from geologic analogs (uranium mineral deposits), and explains how such mechanisms could not apply at Yucca Mountain. Sections 6.3 and 6.4 summarize the lack of potential for critical accumulations by sorption and by colloidal transport, respectively.

- Section 7 describes the criticality evaluations performed on the largest accumulations of fissile material identified in Section 6; all turned out to be far sub-critical.

- Section 8 presents an analysis of the sensitivity of the generally negative (no criticality) results to the input parameters having the greatest uncertainty, particularly to the likely aperture size of the fracture network likely to be found beneath the waste package.

- Section 9 presents an estimate of the consequences of an external criticality, assuming there is an accumulation of a critical mass, which the rest of the study shows to be extremely unlikely, or almost impossible.

- Section 10 gives the major findings of this study.

Since there were no external critical configurations identified in this study, there are no design recommendations. However, the sensitivity of the results to certain of the input parameters demonstrates the need for accurate measurement data to support the re-evaluation of this analysis to be performed in FY 1998.

Detailed information on the uranium mineral deposits discussed in Section 6.1 is given in Appendix A. Detailed information on the models used for the criticality calculations of Section 7 with the three-dimensional Monte-Carlo code, MCNP, is given in Reference 83.

Most of the geologic and geochemical analyses of Sections 5 and 6 were taken from Ref. 4, and the backup details of all such calculations are given therein.

2. WASTE FORM AND WASTE PACKAGE DESCRIPTIONS

Plutonium disposition is concerned with two types of waste forms: immobilized plutonium, and MOX. This section describes the characteristics of each as they were used in the analyses of this report. As mentioned in Section 1, the immobilized Pu form assumed for this study was the glass waste form, which was used to estimate the fissile content and other characteristics of the source term released from the waste package. After most of the calculations for these external criticality studies were completed, and as this document was being prepared, there was a selection process completed between the glass and ceramic waste forms, resulting in the ceramic waste form being chosen. Although much of this analysis will have to be repeated for the ceramic waste form, the results of the analyses for the glass waste form are still of immediate interest for the following reasons:

(1) Of the three waste form parameters which are dominant with respect to criticality (the amount of fissile material, amount of absorber material, and the dissolution rate of the entire waste form) only the last is expected to be significantly smaller for the ceramic than was assumed for the glass waste form, and

(2) Since the criticality results for the glass waste form are generally negative (no identification of a critical configuration which can be achieved by a possible physical scenario), they indicate an upper bound on the magnitude of the external criticality problem for the ceramic waste form as well, since it was chosen because of presumed greater resistance to dissolution.

2.1 Glass Waste Form

The following description of the glass waste form is a condensation of that given in Ref. 2, for the earlier evaluations of immobilized Pu criticality.

2.1.1 Nominal Pu-glass Description

The can-in-canister glass waste form (WF) nominally consists of Lanthanide-Borosilicate (La-BS) glass with 10%, by weight, Pu homogeneously dissolved and an equi-molar ratio of gadolinium (Gd) to act as the primary criticality control material. The La-BS glass was selected because it had the greatest resistance to aqueous corrosion of all the glass alternatives (Ref. 81, p. 4). The Pu bearing glass is poured into cylindrical stainless steel cans (with the outside dimensions of 12.035 cm diameter x 57.535 cm long and 0.3175 cm thick) which are, in turn, supported on a rack/basket, and embedded in a defense high-level waste (HLW) glass filler within a HLW-type canister. A diagram of the configuration is given in Ref. 2, Figure 2.1.1-1. The compositions of the La-BS and HLW filler glass are given in Ref. 2, Appendix A. With an interior volume of 5808 cm^3, 85% filled with the glass waste form having a density of approximately 5.5 gm/cm^3, each can will have approximately 2.56 kg of Pu. With 20 of these cans in a HLW-type canister, the total fissile material in a HLW-type canister will be 51.2 kg Pu.

2.1.2 Optimum Neutron Absorber

Gd has been the nominal choice for neutron absorber because, of all the elements, it has the largest absorption cross section, and is thus the most efficient for absorbing thermal neutrons. However, other elements have better features with respect to other requirements. Samarium (Sm) has been suggested as a lower cost alternative and may be almost as efficient as Gd for absorption of epi-thermal to fast neutrons. Hafnium (Hf) is the least soluble of the three potential candidates (which is important in preventing removal of the neutron absorber over tens of thousands of years), but is also the most expensive. The relative merits of these alternatives were considered in Ref. 1, without any specific conclusion or recommendation. While Gd remains the current choice for neutron absorber (whether included in glass or ceramic), the other two alternatives have not been excluded. These three elements have similar chemical properties, which are different from U and Pu, so none of them would be expected to transport with the fissile material.

2.2 Ceramic Waste Form Description

The ceramic waste form will fit into the same size cans as the glass waste form, and will have the same amount of plutonium and gadolinium. A comprehensive description of an earlier version of the ceramic waste form was given in Ref. 2. The actual waste form chosen in the recent selection process is physically the same as that described in Ref. 2, but the chemical formulation is different. As mentioned above, from the standpoint of criticality, the principal difference between the glass and ceramic waste forms is the much slower dissolution rate expected for the ceramic. This information is provided for completeness only at this point; there is no analysis of the ceramic waste form in this document due to its very recent selection as the preferred disposal option.

2.3 Codisposal Waste Package Description

The WP for immobilized Pu is the same for both glass and ceramic WFs, since both WFs will be emplaced into the same HLW size canister. For this reason the WP will be similar to the Civilian Radioactive Waste Management System (CRWMS) current design for HLW WP. For this study, the WP was nominally loaded with four canisters, since that was the capacity of the nominal canister design. As this study was being completed it was decided to enlarge the waste package somewhat to accommodate five canisters in the interest of greater efficiency, but such a design is not considered as part of this study. The cross section of a four canister package is given in Ref. 2, Figure 2.3-1. Based on the recommended reduced loading given in Ref. 2, the nominal waste package loading is the codisposal configuration containing only one immobilized plutonium canister and 3 (or 4) HLW canisters.

The WP for the immobilized Pu WFs will be constructed of the same materials as the waste package for commercial SNF. It consists primarily of a corrosion allowance outer barrier and a corrosion-resistant inner barrier. The outer barrier is carbon steel, 10 cm thick, and the inner barrier is presently planned be a high nickel steel, Alloy 625. A search is presently under way to replace Alloy 6 with a more corrosion material, and C-22 seems to be a likely possibility.

The WFs are contained within the WPs in stainless steel canisters having dimensions approximately 3 meters in overall length, 61 cm outer diameter, and 1 cm thick. The WP size

to accommodate these canisters is approximately 3.4 meters overall length. The 4 canister WP therefore has an inner diameter of at least 150 cm. The 5 canister WP will have a slightly larger diameter.

2.4 MOX Waste Form and Waste Package Description

The initial fuel composition is based on a design proposed by Westinghouse (Ref. 75), and the spent fuel composition is based on a set of reactor burnup calculations performed by Oak Ridge National laboratory (ORNL) (Ref. 76). The spent fuel is a standard Westinghouse 17x17 assembly which has spent 2 or 3 cycles in a reactor, and is described in detail in Ref. 75. The most stressing with respect to criticality is the 2 cycle fuel which will have a higher fissile content and a lower concentration of neutron absorbers (actinides and fission products). In particular the 2 cycle SNF will have a total Pu inventory of 13.8 kg per assembly with the fissile material (principally ^{239}Pu) constituting 0.470 of the total Pu. The dissolution rate and chemical composition are given Tables 4.1.1.1-3 and 4.1.1.2-1 of Ref. 4, respectively.

The MOX SNF will be emplaced in the standard 21 PWR waste package planned for commercial SNF. In this waste package, the method of internal criticality control is either borated stainless steel plates or zircaloy clad B_4C control rods, with the latter planned for any type of SNF with the highest criticality risk.

3. APPROACH AND METHODOLOGY

The approach and methodology described here apply generally to both internal and external criticality and to both glass and ceramic WFs. However, most of the illustrations are for internal scenarios and the glass WF. This approach is necessary because the internal scenarios are the precursors to any external criticality, and because the glass WF has many variations in resulting configurations. These distinctions are further explained with the discussion of specific scenarios (including processes following complete WF degradation) in Section 4 and with the discussion of specific configurations (resulting from the specific scenarios, and including configurations with the possibility of near-field external criticality) and the relevance of natural analogs in Section 6.

3.1 General requirements for criticality

As explained in Ref. 2, there are certain events and processes that must be present for a criticality event; however, their presence does not assure that a criticality will occur. For this study, the occurrence of external criticality is determined by calculation of k_{eff}, as a function of the accumulation of the principal fissile species ^{235}U, ^{239}Pu.

The barriers surrounding the Pu-containing-WF must be breached before water can begin the dissolution and transport process. These barriers are the inner and outer barriers of the WP, the stainless steel canister, the filler glass, and the stainless steel can containing the Pu WF (glass or ceramic).

Making the conservative assumption that the filler glass does not prevent the water from attacking the individual waste form cans as soon as the canister is breached based on the fact that it will be highly fractured, the mean time for first water penetration to the WF is 3500+1100 = 4600 years (Ref. 2, p 3-1). It should be noted that although the filler glass may not provide direct protection for the WF, the presence of the degrading filler glass is likely to keep the solution alkaline so that the solubility of Gd is low and Gd will precipitate in the WP as fast as it can be released, thereby delaying the time to the start of Gd-free buildup of fissile material in the clayey precipitate. This is important for the prevention of internal criticality, but has no direct relevance to external criticality.

The geochemical analysis shows that Gd and U/Pu will not precipitate in similar minerals, so any external accumulations of fissile material will be free of the Gd absorber. The same holds true for Hf or Sm.

There are three possible materials available in the repository that could be moderators for criticality of ^{239}Pu or ^{235}U if present in sufficient quantity: water, carbonates, or silica. All three of these are present in the external environment, and are included in the appropriate geochemical and neutronics calculations. As with the internal criticality evaluated in Ref. 2, water, being the most efficient moderator, is required to some degree.

As with the criticality analyses of Refs. 1 and 2, results are presented in terms of a calculated k_{eff} and in terms of WF design parameters relating the possibility of occurrence of configurations having k_{eff} above some threshold value defining criticality. The physical definition of criticality is $k_{eff} \geq 1.0$. However, the present NRC licensing requirement applicable to repository criticality is that the calculated k_{eff} be < 1.0 minus a 5%

administrative (safety) margin and a further decrement for uncertainty and bias. For commercial spent nuclear fuel, this translates into $k_{eff} < 0.91$ including a bias and uncertainty associated with applicable criticality safety benchmark calculations, and uncertainty associated with the spent fuel isotopic compositions. However, for immobilized weapons-grade Pu in which all of the Pu is assumed to be ^{239}Pu (or ^{235}U with time), no burnup credit (or associated uncertainty) is used, leading to an approximate limit of $k_{eff} < 0.93$. This is based on an assumed 2% bias and uncertainty inferred from applicable criticality safety benchmark evaluations (Ref. 84) (approximately twice the worst case as calculated using MCNP).

3.2 Analysis Strategy/Methodology

The following are the principal components of the strategy to identify and evaluate potentially critical external configurations:

A. Generate source terms representing the range of chemistries of the solution released from the waste package, particularly the fissile concentration and pH.

B. Use geochemical (EQ6) calculations to estimate accumulations of fissile material in the invert and immediately adjacent rock. The specific procedures for using EQ6 are described in Section 6.1.1. Note that EQ is not an acronym for "equilibrium".

C. Evaluate the potential for fissile accumulations in the far-field using the following::
   (1) Identify geologic formations which could act as reducing zones (which can potentially cause precipitation of U and Pu) for enhanced accumulations,
   (2) Evaluate the potential transport process for moving the source term to the location of such a reducing zone, and
   (3) Use geochemical calculations to estimate the accumulation which would actually result, as a function of time.
   This study reports (1) only, since the accumulation results have thus far been negative, and do not suggest instances for the further evaluations (2) and (3).

D. Use documented single parameter criticality limits as a very conservative discriminator to identify configurations with no criticality potential. These limits are given in Table 3-2.1 (Ref. 85, p 66).

E. Use MCNP to compute k_{eff} for those potentially critical configurations identified by steps B, C, and D.

Table 3.2-1. Single Parameter Limits for Uniform Nitrate Aqueous Solutions of Fissile Nuclides			
Parameter	^{235}U	^{233}U	^{239}Pu
Mass of fissile nuclide, (kg)	0.78	0.55	0.48
Solution cylinder diameter, (cm)	14.4	11.7	15.4
Solution slab thickness, (cm)	4.9	3.1	5.5
Solution Volume, (l)	6.2	3.6	7.3
Concentration of fissile nuclide, (g/l)	11.6	10.8	7.3
Areal density of fissile nuclide, (g/cm^2)	0.40	0.35	0.25
Atomic ratio of hydrogen to fissile nuclide (lower limit)	2250	2390	3630

4. SCENARIO CONCEPTS
(WF degradation and subsequent processes)

All scenarios are developed as part of a systematic process, to ensure that all credible possibilities have been considered and to identify the most likely of these to be characterized by the sequence of physical and chemical processes. The methodology and definition of scenarios has been described in detail in Ref. 2. In particular, a systematic view of the processes that can lead to potentially critical configurations for Pu immobilized in glass was initially developed for Ref. 2, and is outlined in Figures 5-1, 5-2, and 5-3 of that reference. Additional scenarios were identified by a comprehensive workshop (sponsored by CRWMS M&O Performance Assessment and held in March 1997). The workshop participants were experts in the various processes which could lead to a critical mass accumulation, and they formed task teams to evaluate the many scenarios identified. The ultimate result was a report (Ref. 61) which summarized the scenarios identified by the workshop and subsequent task team deliberations, and applied a screening process which reduced the number of scenarios to 8, two of which were external and are extensions of scenarios already identified in Ref. 2. The analyses of this study are generally consistent with the external criticality scenarios presented in Ref. 61. However, the emphasis here is on the maximum accumulations of fissile material which can occur in both the near- and far-fields, and on whether those maximum accumulations constitute a critical mass. The range of scenario parameters which can lead to the potential near- and far-field accumulations is discussed in the following subsections.

4.1 Scenario Initiators and Source Terms

The scenarios for external criticality all start with the dissolution of the waste form and the generation of a source term which carries the fissile material out of the waste package. The individual processes are described as follows.

4.1.1 Corrosion of steel and breach of barriers

All scenarios leading to criticality begin with intrusion of water into the emplacement drift, incidence on the WP (dripping), followed by water penetration into the WP. For the immobilized Pu waste form, the stainless steel canister containing the individual waste form cans must also be breached sufficiently for the water to attack a major fraction of the waste form surface area. The corrosion of stainless steel used for the cans and canisters in the immobilized Pu waste package, or the corrosion of high nickel alloy used for the corrosion resistant inner barrier for all waste packages, has the potential to produce an acidic pH because of the chromate ion which may be the end result of the oxidation of chromium (or the analogous reaction for molybdenum), which is a significant constituent of all stainless steel or the high nickel alloys. The scenarios considered in this study included both canister stainless steel and the Alloy 625 planned for the waste package inner barrier. The relative effects which these materials contribute to the source term are described in Section 5.2.

The period of the stainless steel corrosion lasts longer than the degradation of both the waste form and the HLW. This leads to a complex chemical evolution that determines the pH and fissile concentrations in the source term. The manner in which source terms reflect the possible overlaps and dissolution rates is described in Section 4.1.3, below.

For the MOX SNF, significant fuel dissolution cannot begin until the zircaloy cladding of the individual fuel rods is significantly breached, exposing the fuel to incoming water or humid air conditions. Because of the corrosion resistance of the zircaloy cladding, significant MOX dissolution is not expected to start for at least 50,000 years following waste package breach. This assumption is consistent with that to be used in TSPA-VA for commercial LEU SNF. It will be seen in the analysis of deposition from the MOX source term, in Section 6.1.5, below, that the amount of external accumulation is primarily influenced by the pH of the source term. Since the low pH period will last as long as the dissolution period of the stainless steel, it will not be particularly sensitive to the time of initiation of the SNF dissolution process (Ref. 4, p. 23, 87).

4.1.2 Dissolution of waste forms

Dissolution of the HLW waste form

While the HLW is dissolving the pH of the solution will be high (as large as 10), and the solubility of U and Pu will be sufficiently high that most of this fissile material can be removed from the waste package as fast as it is released from the immobilized Pu waste form. Although the HLW dissolution rate is high enough that the waste form is likely to be completely degraded within 1200 years of the first exposure of this waste form to water, the duration of the high pH period can be prolonged by random variations and changes in dispersion in the flow path in and among the several (3 or 4) HLW canisters (Ref. 4, Section 7).

Dissolution of Pu waste form

Dissolution of the immobilized Pu waste form will begin after breach of the inner cans containing the immobilized Pu (as glass or ceramic). Corrosion of the cans (precursor to breach of the cans) will begin some time after breach of the canister containing the cans. The precise timing of this delay in the initiation of the corrosion process will be inversely correlated with the degree of fracturing of the filler glass, since an increase in fracturing provides faster paths from the environment external to the immobilized Pu canister within the waste package. Since the delay is likely to be short, relative to the other times involved in the scenario, it will be assumed to be zero (which is also conservative).

Once water has contacted the inner cans, penetration sufficient to support dissolution of the immobilized Pu waste form will take upwards of 3000 years (1/10 of the bulk corrosion time for 3 mm thick stainless steel at 0.1 microns per year corrosion rate). It is expected that the times of initiation and penetration will vary among the 20 inner cans. Complete dissolution of the immobilized Pu waste form could take between 10,000 and 500,000 years following initiation, depending on the intrinsic dissolution/reaction rate of the waste form and the degree of fracturing of the material actually fabricated.

The important issues are: (1) whether this period of immobilized Pu waste form dissolution will have major overlap with the period of high pH, which is caused by the HLW dissolution, and (2) whether the immobilized Pu waste form dissolution period will overlap the period of potential low pH. Because of the uncertainty in the dissolution rates (as a consequence of incomplete specification of the material and incomplete experimental program), and the inherent uncertainty in the sequence of aqueous contact with the various physical forms involved, the scenario development process has not yet evolved to the point of specifying the

sequence of these degradation processes, or their durations. Therefore, we have covered the range of possibilities by considering three values for the source term pH: high (10), neutral (7) and low (4 or 5).

Dissolution of MOX

Although there have been very few dissolution tests of any MOX SNF, it is expected that the dissolution rate will be the same as, or somewhat greater than the rate for commercial SNF. This rate, in turn, is greater than the rate for the corrosion resistant, high nickel alloy which is used for the waste package inner barrier, and which can produce an acidic environment while it is corroding. It is, therefore, possible that most of the MOX SNF degradation can take place in an acidic environment. The resulting source terms are, accordingly, developed for both a neutral and an acidic (low pH) source term.

4.1.3 Mechanisms for the generation of source terms

The external criticality potential of any waste package is completely reflected in the chemical composition of the source term which is produced by that waste package. In this regard, the source term encapsulates the processes described above for degradation of the waste package and its contents. As described in Sections 4.1.1 and 4.1.2, above, the current state of knowledge is represented by three different pH values for the immobilized Pu waste package and by two values for the MOX SNF waste package. These pH values generally cover two distinctly different types of external criticality scenarios: (1) Waste form is degrading in a high pH environment so that U and Pu go directly into solution as the waste form degrades, and will be released from the waste package as it is flushed by the infiltrating water; (2) Waste form is degrading in a neutral or acidic environment in which the U and Pu are very insoluble, so that they precipitate within the waste package as they are released from the degrading waste form. For a scenario which starts out as the second type, the pH may subsequently rise so that the fissile elements may be re-mobilized from the precipitate at a latter time, if some reaction occurs to raise the pH. An example of such behavior would be a belated contact of water onto a HLW canister, with subsequent degradation of the HLW glass and generation of a high pH. Such specific time dependent behavior has not been modeled in the present study because we have focused on the worst case sequence of processes, in order to identify any potentially critical configurations. This search has been negative thus far, but if configurations are identified, the scenarios which lead to them will be quantified using the configuration generator, as was done for the internal criticality study (Ref. 2).

4.2 Accumulation Mechanisms

This section provides a summary of the accumulation reactions which can take place between the source term and the material which it encounters in the near-field (or the immediately adjacent host rock). The calculations and results are described in Section 6.

4.2.1 Chemical reaction with near-field gravel and rock

A precipitation of fissile material could occur in the form of silicates or alkaline silicates as the fissile bearing solution released from the WP and encounters a change in chemistry or unique physical formations which can lead to some removal (e.g. precipitation) of fissile material from the solution. The analyses reported in Section 6.1 show this reaction to be significant only for

the high pH source term. Even at the high pH, however, the amount of fissile material which can be deposited is severely limited by much larger mass of non-fissile solutes which are competing for the available void space. The limited amounts of fissile material which can be deposited are shown by calculations in Section 7, to be insufficient for criticality. Therefore, these analyses demonstrate that near-field chemical reactions cannot form the basis of any scenarios leading to criticality.

4.2.2 Analogs of mineral deposits

The geologic processes which have lead to deposition of high-grade uranium ore bodies after deposition of the host rock (called epigenetic processes) are described in Appendix A of this document. They represent potential mechanisms for accumulation of uranium in the far-field, and are logical candidates for inclusion in scenarios which can lead to criticality. However, as shown in Section 6.2, the geology of Yucca Mountain is inconsistent with the occurrence of the geologic formations necessary to support such processes. These processes can form the basis of scenarios leading to external criticality, but such scenarios will have extremely low probability.

4.2.3 Carbon steel in a pond

A possible mechanism leading to UO_2 or PuO_2 precipitation in the invert could be the existence of a reducing agent in an oxygen starved environment. The oxygen starvation can be provided by a pond of water in a depression in the drift. In addition to a fairly high fissile content in the source term flowing out of the waste package, this scenario also requires a major fraction of the carbon steel (or some other iron-rich steel) to fall into the standing water (pond) with the following two requirements on its condition: (1) small fragments of nearly spherical or cubic shape to maximize the surface area exposed to the oxidizing fissile solutes, and (2) little, or no, oxidation on the surfaces of these fragments (otherwise there would be few reducing sites left on the fragment surfaces). The fact that these requirements are somewhat contradictory further reduces the probability of their satisfaction.

Under such circumstances the fissile ions (UO_2^{+6} or $PuO_2^{+6,+5}$) in solution could be reduced from the hexavalent (soluble) to the quadrivalent (insoluble) state, and consequently precipitate while the reducing agent becomes oxidized. Any significant amount of oxygen present will act much faster on the reducing agent than can the less chemically active fissile species, thereby shutting out the fissile species from any reducing reaction, hence the requirement for oxygen starvation. The reducing media can be provided by the carbon steel from the outer barrier material of all types of waste package and the structural basket for the commercial SNF type of waste package (which is used for MOX). Such processes could form the basis of criticality producing scenarios, but the analysis in Section 6.1.6 suggests that the worst case deposit resulting from this process will not be sufficient for criticality. More importantly, the need for nearly the entire waste package complement of carbon steel to be in a continuing, standing pond makes such scenarios very unlikely.

4.2.4 Adsorption in the near- and far-field

Yet another possible mechanism for accumulation of fissile material in the invert is adsorption onto either zeolites in tuff or degraded concrete or Fe_2O_3, the latter of which could come from the corrosion/oxidation of iron containing metal in the WP barrier (for all waste packages) or

from the corrosion of iron containing WP basket metal (for the commercial SNF package). Since zeolites are also found in abundance in the host rock around the repository, this process is also a candidate for far-field criticality scenarios. It is shown, however, in Section 6.3, that the amount of accumulation by this mechanism is too small to support criticality. Thus, while scenarios involving this path can be assumed to be likely to occur, they will not cause criticality.

4.2.5 Colloid transport

There is some possibility that the effective solubility of plutonium can be greatly increased by colloid formation. There is very little experimental evidence to serve as the basis for developing scenarios incorporating such processes. The conventional wisdom on colloid formation and behavior suggests that if Pu colloids are formed, they would likely be filtered out of the water by any surfaces contacted, specifically along fractures in a concrete invert, or by narrow fractures in the rock below, so this is primarily a near-field mechanism. Furthermore, examination of possible colloid particle composition, in Section 6.4, shows that fissile deposition would be limited by competing materials, just as for the chemical reaction deposition mechanism discussed in Section 4.2.1, above. Some contradictory evidence to this conventional wisdom is cited in Section 6.4.

4.3 Water Accumulation

The last element of any scenario leading to criticality is the provision of sufficient moderator. While it is possible to have a criticality moderated solely by silica, a much larger critical mass would be required than for a water moderated criticality. Therefore, the accumulation of water is usually the last step of any criticality scenario. The principal features, events, and processes for accumulation of water are given by the following list (with the expected persistence of the accumulation given in parentheses):

- Near-field water accumulation
  - Depression beneath the waste package with the fractures sealed by thermal stress or by particulate plugging or chemical precipitation (6 months)
  - Unusually large episodic flow (20 m^3 in 1 week) incident on one location in the drift (1 week)

- Far-field water accumulation
  - Impervious rock layer (perched water)
  - Location in the saturated zone (below the water table)

This listing is consistent with the workshop results summarized in Ref. 61.

5. SOURCE TERMS

The purpose of this section is to describe the concentrations of fissile material in the solution flowing out of the waste package. This solution can be viewed as a source term for the accumulation of fissile material external to the waste package. For this purpose the dissolution of the waste forms and the mobilization of the dissolution products is modeled, using EQ6 in a flow-through mode. This is an option which simulates the mixing of two solutions, whereby the solution inside the package was first diluted for some specified time interval, and then part of the solution removed, thereby simulating to some degree advection of new ground water and transport out of the package. Details of this procedure are given in Attachment II of Ref. 4.

5.1 Composition of Water Entering the Waste Package

The development of the source term begins with the determination of the composition of the water entering the waste package. Examination of the analytical results for J-13 well water by the use of the geochemical code EQ3 (the equilibrium part of EQ3/6) reveals that the measurements are compatible with well established thermodynamic data only if the partial pressure of CO_2 is markedly higher than in the atmosphere. This situation is discussed in more detail in Ref. 2, pp. 5-18 to 5-19. For the present application, the pH values in Ref. 7 were converted approximately to hydroxide concentrations, those values averaged, and the average converted back to an average pH of 7.64. To achieve agreement between analytical and thermodynamic data, the average for alkalinity was adjusted by about half of its analytical standard deviation (8.6 mg/L) from 128.9 mg/L to 133.0 mg/L. These adjusted values were used in modeling the degradation of waste packages containing commercial spent nuclear fuel and for MOX fuel waste packages. In addition during the modeling runs, normal atmospheric partial pressures of CO_2 were used. This results in an immediate adjustment of pH and corresponding loss of carbonate concentration in the water. In other words, the implicit assumption is that not long after entering the open space of a repository, the water will come to equilibrium with the atmosphere, rather than with rock gas which may have a higher concentration of CO_2. Table 5-1, first three columns, shows the composition of the water actually used for the SNF and MOX calculations. The initial water composition for modeling the degradation of immobilized plutonium was the same as given in Ref. 7 along with EQ3 input constraints for being in equilibrium with atmospheric CO_2 and O_2 and the electrical balance adjusted by modifying the total chloride ion concentration as needed. Chloride was chosen for the electrical balancing because it tends to have little effect on the chemical calculations; this results from the fact that with most elements it forms only weak complexes and that the solids present in the system under consideration contain little or no chloride. This resulted in a solution very nearly the same as described above, except for a significant change in chloride concentration (last 3 columns of Table 5-1). This difference in chloride concentration has little effect because the dissolution of the HLW glass very quickly results in substantial changes that dominate the aqueous chemistry.

The concentrations of dissolved U and Pu are not sensitive to differences in chloride concentration nor, except at high pH, to differences in sodium or carbonate concentrations. Consequently, the results of the calculations provided in Ref. 2 were used for calculations evaluating the possible deposition of fissile isotopes dissolved in neutral or acidic effluent from immobilized plutonium waste packages in invert or rock below the waste package.

Table 5-1. Calculation of J-13 Water Composition (nominal: first 3 columns, and alternative: second 3 columns)

Component	Molality	Mole Fr.		Component	Molality	Mole Fr.
Na	1.99e-03	1.20e-05		Na	1.99e-03	1.20e-05
Si	1.02e-03	6.11e-06		Si	1.02e-03	6.11e-06
Ca	3.24e-04	1.95e-06		Ca	3.24e-04	1.95e-06
K	1.29e-04	7.74e-07		K	1.29e-04	7.74e-07
C	2.18e-03	1.31e-05		C	1.45e-04	8.69e-07
F	1.15e-04	6.89e-07		F	1.15e-04	6.89e-07
Cl	2.01e-04	1.21e-06		Cl	2.15e-04	1.29e-06
N	1.42e-04	8.53e-07		N	1.42e-04	8.53e-07
Mg	8.27e-05	4.97e-07		Mg	8.27e-05	4.97e-07
S	1.92e-04	1.15e-06		S	1.92e-04	1.15e-06
B	1.24e-05	7.44e-08		B	1.24e-05	7.44e-08
P	1.27e-06	7.63e-09		P	1.27e-06	7.63e-09
H	1.11e+02	6.67e-01		H	1.11e+02	6.67e-01
Al	1.48e-08	8.90e-11		O	5.55e+01	3.33e-01
Ba	1.00e-10	6.00e-13		Totals	1.67e+02	1.00e+00
Ce	1.00e-24	6.00e-27				
Cr	3.45e-07	2.07e-09				
Cu	1.00e-10	6.00e-13				
Cs	1.00e-10	6.00e-13				
Fe	1.15e-04	6.89e-07				
Gd	1.00e-14	6.00e-17				
La	1.00e-14	6.00e-17				
Li	1.00e-10	6.00e-13				
Mn	7.28e-07	4.37e-09				
Mo	1.00e-10	6.00e-13				
Nd	1.00e-14	6.00e-17				
Ni	1.00e-10	6.00e-13				
Pb	1.00e-10	6.00e-13				
Pu	1.00e-14	6.00e-17				
Sm	1.00e-10	6.00e-13				
Sr	1.00e-10	6.00e-13				
Ti	1.00e-10	6.00e-13				
U	1.00e-14	6.00e-17				
Zn	1.00e-10	6.00e-13				
Zr	1.00e-20	6.00e-23				
O	5.55e+01	3.33e-01				
Totals	1.67e+02	1.00e+00				

J-13 water. Columns 1-3: Adjusted for pH 7.6397 and log fO2 = -2.5390 to be consistent with thermodynamic data. Original molalities from Ref. 7; adjustments in EQ6 run j13avg20.6o, Ref. 4, Section 9.2. These data used for oxide fuel calculations. Columns 4-6 correspond to original data, balanced on Cl- and for log fO2 = -3.500 These data were used for runs with glass waste before a method was devised to make a suitable adjustment to the raw data. The effect on the results is insignificant because the dissolution of the HLW quickly dominates the chemistry.

5.2 pH Range of the Source Term

As indicated in Section 1, this waste form was modeled as plutonium and gadolinium in a lanthanum-borosilicate (La-BS) glass because this was the one form for which there was the most data. As this analysis was in the final publication process (September 1997) a down selection process chose ceramic as the matrix for immobilized plutonium. The potential accumulations from the ceramic waste form will be analyzed in subsequent studies; however, it is expected that the analyses for La-BS glass reported here will be conservative with respect to the ceramic waste form, because of the expected lower dissolution rate for the ceramic waste form. Therefore, it is appropriate to present the results of the La-BS glass waste form analyses as a conservatively bounding analysis.

At early times, the composition of the effluent was taken from a stage in the EQ3/6 simulation of the reaction inside the waste package at which the pH had risen nearly to its maximum value, but before the ionic strength had increased to the point that no confidence could be placed in the result. This composition and the time of its occurrence are discussed in more detail in subsections below. For later times, compositions were calculated on the basis that most of the high ionic strength alkaline initial solution would have been flushed out and that the chemistry was essentially the same as would result from influx of J-13 water with the oxidized uranium and plutonium solids that would exist at a given pH at saturation as discussed in Ref. 2. Nevertheless, the algorithm for simulating flushing and transport (described in the first paragraph of Section 5, above, and in Ref. 4) was exercised for an infiltration rate of 10 mm/Yr (see files allinglsI10mm, allinglsII10mm, allinglsIII10mm, allinglsIV10mm, allinglsV10mm, alloutglsI10mm, alloutglsII10mm, alloutglsIII10mm, alloutglsIV10mm, and alloutglsV10mm, Ref. 4, Section 9.2) with the assumption that Cr would oxidize fully (Ref. 4, Assumption 4.3.9). This analysis showed that the pH still rose to a high value, 9.9274, in about 250 years (see file alloutglsII10mm, Ref. 4, Section 9.2) compared to 10.04 for the closed system case, but was no longer highly alkaline after about 330 years (see file alloutglsIII10mm), about half as long as in the closed system case. Ionic strength reached a high of 1.456 in marked contrast to the continually increasing value to totally unrealistic values for the closed system; in the closed system at 250 years the ionic strength was calculated as 4.25, and, because this is too high to model correctly, even approximately, with the available data for activity coefficients, the solution characteristics for this stage were not used. Thus, the flushing has a large effect on the total dissolved solids in the system, but only a modest effect on the pH as compared to the highly conservative case of a closed system. The largest causes of the initial rapid rise in pH and ionic strength, as well as the very low pH that could result from complete oxidation of Cr and Mo, thus appear to be the high (conservative) rates of metal corrosion used in the models.

Following the onset of corrosion of the HLW in J-13 water, the pH gradually begins to increase as alkaline glass degradation products are formed. The solution composition was modeled by EQ6 as the contents of the waste package were dissolved (case j13avwp50.6o of Ref. 4, Section 9.2). For about 600 years the effluent from the package was simulated to have a pH of about 10. The effluent becomes neutral (about pH 7) after the high pH period. The neutral condition lasts about 1200 years after which the effluent pH decreases to nearly 5 for another 8000 years after which time it increases to approximately 6.5. The acid condition after 1200 years is due to the oxidation products of stainless steel. The relatively low pH before 8000 years is due to the oxidation of the stainless steel of the canisters. Following that time the canister steel has mostly corroded and the only acidification is provided by the much more

slowly corroding waste package inner barrier, Alloy 625, which accounts for the increase in pH. The 8000 years transition time between the strong and weak acidification would be increased by a slower corrosion rate for the canister stainless steel. During the entire degradation period the solution remains oxidizing. Solutions with these three conditions were used as feed solutions for reactions with the environment external to the waste package.

5.3 Fissile Concentrations in Source Terms from the Immobilized Plutonium Waste Package

5.3.1 Source Term at pH 10

For the present analysis, a solution composition near the maximum pH, but at a low enough ionic strength to stay within reasonable bounds, was chosen (see step 824 of EQ6 output file j13avwp50.6o, Section 9.2 of Ref. 4). Specifically, this was pH 10.0031 and ionic strength 2.51 at 140 years post-closure. Under these conditions the solubilities of U and Pu are near their maximum values; consequently, solutions resembling the one chosen are the most likely to produce a sufficient concentration of fissile material to give rise to a criticality in the invert. The pH is simulated to remain high for 600 years, which is a short time compared to time-frames of interest. Consequently, the total mass of ^{235}U and ^{239}Pu that could be released while the pH is high may be small. The simulated solution chosen contains 6111 ppm total U and 78.3 ppm Pu. All the Pu would have been released from the La-BS glass as would all the ^{235}U. The ^{235}U arises from the decay of ^{239}Pu, here simulated as at 5000 years post-closure. It is assumed that the ^{235}U from the La-BS glass will mix with the ^{238}U from the HLW glass before any U or Pu solids precipitate or are otherwise immobilized within the waste package. In this case the percentage of ^{235}U in the effluent from the waste package will be about 3.31%, which is conservative in view of the fact that no preferential early removal of ^{235}U would occur immediately upon release from the La-BS glass.

The composition described above is very conservative because it was developed for no flow through the package during the dissolution. With no flow, the concentrations become much higher than with the flushing effect of a flow through situation. At infiltration rates up to 1 mm per year the flushing effect may be minimal. However, some results below were reported for 5 mm/Yr and 10 mm/Yr infiltration rates. A dissolution case with flushing (EQ6 output files alloutglsI10mm, alloutglsII10mm, alloutglsIII10mm, alloutglsIV10mm, and alloutglsV10mm -- see Section 9.2, of Ref. 4) was run to test the sensitivity of the results. It was found that at 10 mm/Yr infiltration the pH 10 (actually 9.93) condition would last less than 300 years (compared with 600 years for the non-flushing cases). It would also be expected that the pH 10 condition would last less than 400 years at 5 mm/Yr due to the same effect. The flushing dissolution case at 10 mm/Yr gave the same length of dissolution time (140 years), a higher maximum concentration of uranium in solution, 7263 ppm versus 6111 ppm, and a lower maximum plutonium concentration, 10.1 ppm versus 78.3 ppm.

5.3.2 Source Term at pH 7

For the simulations of the reactions, a representative solution chemistry was chosen. The results from EQ6 output file j13avwpsoly45.6o (see Ref. 4, Section 9.2) were taken. This solution at pH 7.01 an ionic strength of 3.5E-03 (molality scale). The solution contained 1.929E-03 ppm U and 1.56E-07 ppm Pu.

5.3.3 Source Term at pH 5

For the simulations of the reactions, a representative solution chemistry was chosen. The results from Step 14 of EQ6 output file j13avwpsoly40.6o (see Ref. 4, Section 9.2) were taken. This solution at pH 5.5 has an ionic strength of 2.4 molal. The solution contained 4.71E-03 ppm U and 6.15E-06 ppm Pu.

5.4 Source Term from a Degraded MOX Waste Package

The source term from a degraded MOX waste package was calculated in a manner similar to that used for the immobilized Pu waste form, but with the dissolution rate given in Table 4.1.1.1-3 and the chemical compositions given in Table 4.1.1.2-1, both of Ref. 4. The solution concentration is given in Step 632 of the EQ6 output file j13avmoxa1.6o (Ref. 4, Section 9.2).

The MOX waste package does not contain any components such as the HLW glass which could produce a high pH. It is most likely that the water degrading the MOX SNF will remain close to neutral pH. However, it is possible that if water is ponding in the waste package it will act to corrode the inner barrier material sufficiently to generate chromate ions and lower the pH. Therefore, to be conservative, a low pH case was also chosen with a pH 4.09 and an ionic strength of 0.173 molal. The solution contained 782.6 ppm U and 1.3E-03 ppm Pu. As a further conservatism, all of the Pu in the MOX SNF is assumed to remain undecayed (since Pu is more reactive with respect to criticality than is the U into which it decays with a half-life of 24,000 years). Therefore, the uranium is characteristic of depleted uranium with a ^{235}U content of only 0.1675 wt%.

6. ACCUMULATIONS OF FISSILE MATERIAL

6.1 Near-Field Accumulations

6.1.1 Techniques Used for Flow Centered EQ3/6 Computations

The option for "Fluid-Centered Flow-Through Open System" in EQ6 was used to estimate the "extended distance deposit" over a path length traveled during the time covered by the reaction calculation. This type of simulation defines the extended distance deposit; the solution is permitted to react with solid materials (in this case tuff or concrete) for some specified interval (time or reaction progress), then moved away from the solid reaction products produced and allowed to react with the same initial solids for a further interval. In this way the model simulates reaction of the solution as it percolates through a rock. Whereas this corresponds only to a single portion, or packet, of solution through the rock, successive modeling runs were set up that simulate successive packets through the now altered rock. In other words, the second packet would react both with remaining unaltered rock and with the alteration products produced by the first packet. This requires dividing the path through the rock into appropriate reaction zones, each with a characteristic mineralogy. The changing mineralogy from zone to zone necessitates several computer runs for the transit of the second packet through rock. The solution entering each zone was specified in the input file for each of these runs to be the same as that exiting the preceding upstream zone. A more detailed discussion of the modeling approach can be found in Attachment III of Ref. 4. Prior studies have shown that zones of consistent mineralogy will develop which migrate slowly downstream as successive packets of solution are passed through (Refs. 8, 9, and 10). Some further verification of this was done during the simulations of reactions of immobilized plutonium package solutions with crushed tuff. The results are discussed in the section on the reactions of the source term from the immobilized plutonium package with tuff. (Section 6.1.3, below)

The output from the EQ6 calculations was interpreted in terms of deposition as a function of distance by the following spreadsheet process. Data from the EQ6 output file was transferred electronically as text files which were then converted to input spreadsheets. These input spreadsheets were then processed in summary spreadsheets by linking formulas. All of the spreadsheets used are documented electronically as Microsoft Excel® files in Section 9.2 of Ref. 4. The tables in the following sections are condensed versions of these spreadsheets.

The spreadsheets for the extended distance deposit calculate the deposition profile through the flow path as each successive kg of water flows through. The build up of the deposit and its composition of fissile material are tabulated as a function of distance, infiltration rate, and total duration of the deposition period. The deposition period is the smallest of the period during which the pH condition persists, or the time it takes for the solid to plug the flow path, or the time it takes to remove all fissile material from the package (this limit did not occur for any of the cases). The fraction of voids filled with the total solid and the fraction filled with fissile material are also tabulated versus distance.

6.1.2 Technique used for Pond-Centered EQ6 Calculations

Local deposition of uranium on the surface of waste package fragments in a low oxygen environment can be approximated by a simple EQ6 run with no replenishment of the water. This is conservative because the limited oxygen supply will be depleted by the oxidation

process so that the uranium or plutonium can more successfully compete for the available reducing agent sites. The results of these calculations are given in Section 6.1.6, below.

6.1.3 Reaction of Source Term with Crushed Tuff Invert

This section presents results of modeling the reaction of the source term from the immobilized plutonium package reacting with the crushed tuff invert and the fractured host rock immediately below.

To develop the mineral composition of the vitric tuff for input to the calculations, the chemical composition of each of 6 rock samples was distributed into rock components (SiO_2, Al_2O_3, etc.), and then the average of the six samples was taken on a component by component basis. This process is documented in Table 4.1.3-1 of Ref. 4. The resulting average was used as a "special reactant" for input to EQ6. To model a devitrified tuff, this composition was used as input to a petrological calculation of the norm, i.e. a calculation to distribute the various components of the rock among minerals that are found in welded tuff.

6.1.3.1 Reaction with tuff invert of pH 10 solution from immobilized plutonium waste package

6.1.3.1.1 Low flow rate (1 mm/Yr) and nominal duration of high pH

A simulation of this reaction in EQ6 (output file wp10t0a.6o, Ref. 4, Section 9.2) shows that when the solution first enters the invert, its composition changes slowly as it reacts with the tuff producing small quantities of alteration minerals, but neither uranium nor plutonium solids are produced (deposited). The alteration of the tuff principally consists of a recrystallization of the tuff to a mixture of quartz and feldspar. It should be noted that, as the solution flows deeper into the invert and finally into the host rock below, there is further reaction and change of solution composition. At the next step of the simulation a small quantity of solid $Na_4UO_2(CO_3)_3$ is formed primarily due to dissolution of additional sodium from the tuff. The small decrease in pH causes a concomitant shift in the proportions of carbonate and bicarbonate ions in solution and consequent destabilization of the plutonyl carbonate aqueous complex primarily responsible for the solubility of plutonium. Thus, PuO_2 also precipitates.

Table 6.1-1 shows the results for the reaction of the alkaline solution with the tuff; these results are presented in the form of a deposition profile which is the net result of a 600-year deposition process (the duration of pH 10 condition) resulting from an infiltration rate of 1 mm/Yr. The deposit is distributed over a distance of 18.2 m extending through the 0.7 m invert and into the rock fractures below. To develop this analysis, the flow path was discretized into finite lengths or "cells". The boundaries of these cells are points where there is a significant shift in the mineralogy of the deposit. (The choice of boundaries is detailed in the workbook WP10T0A.XLS, worksheet "All Solids" of Ref. 4, Attachment I.)

The format of Table 6.1-1 is used for presenting the other cases, so it is useful to explain the column headings. The first column is the cell number (which comes from the correspondence between time and principal mineral deposition). The second column is the travel time into the rock, which is taken to be equal to the time for the reaction to progress through the cell (not deposition time defined in Section 6.1.1). The third column is the distance traveled into the rock, which is the travel time multiplied by the flow velocity (which is equal to the infiltration

rate divide by a factor equal to the average voidspace, including fracture, because the flow is restricted to the invert void space or the rock fractures). To clarify the relation between cell, or layer, and distance, the cell boundaries are indicated by the distance markings in the figures corresponding to each of the tables following the format of Table 6.1-1. The fourth through seventh columns contain total masses (of indicated species) deposited in each layer (cell) and covering the entire area of the waste package footprint (5.5 m^2). The fourth column is the total solids deposited, which is mostly non-fissile material. In fact, most of the fracture volume is filled with this non-fissile material which competes for deposition volume with the fissile material (Pu) and thereby severely limits the amount of fissile material which can accumulate. The fifth column is the total uranium, which is mostly ^{238}U from the degrading HLW glass. The sixth column is the total Pu, which for this analysis is assumed to be all ^{239}Pu. The seventh column is the total fissile mass, which is the sum of the ^{239}Pu and ^{235}U (the latter resulting from 6000 years of decay of ^{239}Pu). The eighth column is the linear density of fissile material (the result of dividing the fissile mass by the cell thickness). The ninth column is the percent of the void space (or fracture volume) which has been filled by the end of the indicated duration (600 years in the case of Table 6.1-1). The tenth column is the fraction, of the void space or fracture volume) which is filled with fissile material, and the last column is the weight percent of fissile material as a fraction of the total U + Pu. Since the criticality calculations in sections 7, 8, and 9 conservatively consider only those neutron absorbers naturally present in the rock or invert, and not those which are likely to be co-deposited with the fissile material, this "effective enrichment" parameter serves as an important margin of safety.

The first cell extends from the entry point to where the uranium and plutonium species begin to precipitate. The second cell extends to the point where a new mineral, borax, is added to the precipitating solid. It should be noted that, in keeping with the conservative approximations of this analysis, the boron in the mineral borax is not included in the criticality calculations, even though it is likely to be co-deposited with the fissile elements in the invert void space and the adjacent rock fractures. The third cell extends to where another new mineral, albite (low temperature type) is added to the solid composition. Cell 4 extends to a somewhat arbitrary point where no significant additional uranium plus plutonium solids are forming. Cell 5 extends to the point where the source term solution has been sufficiently reacted that it is in equilibrium with the rock and no further reactions will take place. The first three cells in the profile are in the crushed tuff of the invert. Cell 4 is partly in the invert and partly in the immediately adjacent rock. Cell 5 is completely in the rock. Note that in the first three cells there is a steady decrease in the fraction of void space filled with solids. A sudden increase in cell 4 of the fractures filled is due to a shift in the mineralogy (onset of more solid solutions and low density minerals). A further shift in cell 5 is a combination of changing mineralogy and a different availability of void space (different porosity).

It should be noted that the time for an element of water to go from the beginning of the first layer to the end of the fifth layer (9.65×10^5 days or 2644 years) bears no direct relation to the duration of the ph > 10 condition. This latter can be viewed as the width of a pulse of high fissile concentration and is the determinant of the amount of material accumulated in a given layer, since after the pulse is over there will no longer be sufficient fissile dissolved in the water, or sufficient reaction with the rock, to produce a significant fissile deposit. As explained below these pulse widths are 600, 6000, 300, and 3000 years corresponding to the results presented in Tables 6.1-1,4 respectively, with the 6000 and 3000 years durations being too long to maintain a pH > 10, and are included only to demonstrate (in Section 7, below) that

even such extreme conditions will result in an accumulation of less than that required for criticality by over an order of magnitude.

The total amount of fissile material simulated to be deposited in the invert and rock is only 356 g distributed over the 18 m flow path with most of it concentrated in the first 200 cm (see Figure 6.1-1). Furthermore, the density of fissile material (column 8 of the table) drops off sharply beyond the 3rd cell (layer) so the only deposit which could function in a critical mass is in the first 3 layers, which totals only 70 g of fissile material. Part of the reason for this small amount of fissile material is that throughout the deposition path, the percent of void space predicted to be filled with fissile material is extremely small (less than 0.02% for Table 6.1-1, and never more than 0.08% in the most conservative case of Table 6.1-4, described below, which will be used for comparison with the concentrations found to be critical in Section 7). The highest linear density point (near the top) is calculated to have only about 0.5 g of fissile material in a 1 mm depth distributed over a 5.5 m^2 area.

Table 6.1-1. Deposition from the Reaction of pH 10 Solution from the Immobilized Plutonium Package with a Crushed Tuff Invert for a 600-year Duration of pH 10 Conditions and 1 mm/Yr Infiltration Rate (EQ6 Output File wp10t0a.6o, Ref. 4, Section 9.2)

Cell	Travel Time	Distance	Accumulation During The Deposition Time					% Void	% Void	Fissile
No.	Into Rock	Traveled	Total Solids	Uranium	Plutonium	Fissile	Fissile	Filled With	Filled With	wt% of
	days	mm	grams	grams	grams	grams	g/mm	Solids	Fissile	U+Pu
1	2.19E+03	2.00E+01	1.67E+04	2.60E+02	2.48E+00	1.06E+01	5.30E-01	19.1726%	0.0159%	4.05%
2	5.73E+03	5.23E+01	2.70E+04	4.12E+02	4.11E+00	1.70E+01	5.25E-01	11.8405%	0.0096%	4.09%
3	2.11E+04	1.93E+02	1.17E+05	1.70E+03	1.67E+01	7.00E+01	4.99E-01	14.0116%	0.0108%	4.07%
4	9.65E+04	1.09E+03	5.43E+05	4.51E+01	3.45E+01	3.59E+01	4.00E-02	24.7499%	0.0005%	45.13%
5	9.65E+05	1.82E+04	6.26E+06	0.00E+00	2.22E+02	2.22E+02	1.30E-02	17.0949%	0.0002%	100.00%
Total			6.96E+06	2.42E+03	2.80E+02	3.56E+02				13.18%

6.1.3.1.2 Low flow rate (1 mm/Yr) and 10x nominal duration of high pH

Calculations were made for a factor of 10 increase in the duration of the high pH (10) which would correspond to a factor of 10 decrease in rate constants for the dissolution rate of the HLW glass responsible for the high pH. Such a decrease could represent the uncertainty in the glass dissolution rate, or a reduction in the amount of glass exposed to aqueous attack at any given time, which would amount to a reduction in the "effective dissolution rate." Of course, such a reduction in effective dissolution rate would likely reduce the maximum pH, so maintenance of this high pH for Table 6.1-2 shows the same scenario as Table 6.1-1 but with a deposition pattern for 6000 years duration of high pH and infiltration rate of 1 mm/Yr. The effects of this large increase in pH duration were mitigated in the simulation since the calculations indicate that the flow path would be sealed by deposits after 2400 years. The maximum accumulation of fissile material in the flow path would be less than 0.06% at the highest point. While there would be nearly 1.5 kg of fissile material in the deposit, it would be distributed over the flow path. Over 80% of the total fissile material would be spread out at a low density (Cells 4 and 5), less than 0.2 g/mm and the fraction of voids filled with fissile material would be less than 0.01%. As with the previous case, it will be seen that this fissile mass is much too small to support criticality.

6.1.3.1.3 Higher flow rate (10 mm/Yr) and nominal duration of high pH

A separate dissolution run was made (details given in Section 7.4.2.1.1 of Ref. 4) to investigate what would happen to the duration of the pH level and fissile mass concentrations if the infiltration rate were high. The high-flushing rate run showed that the duration of pH 10 was reduced by half and plutonium and uranium concentrations were reduced by a factor of 5 (Ref. 4). Therefore, if the infiltration rate was 10 mm/Yr, a higher deposition rate would be predicted. However, at such a high infiltration rate, the duration of high pH condition drops to 300 years and results in a lower concentration of fissile mass than for the 1 mm/year case as shown in Table 6.1-3.

6.1.3.1.4 High flow rate (10 mm/Yr) and 10x nominal duration of high pH

If the 10 mm/Yr selection were combined with a factor of 10 increase in pH duration (to 3000 Yr) the result shown in Table 6.1-4 would be obtained. Figure 6.1-2 shows a graphical representation of the buildup of solids and fissile material for the 10 mm/Yr, 3000 Yr case. In this case the voids would be nearly filled but the fraction of voids filled with fissile material would be still less than 0.08% at the highest point, and, while the total amount of fissile material in the deposit would be nearly 18 kg, it is mostly distributed over 190 m of depth, at a very low density. Since this case gives the highest accumulation of fissile material, the result will be used for comparison with the minimum critical masses identified in Section 7, below. The mass actually used for comparison will be 4.9 kg, since this is the total deposited at a reasonably high density, in the first 3 cells (layers) and to a depth of 3.35 meters.

Table 6.1-2. Deposition from the Reaction of pH 10 Solution from the Immobilized Plutonium Package with a Crushed Tuff Invert For a 6000-year Duration of pH 10 Conditions and 1 mm /Yr Infiltration Rate (EQ6 Output File wp10t0a.6o, Ref. 4, Section 9.2).

Cell	Travel Time	Distance	Accumulation During The Deposition Time					% Void	% Void	Fissile
No.	Into Rock	Traveled	Total Solids	Uranium	Plutonium	Fissile	Fissile	Filled With	Filled With	wt% of
	days	mm	grams	grams	grams	grams	g/mm	Solids	Fissile	U+Pu
1	2.19E+03	2.00E+01	6.74E+04	1.05E+03	1.00E+01	4.28E+01	2.14E+00	77.4653%	0.0641%	4.05%
2	5.73E+03	5.23E+01	1.09E+05	1.66E+03	1.66E+01	6.87E+01	2.12E+00	47.8407%	0.0389%	4.09%
3	2.11E+04	1.93E+02	4.74E+05	6.88E+03	6.74E+01	2.83E+02	2.01E+00	56.6130%	0.0437%	4.07%
4	9.65E+04	1.09E+03	2.19E+06	1.82E+02	1.39E+02	1.45E+02	1.62E-01	100.0000%	0.0021%	45.13%
5	9.65E+05	1.82E+04	2.53E+07	0.00E+00	8.98E+02	8.98E+02	5.25E-02	69.0706%	0.0006%	100.00%
Total	N/A	N/A	2.81E+07	9.77E+03	1.13E+03	1.44E+03	N/A	N/A	N/A	13.18%

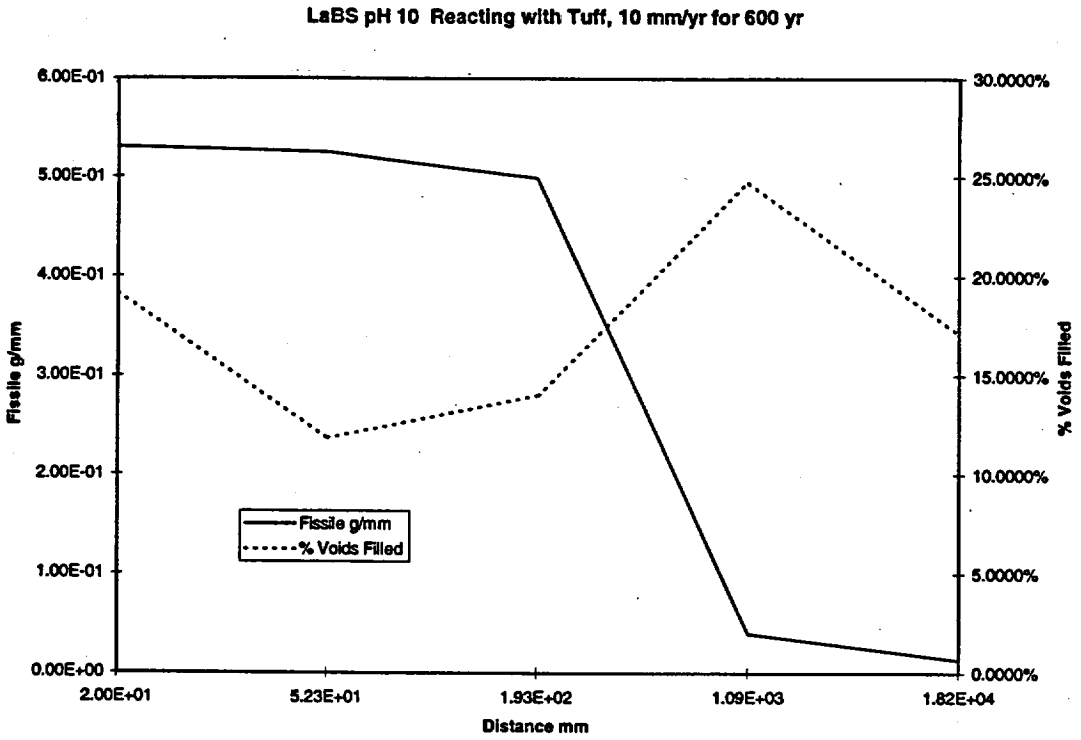

Figure 6.1-1. Amount of Fissile Material and Percentage of Voids Filled for Immobilized Plutonium pH 10 Reacting With Tuff at 1 mm/yr for 600 years.

Table 6.1-3. Deposition from the Reaction of pH 10 Solution from the Immobilized Plutonium Package with a Crushed Tuff Invert for a 10 mm /yr Infiltration Rate and 300 year Deposition Time (EQ6 Output File wp10t0a.6o, Ref. 4, Section 9.2).

Cell	Travel Time	Distance	Accumulation During The Deposition Time					% Void	% Void	Fissile
No.	Into Rock	Traveled	Total Solids	Uranium	Plutonium	Fissile	Fissile	Filled With	Filled With	wt% of
	days	mm	grams	grams	grams	grams	g/mm	Solids	Fissile	U+Pu
1	2.19E+03	2.00E+02	8.35E+04	1.30E+03	1.24E+01	5.30E+01	2.65E-01	9.5863%	0.0079%	4.05%
2	5.73E+03	5.23E+02	1.35E+05	2.06E+03	2.05E+01	8.50E+01	2.63E-01	5.9203%	0.0048%	4.09%
3	2.11E+04	3.35E+03	5.86E+05	8.52E+03	8.34E+01	3.50E+02	1.24E-01	8.7024%	0.0067%	4.07%
4	9.65E+04	1.82E+04	2.71E+06	2.25E+02	1.73E+02	1.80E+02	1.21E-02	7.4133%	0.0002%	45.13%
5	9.65E+05	1.89E+05	3.13E+07	0.00E+00	1.11E+03	1.11E+03	6.49E-03	8.2180%	0.0001%	100.00%
Total	N/A	N/A	3.48E+07	1.21E+04	1.40E+03	1.78E+03	N/A	N/A	N/A	13.18%

Table 6.1-4. Deposition from the Reaction of pH 10 Solution from the Immobilized Plutonium Package with a Crushed Tuff Invert for a 10 mm/yr Infiltration Rate and 3000 year Deposition Time. (EQ6 Output File wp10t0a.6o, Ref. 4, Section 9.2)

Cell	Travel Time	Distance	Accumulation During The Deposition Time					% Void	% Void	Fissile
No.	Into Rock	Traveled	Total Solids	Uranium	Plutonium	Fissile	Fissile	Filled With	Filled With	wt% of
	days	mm	grams	grams	grams	grams	g/mm	Solids	Fissile	U+Pu
1	2.19E+03	2.00E+02	8.35E+05	1.30E+04	1.24E+02	5.30E+02	2.65E+00	95.8628%	0.0794%	4.05%
2	5.73E+03	5.23E+02	1.35E+06	2.06E+04	2.05E+02	8.50E+02	2.63E+00	59.2026%	0.0482%	4.09%
3	2.11E+04	3.35E+03	5.86E+06	8.52E+04	8.34E+02	3.50E+03	1.24E+00	87.0240%	0.0672%	4.07%
4	9.65E+04	1.82E+04	2.71E+07	2.25E+03	1.73E+03	1.80E+03	1.21E-01	74.1326%	0.0015%	45.13%
5	9.65E+05	1.89E+05	3.13E+08	0.00E+00	1.11E+04	1.11E+04	6.49E-02	82.1795%	0.0008%	100.00%
Total	N/A	N/A	3.48E+08	1.21E+05	1.40E+04	1.78E+04	N/A	N/A	N/A	13.18%

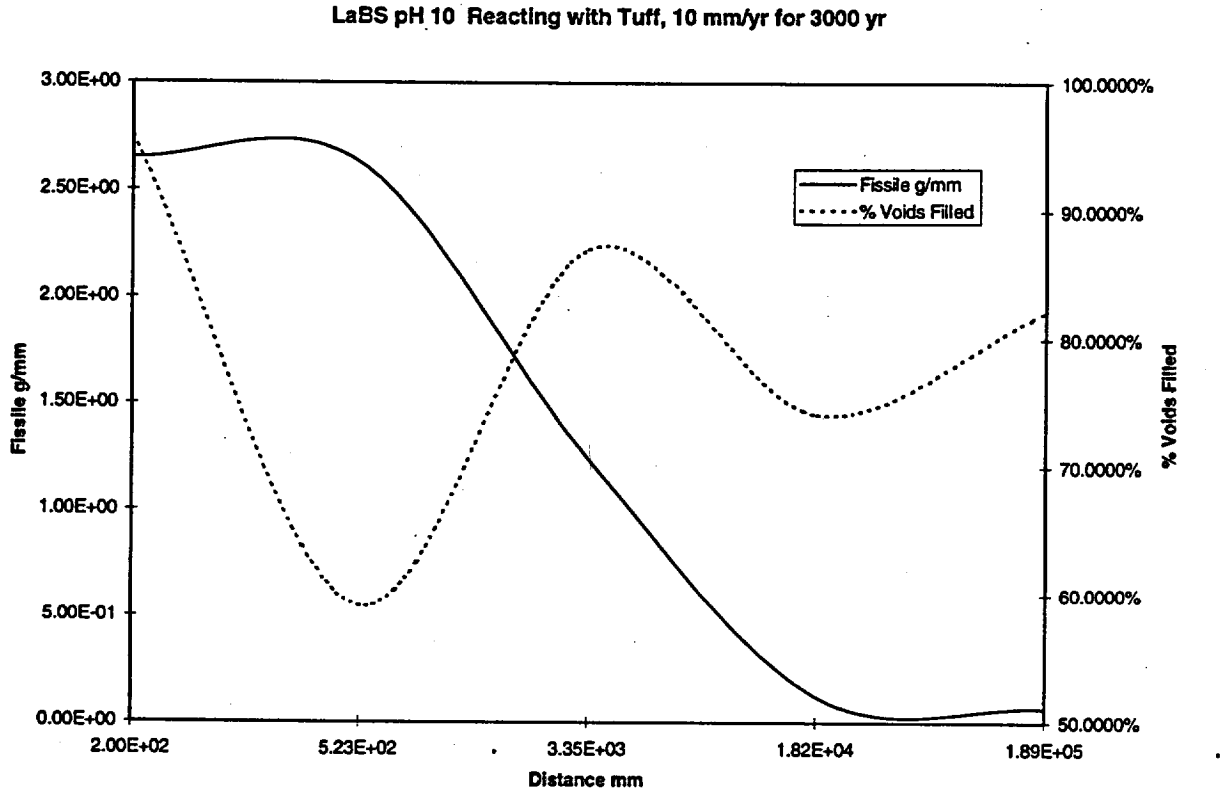

Figure 6.1-2. Amount of Fissile Material and Percentage of Voids Filled for Immobilized Plutonium pH 10 Reacting With Tuff at 10 mm/yr for 3000 years.

6.1.3.1.5 Sensitivity to alternative assumptions

Some Pu decayed to U

The chemistry modeling results discussed above do not account for further decay of ^{239}Pu to ^{235}U. The duration of 6000 years would be about 1/4 the half-life, and some significant amount of plutonium will have become uranium. This will likely increase the fissile contents by some small amount since more uranium tends to deposit than plutonium. The effect of decay would not be sufficient to change the likelihood of any criticality condition.

Simulation of continuous flow with discrete passes

Studies were done to explore whether the presence of reaction products from the first pass would have a significant effect on the behavior of the second pass fluid, etc. The original modeling scheme considered the need to model each pass if necessary (see Attachment III of Ref. 4 for detailed discussion of modeling scheme). Table 6.1-5 shows the deposition pattern for the two subsequent passes in cell 2. During the course of the three passes, 1.929E-02 g of fissile material would be deposited in 24.1 g of altered tuff, which amounts to 0.08 wt%. The simulated deposition history for this material was 5.13E-03 g during the first pass, a rather larger amount on the second pass, 8.67 E-03 g, but less again during the third pass, 5.50E-03 g. Whereas additional passes were not done, it is expected that the amounts precipitated per pass will continue to decrease because the alteration of the tuff will make it less reactive. In other words the chemistry is expected to permit only one maximum amount deposited per pass. The amount of solids that do not contain fissile material also increases; this increase is sufficient that the percentage of fissile material in the deposited solids decreases with each successive pass.

Thus, gradually the tuff invert would be converted to altered material, mostly quartz and feldspar, with a fissile content amounting to less than 0.1 wt%. Because cells deeper than cell 2 would already be partially altered before the fissile bearing solution could reach them, the amount of reaction, hence amount of precipitated U and Pu, would be smaller, i.e. less than 0.1 wt%. The chemical calculations do not permit modeling the geometry. In fact it would be difficult to establish the ratio of reactive solution to invert and the manner of contact between them. This means that the cells may be layers that develop on crushed tuff fragments, or altered pieces of tuff that lie above others, or, more likely, some combination of both. The results indicate some small increase in fissile material but it would not be a significant increase in terms of criticality concerns. This result confirms the results of Lichtner (Refs. 8 and 9) that were discussed in Section 7.2.1 of Ref. 4.

Table 6.1-5. Deposition in Cell 2 From Three Passes for Reaction of Immobilized Plutonium pH 10 Solution With Crushed Tuff

	Uranium	Plutonium	Total Solids	Fissile	Fissile
	grams	grams	grams	grams	wt% of U+ Pu
Pass 0	1.24E-01	1.24E-03	8.14E+00	5.13E-03	4.0877%
Pass 1	3.36E-01	3.29E-03	1.80E+01	1.38E-02	4.0686%
Pass 2	4.70E-01	4.58E-03	2.41E+01	1.93E-02	4.0660%
(Each "pass" has one kg of water flowing through the system).					

Whereas subsequent to deposition of Pu or U it would be conceivable that through-flowing water could dissolve the minerals of the invert faster than the fissile solids, leaving behind a residual concentration, the modeling scheme and results described above provide no hint that this will in fact occur. Moreover, the simulation indicates that 90% or more of the invert would need to be dissolved even to reach a 1 wt% concentration of fissile material. This would be highly unlikely in view of the low solubility of the clay minerals, quartz, and feldspar.

Large surface area

As was discussed above, a special case with a large surface area of reactants (to model an extremely high degree of fracturing) was also run. Table 6.1-6 presents the Large Area results for a deposition history of 600 years and 1 mm/Yr infiltration rate. The depositions occur much sooner (near the entrance to the invert) than for the base case. The change in area (and thus the effective reaction rate) seems only to change the position, not the composition, of the deposited material. This would be expected since the relative rates for the reactants has not changed, only the overall rate. Because the deposits occur over a shorter distance, they soon plug the flow path (in less than 6 years). This results in diversion of flow and consequent spreading out of the deposit over a larger area. Thus, the result would be even less likely to cause a significant accumulation than the smaller surface area case.

Table 6.1-6. Large Area Case for Reaction of pH 10 Immobilized Plutonium Package Effluent with Crushed Tuff Invert, 600 year Duration of pH 10 and 1 mm/Yr Infiltration Rate (EQ6 Output File wp10t01a.6o, Ref. 4, Section 9.2)

Cell	Travel Time	Distance	Accumulation During The Deposition Time					% Void	% Void	Fissile
No.	Into Rock	Traveled	Total Solids	Uranium	Plutonium	Fissile	Fissile	Filled With	Filled With	wt% of
	dayss	mm	grams	grams	grams	grams	g/mm	Solids	Fissile	U+Pu
1	1.10E+01	1.01E-01	4.38E+02	6.72E+00	6.61E-02	2.76E-01	2.75E+00	99.9999%	0.0838%	4.07%
2	3.82E+01	3.49E-01	1.03E+03	1.57E+01	1.54E-01	6.45E-01	2.37E-02	71.4143%	0.0564%	4.07%
3	1.75E+02	1.60E+00	5.13E+03	4.26E+01	3.26E-01	3.39E-01	2.49E-03	73.9871%	0.0015%	45.13%
4	1.75E+03	1.60E+01	5.91E+04	0.00E+00	2.10E+00	2.10E+00	1.33E-03	85.3051%	0.0007%	100.00%
Total	N/A	N/A	6.57E+04	2.28E+01	2.64E+00	3.36E+00	N/A	N/A	N/A	13.18%

Multiple package effects

It has been suggested that the effects of source terms from multiple packages could increase the accumulation of fissile material. The analyses of Section 6.1.3 generally, and the previous paragraph in particular, show that a local accumulation of fissile material is limited primarily by the geologic formation, not the amount of material available from the source term over some period of time. Furthermore, the packages with immobilized plutonium or highly enriched uranium will be spaced far apart (with many low enriched SNF packages in between). These limitations will be further quantified for license application.

6.1.3.1.6 Chemical changes resulting from reaction of tuff with the pH 10 solution exiting the immobilized plutonium waste package

In the reaction between the alkaline effluent and tuff, the controlling factors for the system appear to be the sodium and carbonate solution content conditions. During the passage of fluid, the pH change would be minor but decreasing. The carbonate species result from the presence of atmospheric levels of CO_2 in the repository air which would be in contact with the solution. The dominant carbonate solution species (which would be typical for the various runs), is CO_3^{--} . The dominant aqueous species for U and Pu are the carbonate complexes:

$UO_2(CO_3)_3^{4-}$

$PuO_2(CO_3)_3^{4-}$

Seven reactions involving aqueous Pu and U consume H^+ and one such reaction generates H^+. In addition the carbonate system promotes a large buffering capacity. The consumption of H^+ by the tuff dissolution processes coupled with the combining of H^+ with aqueous species is compensated by the generation of H^+ from processes forming Pu and U solids. The pH remains nearly constant owing to buffering by the reaction:

$CO_3^{--} + H^+ = HCO_3^-$

The U solid formation reaction, in terms of EQ6 basis species, is:

$$4Na^+ + 3HCO_3^- + UO_2^{++} = Na_4UO_2(CO_3)_3 + 3H^+$$

This shows the precipitation of UO_2^{++} as $Na_4UO_2(CO_3)_3$ solid would be dependent on the fourth power Na^+ and the third power HCO_3^- solution content. Furthermore, the dissolution of $Na_4UO_2(CO_3)_3$ would be dependent on the third power of the H^+ solution content. Generation of H^+ would drive this reaction in the direction which would dissolve $Na_4UO_2(CO_3)_3$. However, the generation of the H^+ is not significant compared to the influence of the Na, especially in view of the buffering of the pH by the carbonate-bicarbonate system. Generation of HCO_3^- would drive the reaction to form $Na_4UO_2(CO_3)_3$ solid. The HCO_3^- solution content decreases as the reaction proceeds, which would be expected to promote dissolution of $Na_4UO_2(CO_3)_3$. Since $Na_4UO_2(CO_3)_3$ solid does form, HCO_3^- cannot be a dominant driving force for $Na_4UO_2(CO_3)_3$ formation under the constant CO_2(g) pressure conditions (assumed in the modeling to apply to the repository system). However, as discussed below, the generation of Na^+ can be a significant driving force.

The dominant aqueous species in the high pH effluent-tuff system would be $UO_2(CO_3)_3^{---}$. Therefore the following set of reactions applies to the formation of $Na_4UO_2(CO_3)_3$ solid:

$$4Na^+ + 3HCO_3^- + UO_2^{++} = Na_4UO_2(CO_3)_3 + 3H^+$$
$$UO_2(CO_3)_3^{---} + 3H^+ = UO_2^{++} + 3HCO_3^-$$

$$4Na^+ + UO_2(CO_3)_3^{---} = Na_4UO_2(CO_3)_3$$

Here, in terms of the net reaction, the formation of $Na_4UO_2(CO_3)_3$ solid would be dependent on the fourth power of the solution Na^+ content.

The Pu solid formation reaction, in terms of EQ6 basis species, is:

$$Pu^{++++} + 2H_2O = PuO_2 + 4H^+$$

Here the PuO_2 dissolution would be dependent on the fourth power of the H^+ solution content. Generation of H^+, if it underwent a significant concentration increase, would drive the reaction to dissolve PuO_2 solid. However, the dominant Pu species in solution is $PuO_2(CO_3)_3^{---}$ not Pu^{++++}. Therefore, the following set of reactions apply to the formation of PuO_2 solid:

$$PuO_2(CO_3)_3^{---} + 3H^+ = PuO_2^{++} + 3HCO_3^-$$

$$PuO_2^{++} + 2H^+ = Pu^{++++} + 0.5O_2(g) + H_2O$$

$$Pu^{++++} + 2H_2O = PuO_2 + 4H+$$

$$\overline{PuO_2(CO_3)_3^{---} + H^+ + H_2O = PuO_2 + 3HCO_3^- + 0.5O_2(g)}$$

Whereas subsequent to deposition of Pu or U it is conceivable that through flowing water could dissolve the minerals of the invert faster than the fissile solids, leaving behind a residual concentration. The modeling scheme and results described above provide no hint that this will in fact occur. Moreover, the simulation indicates that 90% or more of the invert would need to be dissolved even to reach a concentration of fissile material of 1%. This is highly unlikely in view of the low solubility of the clay minerals, quartz, and feldspar.

6.1.3.2 Reaction of pH 7 solution, from the immobilized Pu waste package, with crushed tuff invert

The same analysis was done for the pH 7 solution as was done for the pH 10 solution. The results are documented in EQ6 output file "wp7t0.6o" (Ref. 4, Section 9.2). The EQ6 calculations showed that no uranium or plutonium was deposited by the solution. The dissolved uranium and plutonium are instead carried out of the system by the flowing water. Some alteration of the tuff occurred but this did not foster any deposition of fissile material. No further analysis was performed.

These results indicated that no pH 7 solution from any of the waste packages is likely to produce a deposit of any uranium or plutonium in the invert or rock when it reacts with tuff. Based on this, all other modeling of pH 7 solutions was suspended.

6.1.3.3 Reaction of pH 5 solution, from the immobilized Pu waste package, with crushed tuff invert

Modeling of the source term (described in Section 5.3, above) shows a pH 5 solution could last for at least 8000 years (the minimum duration of the stainless steel corrosion process). Modeling of the reaction of this solution with crushed tuff was also carried out. The results are documented in EQ6 output file "wp5t0.6o" (Ref. 4, Section 9.2). Table 6.1-7 shows how a deposit will build up for a 1 mm/Yr infiltration rate. A large deposit of alteration products would be produced which plugs the flow path about 22 cm into the invert after about 2440

years. At the time the flow path is plugged, a 1.5E+04 kg deposit has formed which contains a total of only 0.0016 g of fissile material. The fraction of voids filled with fissile material would be then less than 0.0001%. At higher infiltration rates the results are of course the same: plugged path at 2440 years. This reaction will not produce a significant accumulation of fissile material and will not result in any criticality.

Table 6.1-7. Deposition Resulting from Reaction of Immobilized Plutonium pH 5.5 Solution With Crushed Tuff Invert, 1 mm/Yr Infiltration Rate, 2440 year Deposition (EQ6 Output File wp5t0.6o, Ref. 4, Section 9.2).

Cell	Travel Time	Distance	Accumulation During The Deposition Time					% Void	% Void	Fissile
No.	Into Rock	Traveled	Total Solids	Uranium	Plutonium	Fissile	Fissile	Filled With	Filled With	wt% of
	days	mm	grams	grams	grams	grams	g/mm	Solids	Fissile	U+Pu
1	3.84E-03	3.51E-05	1.92E-02	0.00E+00	0.00E+00	0.00E+00	0.00E+00	9.8572%	0.0000%	0.00%
2	3.84E+03	3.51E+01	1.24E+05	5.10E-04	0.00E+00	1.60E-05	4.55E-07	75.6864%	0.0000%	3.13%
3	1.53E+05	2.20E+03	4.70E+06	1.77E-02	2.54E-05	5.78E-04	2.67E-07	100.0000%	0.0000%	3.27%
4	5.01E+05	9.07E+03	1.03E+07	2.85E-02	6.34E-05	9.57E-04	1.39E-07	55.5012%	0.0000%	3.34%
Total			1.51E+07	4.67E-02	8.88E-05	1.55E-03				100.00%

6.1.4 Reaction of Immobilized Plutonium Package Solutions with Concrete or Grout

This section presents results of modeling analyses of the reaction of immobilized plutonium solutions with a concrete or grout invert.

The composition for the cement was put into the form of a "special reactant" for input to EQ6 and the code run to ascertain the likely makeup of the cement at long times in the presence of J-13 well water and atmospheric CO_2. For this purpose, rates of reaction were not needed; it was instead assumed that over the time frame of a few thousand years before waste package breach the cement would have reacted to equilibrium with the water and atmosphere. This degraded cement, which contained mostly calcite with lesser amounts of clay minerals, zeolites, and quartz, was then combined with an appropriate proportion of crushed tuff as aggregate. Because the silicate minerals, or glass, of the tuff react much more slowly than cement, it was assumed that the tuff aggregate would not have changed before waste package breach. It was also assumed that the organic components added to the cement would all have decayed or altered to inorganic compounds, such as CO_2 and water, before waste package breach. Consequently, the organics were not included in the chemistry for modeling the degradation of the cement. The size distribution of the aggregate was taken from Ref. 6, pp. 2 and 3. These data were used to estimate the surface area of aggregate needed for modeling the rates of reaction. Attachment I of Ref. 4 shows the details of this calculation. The chemical and mineralogical compositions of the tuff were the same as described in Section 4.1.3 of Ref. 4. Table 7.4.2-8 of Ref. 4 provides details of the composition, masses, surface areas, and corrosion or degradation rates of the cement and aggregate, and physical parameters for the concrete.

6.1.4.1 Reaction of Immobilized Plutonium pH 10 Solution With Concrete

The reaction of the immobilized plutonium pH 10 solution with a concrete invert was also investigated. The results are documented in the EQ6 output file "LaBSconcrete1simp7.6o" (see Section 9.2 of Ref. 4). This was a difficult case to obtain results in EQ6 largely because of the low reactivity between the alkaline solution and the alkaline concrete. About 77 grams of solid are produced per kg of water reacted with no uranium in the deposit. The solid contains less than 0.001% plutonium. The pH 10 condition lasts for 600 years and the flow cross section would be 5.52E+04 cm^2. Based on this, there would be 33 kg of water contacting the solid during the pH 10 period. This gives 2.55 kg of solid containing less than 0.03 g of Pu and no uranium. No further analysis was carried out because it was clear that this mechanism would produce no significant deposit of fissile material over any realistic time frame.

6.1.4.2 Reaction of Immobilized Plutonium pH 5 Solution With Concrete

The reaction of the immobilized plutonium pH 5 solution with a concrete invert was also investigated. The results are documented in the EQ6 output file "LaBSconcrete5t0.6o" (see Section 9.2 of Ref. 4). This was a difficult case to obtain results in EQ6 largely because of the low reactivity between the solution and the concrete. About 200 grams of solid are produced per kg of water reacted. In these solids there is no uranium and only 6.8 E-09 g of plutonium. At an infiltration rate of 1 mm/Yr with a flow cross section (package footprint) of 5.52E+04 cm^2 and an 8000-Yr duration of pH 5 conditions, the total amount of water reacting is 440 kg. Therefore about 88 kg of solid would be deposited containing 2.9E-06 g of plutonium and no uranium. If the flow were intermittent (unsteady of a steady 1 mm/Yr) the total amount, and composition, of solid deposited would be approximately the same as for the steady flow, but the process would take correspondingly longer. (Therefore, the steady state is conservative by comparison with the intermittent case.) No further analysis of the as carried out because it was clear that this mechanism would produce no significant deposit of fissile material over any realistic time frame.

6.1.4.3 Reaction of Immobilized Plutonium pH 7 Solution With Concrete

Based on the results obtained with tuff reactions modeling of this case was suspended. It is not expected that any effect will be obtained from reaction of a neutral solution such as this with concrete.

6.1.5 MOX Reactions with Concrete and Crushed Tuff

This section presents the results of modeling of the reaction of the source term from a MOX waste package with the materials most likely to be encountered in the volume immediately beneath the waste package.

6.1.5.1 Reaction of MOX pH 4 Solution With Crushed Tuff Invert

A pH 4 solution is calculated to flow from the dissolving MOX package contents for about 50 years. The reaction of this solution with the crushed tuff invert was modeled. Cells 1 and 2 were combined for these evaluations because the distance traveled in cell 1 was < 1 μm.

The results for a 1 mm/Yr infiltration rate are summarized in Table 6.1-8. A very large quantity of solid would be formed over a 286 mm path in the invert. This solid contains only about 0.38 g of fissile material over the entire path and fills less than 3% of voids at the highest point of accumulation. Figure 6.1-3 shows the pattern of fissile mass accumulation and the filling of the voids. Most of the material would be located in the first mm of the invert but it does not represent a significant amount of fissile material.

Table 6.1-8. Deposition from the Reaction of MOX Package pH 4 Solution with Tuff Invert, 1 mm/Yr Infiltration Rate for 50 years (EQ6 Output File wpmox4t0.6o, Ref. 4, Section 9.2).

Cell	Travel Time	Distance	Accumulation During The Deposition Time					% Void	% Void	Fissile
No.	Into Rock	Traveled	Total Solids	Uranium	Plutonium	Fissile	Fissile	Filled With	Filled With	wt% of
	days	mm	grams	grams	grams	grams	g/mm	Solids	Fissile	U+Pu
1 & 2	3.84E+02	3.51E+00	5.86E+02	2.27E+02	0.00E+00	3.81E-01	1.09E-01	2.6439%	0.0015%	0.168%
3	1.53E+03	1.40E+01	1.40E+03	2.15E+00	3.50E-04	3.96E-03	3.78E-04	1.4075%	0.0000%	0.184%
4	6.09E+03	5.56E+01	3.44E+03	1.62E-02	2.29E-05	5.01E-05	1.20E-06	1.0121%	0.0000%	0.309%
5	3.13E+04	2.86E+02	1.90E+04	0.00E+00	1.06E-06	1.06E-06	4.60E-09	1.1675%	0.0000%	100.000%
Total			2.45E+04	2.30E+02	3.74E-04	3.85E-01				

If the dissolution rates in the package were overestimated by a factor of 10, the pH 4 condition could persist for as much as 500 years. This case is shown in Table 6.1-9 and is plotted in Figure 6.1-4. More than 4 kg of solid material accumulates in the top 3.5 mm of the invert filling about 26% of the void space at the highest point. But the total fissile material in this region is less than 4 g. The total fissile material in the whole deposit (spread over a 286 mm depth) is only 3.9 g. If the infiltration were 10 mm/Yr and the pH were 10 for 500 years, this total would be 39 g. As previously discussed, the flushing effects at 10 mm/Yr would greatly reduce the time of pH 10 and the fissile material concentrations so that the 39 g figure would be considerably less. Therefore, even in the largest bounding cases, this reaction does not produce a significant quantity of fissile material.

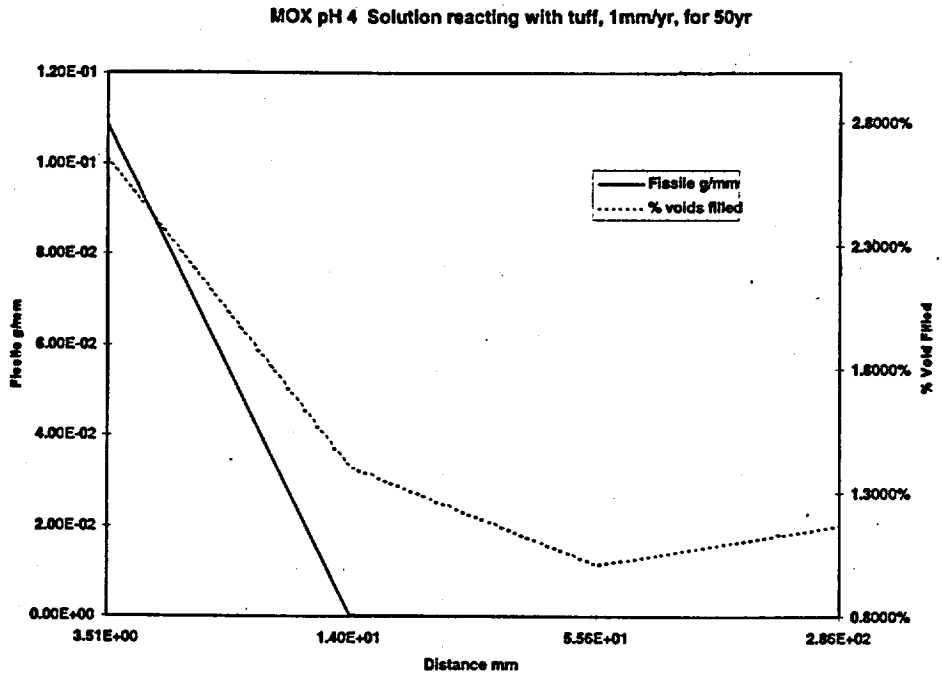

Figure 6.1-3. Amount of Fissile Material and Percentage of Voids Filled for MOX pH 4 Reacting With Tuff at 1 mm/Yr for 50 years

Table 6.1-9. Deposition from the Reaction of MOX Package pH 4 Solution With Tuff Invert, 1 mm/Yr Infiltration Rate for 500 years (EQ6 Output File wpmox4t0.6o, Ref. 4, Section 9.2).

Cell	Travel Time	Distance	Accumulation During The Deposition Time					% Void	% Void	Fissile
No.	Into Rock	Traveled	Total Solids	Uranium	Plutonium	Fissile	Fissile	Filled With	Filled With	wt% of
	days	mm	grams	grams	grams	grams	g/mm	Solids	Fissile	U+Pu
1 & 2	3.84E+02	3.51E+00	5.86E+03	2.27E+03	0.00E+00	3.81E+00	1.09E+00	26.4390%	0.0147%	0.168%
3	1.53E+03	1.40E+01	1.40E+04	2.15E+01	3.50E-03	3.96E-02	3.78E-03	14.0750%	0.0000%	0.184%
4	6.09E+03	5.56E+01	3.44E+04	1.62E-01	2.29E-04	5.01E-04	1.20E-05	10.1211%	0.0000%	0.309%
5	3.13E+04	2.86E+02	1.90E+05	0.00E+00	1.06E-05	1.06E-05	4.60E-08	11.6751%	0.0000%	100.000%
Total			2.45E+05	2.30E+03	3.74E-03	3.85E+00				

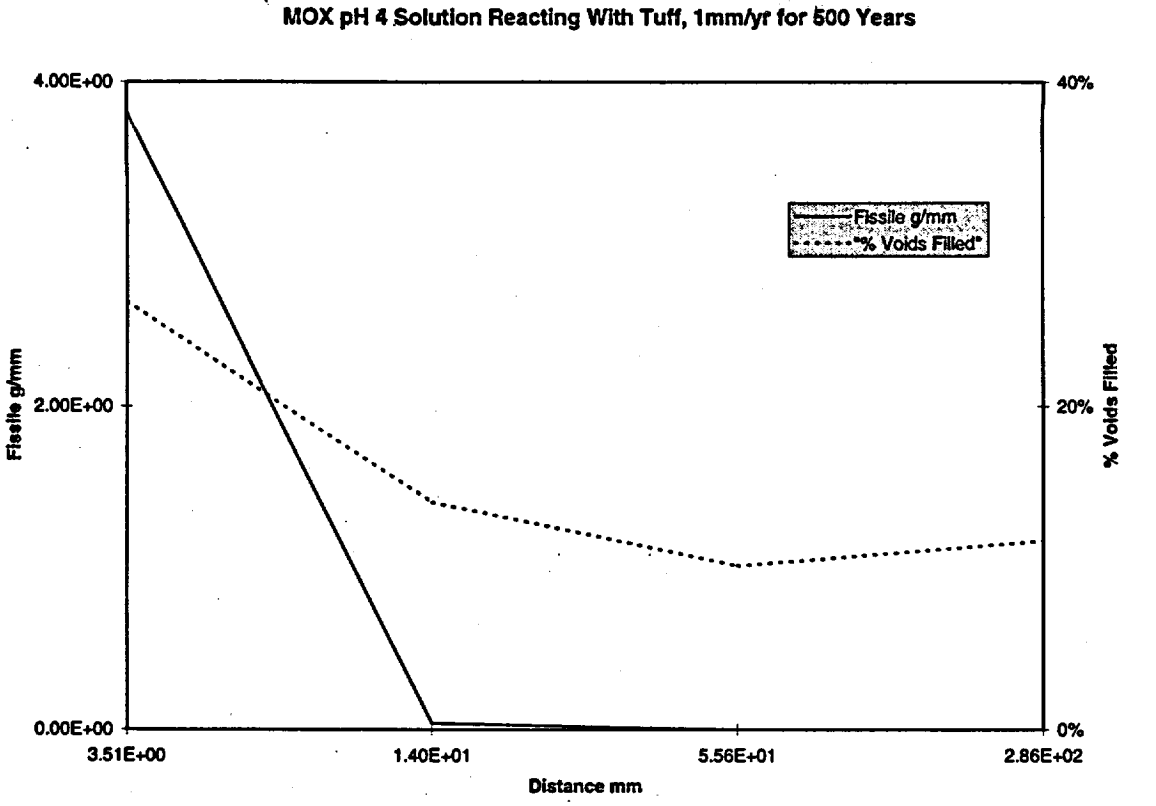

Figure 6.1-4. Amount of Fissile Material and Percentage of Voids Filled for MOX pH 4 Reacting With Tuff at 1 mm/yr for 500 years

6.1.5.2 Reaction of MOX pH 7 Solution With Tuff Invert

This case was not run because the results with neutral solutions for the immobilized plutonium package indicated that little or no fissile material would be formed from any neutral solutions.

6.1.5.3 Reaction of MOX pH 4 Solution With Concrete

Based on results obtained for immobilized plutonium and the results for pH 4 with tuff this case was not run since no significant deposition of fissile material would be expected.

6.1.5.4 Reaction of MOX pH 7 Solution With Concrete

This case was not run because the results with neutral solutions for the Immobilized Plutonium package indicated that little or no fissile material would be formed from any neutral solutions.

6.1.6 Reaction of pH 10 Source Term With Carbon Steel

As discussed in Sections 4.2.3 and 6.1.2, above, it is possible for carbon steel to act as a reducing agent for uranium or plutonium in solution, and hence to cause precipitation which, over time, leads to accumulation of the fissile material.

This scenario includes the existence of altered steel fragments in a pool of water below the waste package. If the pool is sufficiently deep, a no or low free oxygen condition may be maintained. The cases investigated covered a range of oxygen contents of the water ranging from a completely anoxic condition to atmospheric oxygen content. For simplicity, and conservatism, the carbon steel fragments were modeled as simply fragments of iron in the pool. These fragments would act as a reducing agent to the solution entering especially if there was a limited oxygen supply. The deposit is envisioned as a slab covering the bottom of the pond in the footprint of the package. The model visualizes a slab forming on the layer of steel fragments forming a slab at the bottom of the pond. The thickness of such a slab is calculated.

6.1.6.1 Reaction of pH 10 Source Term With Carbon Steel With No Gaseous Oxygen Present

This case was investigated because of the potential for precipitation of fissile material due to direct reduction of uranium and plutonium species by the iron in an anoxic environment.

The simulations indicate the oxygen fugacity is never lowered enough to reduce the uranium to where it would precipitate. However, at a 10 mm/Yr infiltration rate, a significant amount of plutonium is simulated to be reduced and precipitated reaching equilibrium in about 3 years as the fluid contacts the iron. Table 6.1-10 shows the simulated accumulated deposit for various infiltration rates. At 10 mm/Yr, the pH condition will last about 300 years. For this case, the deposit was calculated to contain nearly 1.5 kg of fissile material (all as PuO_2). However, note that the concentrations would probably be reduced by a factor of 5 due to flushing effects during dissolution at this very high infiltration rates. Thus the deposit is likely to contain about 500 g of Pu. The slab scenario views the deposit as a very thin (0.05 mm) slab. However, if the steel fragments were more local the deposit could be much thicker with a smaller areal extent (approaching a cube or sphere). In any case this extreme bounding case should not pose a criticality concern since the minimum critical thickness of an optimal fissile solution is 5.5 cm for ^{239}Pu and 4.9 cm for ^{235}U (Table 3.2-1).

Table 6.1-10. Deposition from Reaction of pH 10 Solution from the Immobilized Plutonium Package with Carbon Steel Fragments with No Gaseous Oxygen Present (Anoxic Condition)

Deposition	Infiltration Rate	Accumulation For The Deposition Period				Fissile	Slab Deposit**
Time Yr*	mm/Yr	Total Solids	Uranium	Plutonium	Fissile	wt% of	Thickness
		grams	grams	grams	grams	U+Pu	cm
600	1.00E-01	4.73E+01	.0	2.94E+01	2.94E+01	100.00%	1.10E-04
600	1.00E+00	4.73E+02	0	2.94E+02	2.94E+02	100.00%	1.10E-03
400	5.00E+00	1.58E+03	0	9.81E+02	9.81E+02	100.00%	3.65E-03
300	1.00E+01	2.36E+03	0	1.47E+03	1.47E+03	100.00%	5.48E-03
*	Equals the duration of pH 10 condition which is less at higher infiltrations due to flushing effects.						
**	The deposit is viewed as a slab of this thickness spread out over an area = to the package footprint. The deposit could be accumulated in a smaller area (where there is iron).						

As with other cases, the possibility that the pH 10 condition could endure longer was investigated. Table 6.1-11 shows results if the duration of pH 10 conditions should last 10 times longer. In this case, large quantities of Pu are formed even at 1 mm per year infiltration rates. A deposit of 14.7 kg of PuO_2 (about 10% of the total Pu in the package) in a slab 0.5 mm thick is shown for a 10 mm/Yr infiltration rate. This mass of Pu could be a significant

criticality concern if optimally configured. However, as noted in the previous paragraph, thin slab accumulations such as these would be subcritical. Even considering flushing effects this would still represent nearly 5 kg of Pu and would be a definite criticality concern. However, anoxic conditions are probably not realistic for a duration of 3000 years due to diffusion of oxygen into the system. Such long times are likely to permit the water to be oxygenated to an extent which would permit the oxygen to tie up the reducing sites on the iron.

Table 6.1-11. Deposition from Reaction of pH 10 Solution from the Immobilized Plutonium Package with Carbon Steel Fragments with No Gaseous Oxygen Present (Anoxic Condition) - Long Duration of pH 10

Deposition Time	Infiltration Rate	Accumulation For The Deposition Period				Fissile	Slab Deposit**
Yr*	mm/Yr	Total Solids	Uranium	Plutonium	Fissile	wt% of	Thickness
		grams	grams	grams	grams	U+Pu	cm
6000	1.00E -01	4.73E+02	0	2.94E+02	2.94E+02	100.00%	1.10E-03
6000	1.00E+00	4.73E+03	0	2.94E+03	2.94E+03	100.00%	1.10E-02
4000	5.00E+00	1.58E+04	0	9.81E+03	9.81E+03	100.00%	3.65E-02
3000	1.00E+01	2.36E+04	0	1.47E+04	1.47E+04	100.00%	5.48E-02
* Equals the duration of pH 10 condition which is less at higher infiltrations due to flushing effects.							
** The fissile deposit is viewed as a slab of this thickness spread out over an area = to the package footprint.							
The deposit could be accumulated in a smaller area (where there is iron).							

6.1.6.2 Reaction of pH 10 Source Term With Carbon Steel With 10% Normal Level of Gaseous Oxygen

The interaction of the solution with steel fragments was also investigated for the case where there are small amounts of oxygen present (10% of atmospheric). The results are shown in Table 6.1-12. In this case plutonium is not reduced as with the anoxic case. The iron oxidizes and the pH gradually increases. The time for complete reaction with the iron (equilibrium) is approximately 2000 years. In such a case the water may flush out of the pond before significant reaction. In the model, the water does react with the steel, which is probably a very conservative scenario. The principal uranium product in the simulation is $Na_4UO_2(CO_3)_3$ which is a small percentage of a very large accumulation of minerals (the uranium metal represents about 0.2% of the total weight of solid). At an infiltration rate of 10 mm/Yr there is a kg of fissile material in a slab which is 63 cm thick. There are several problems with the result in view of the scenario:

1. The slab is so thick that the iron would long have been masked from the solution and reaction rates would likely have become near zero early in the process.

2. The slab is so thick as to have displaced all the water from the pond and the steel under the slab would have reacted with all the oxygen dissolved in the interstitial water in the slab, or, if the pore water has dried up, been exposed to enough atmospheric moisture that all the steel has corroded. In either case the 10% oxygen assumption is not valid.

3. The 2000 year reaction time is almost 10 times longer than the calculated duration of the pH condition.

4. The amount of iron required to produce the deposit is 9.3E+06 g. The total mass of the corrosion allowance vessel is 8.2E+06 g. Therefore it would take more than all the iron available to produce the deposit.

In view of all of these improbable or even impossible occurances, the result is viewed as not realistic.

Table 6.1-12. Deposition from Reaction of pH 10 Solution from the Immobilized Plutonium Package with Carbon Steel Fragments with 10% of Normal Atmospheric Gaseous Oxygen Level, Expected Duration of pH Condition

Deposition Time		Accumulation For The Deposition Period				Fissile	Slab Deposit**
Yr*		Total Solids	Uranium	Plutonium	Fissile	wt% of	Thickness
		grams	grams	grams	grams	U+Pu	cm
600	1.00E-01	2.96E+05	6.33E+02	2.82E-01	2.01E+01	3.17%	1.26E+00
600	1.00E+00	2.96E+06	6.33E+03	2.82E+00	2.01E+02	3.17%	1.26E+01
400	5.00E+00	9.86E+06	2.11E+04	9.41E+00	6.70E+02	3.17%	4.19E+01
300	1.00E+01	1.48E+07	3.16E+04	1.41E+01	1.00E+03	3.17%	6.28E+01

* Equals the duration of pH 10 condition which is less at higher infiltrations due to flushing effects.

** The deposit is viewed as a slab of this thickness spread out over an area = to the package footprint.
The deposit could be accumulated in a smaller area (where there is iron).

Table 6.1-13 shows the result if the duration of pH 10 is increased by a factor of 10. At infiltration rates of 5 mm/Yr and above the modeling results would indicate that the entire uranium inventory of the package (1.32E+02 moles) is seen as deposited on the steel as $Na_4UO_2(CO_3)_3$ (7.15e+04 g). In view of the conflict between the result and requisite conditions (see discussion above), the result is not considered realistic.

Table 6.1-13. Deposition from Reaction of pH 10 Solution from the Immobilized Plutonium Package with Carbon Steel Fragments with 10% of Normal Atmospheric Gaseous Oxygen Level, Duration of pH Condition Increased by a Factor of 10

Deposition Time	Infiltration Rate	Accumulation For The Deposition Period				Fissile	Slab Deposit***
Yr	mm/Yr	Total Solids	Uranium	Plutonium	Fissile	wt% of	Thickness
		grams	grams	grams	grams	U+Pu	cm
6000*	1.00E-01	2.96E+06	6.33E+03	2.82E+00	2.01E+02	3.17%	1.26E+01
6000*	1.00E+00	2.96E+07	6.33E+04	2.82E+01	2.01E+03	3.17%	1.26E+02
1356**	5.00E+00	3.34E+07	7.15E+04	3.19E+01	2.27E+03	3.17%	1.42E+02
678**	1.00E+01	3.34E+07	7.15E+04	3.19E+01	2.27E+03	3.17%	1.42E+02

* Equals the duration of pH 10 condition which is less at higher infiltrations due to flushing effects.

**Uranium supply in the package is used up before pH condition is over.

*** The deposit is viewed as a slab of this thickness spread out over an area = to the package footprint.
The deposit could be accumulated in a smaller area (where there is iron).

6.1.6.3 Reaction of pH 10 Source Term With Carbon Steel With Atmospheric Levels of Gaseous Oxygen

The reaction of the solution with steel under atmospheric conditions was also investigated. Table 6.1-14 shows the results. The time to equilibrium was only about 3 years. No uranium was precipitated and small quantities of plutonium were precipitated. At the highest infiltration rate there was only 243 g of fissile material (all PuO_2) in a slab 89 cm thick. This large thickness conflicts with the scenario. If the slab were this thick, the solution would be completely isolated from the steel. This would be the case for a very long time and reaction rates would have fallen to near zero early in the process. Such a large slab would divert all the water away from the region early in the process. The case of a longer pH 10 duration produces a 1 kg quantity of fissile material (all PuO_2) but it is contained in a 4.5 m thick slab containing 1.3E+05 kg of deposit. This result is even more implausible than the shorter duration case.

Table 6.1-14. Deposition from Reaction of pH 10 Solution from the Immobilized Plutonium Package with Carbon Steel Fragments with Normal Atmospheric Gaseous Oxygen Level

Deposition Time	Infiltration Rate	Accumulation For The Deposition Period				Fissile	Slab Deposit**
Yr*	mm/Yr	Total Solids grams	Uranium grams	Plutonium grams	Fissile grams	wt% of U+Pu	Thickness cm
600	1.00E-01	2.58E+05	0	2.43E+00	2.43E+00	100.00%	8.91E-01
600	1.00E+00	2.58E+06	0	2.43E+01	2.43E+01	100.00%	8.91E+00
600	5.00E+00	1.29E+07	0	1.22E+02	1.22E+02	100.00%	4.46E+01
600	1.00E+01	2.58E+07	0	2.43E+02	2.43E+02	100.00%	8.91E+01

* Equals the duration of pH 10 condition which is less at higher infiltrations due to flushing effects.

** The deposit is viewed as a slab of this thickness spread out over an area = to the package footprint. The deposit could be accumulated in a smaller area (where there is iron).

6.1.7 Summary of Calculated Accumulations

Table 6.1-15 summarizes the potential accumulations beneath the waste package footprint calculated in the computer simulations described in preceding sections.

6.1.8 Deposition profiles

The most relevant parameters for the first 4 cases of Table 6.1-15 (which are the only cases with any significant deposition) are analyzed further in Table 6.1-16. For convenience of reference, the maximum realistic accumulation of fissile material is also given.

For comparison with the criticality calculations in Section 7, we will use the third case from Table 6.1-16 which is the most conservative because it yields the highest deposition of fissile material (4.88 kg) and the highest percentage of fissile mass in the voidspace (0.08).

Table 6.1-15 Accumulations of Fissile Material Calculated by EQ3/6 Simulations Tuff or Concrete Inverts from Waste Packages Containing Immobilized Plutonium, or MOX

Waste form	pH	Invert medium	Accumulation duration (yrs)	Maximum accumulation of fissile material (g)*	Section
1. Immobilized Pu	10	Tuff	300	490 (1750)†	6.1.3.1.3
2. Immobilized Pu	10	Tuff	600	133.5 (356)†	6.1.3.1.1
3. Immobilized Pu	10	Tuff	3000	4880 (17800)†	6.1.3.1.4
4. Immobilized Pu	10	Tuff	6000	539.5 (1440)†	6.1.3.1.2
5. Immobilized Pu	7	Tuff	600	Nil	6.1.3.2
6. Immobilized Pu	5	Tuff	8000	0.0016	6.1.3.3
7. Immobilized Pu	10	Concrete	600	0.03	6.1.4.1
8. Immobilized Pu	7	Concrete	N/A	Smaller than case 5	N/A
9. Immobilized Pu	5	Concrete	8000	2.9×10^{-6}	6.1.4.2
10. MOX	7	Tuff	N/A	Smaller than case 5	N/A
11. MOX	4	Tuff	500	3.85	6.1.5.1
12. MOX	7	Concrete	N/A	Smaller than case 5	N/A
13. MOX	5	Concrete	N/A	Smaller than case 9	N/A

* Maximum accumulation in the invert, over an area equal to the waste package footprint: 5.5 m^2 for the immobilized Pu emplacement and 6.8 m^2 for the commercial SNF waste package.

† The values in parentheses are distributed over tens of meters path length, the other values are distributed over approximately 3 meters (or less), which greatly enhances the potential for criticality.

Notes:

- All cases are for infiltration rate = 1 mm/yr, except cases 1 and 3 which are for 10 mm/yr.
- The expression N/A has been used to indicate that a time period and section number are not relevant for those cases which were not run because the are completely dominated by cases already shown to have negligible fissile mass accumulation.

Table 6.1-16. Relevant Parameters for the Four Cases having Significant Accumulation of Fissile Material.

Section	Accumulation duration (yrs)	Infiltration rate (mm/yr)	Depth (meters)	Fissile accumulation (grams)	% voidspace (max) filled with fissile mass
6.1.3.1.3	300	10	3.35	490	0.008
6.1.3.1.1	600	1	1.09	133.5	0.016
6.1.3.1.4	3000	10	3.35	4880	0.079
6.1.3.1.2	6000	1	1.09	539.5	0.064

6.2 Evaluation of Potential Far-Field Criticality Using Natural Analogs for Uranium Ore Deposition at Yucca Mountain

The purpose of this section is to present an analysis of the mechanisms with the potential for far-field accumulation from the waste package source term. The analogies between ore body formation and potential far-field criticality configurations are explored.

6.2.1 Introduction/Overview

As a result of the TSPA Abstraction/Testing workshop on criticality held on March 18-20, 1997 in Las Vegas, NV, a series of potential scenarios was developed and later refined that potentially could result in a future criticality event in the far-field (the far-field being defined in this case as encompassing the host rock from the drift wall up to and including the accessible environment). A plan was developed to look at these scenarios with the hypothesis that many of the possible scenarios for external criticality could be screened out on the basis of available literature and simple physical or geochemical calculations. The initial results of this effort were presented in Ref. 61. In this section, the available literature is screened for comparison to the physical environment at Yucca Mountain and conclusions are drawn with respect to the scenarios that were identified previously.

One concern of the far-field problem is that the waste placed in the repository, over geologic time, will act as a source of transportable uranium, thus enabling one of the conditions needed for uranium mineral deposition in the far-field. The hypothesis is that epigenetic (i.e. mineralization deposited much later than the host rock) uranium ore deposits documented in the literature should provide some understanding as to the environmental conditions/setting necessary for significant uranium mineral deposition in the far-field and define the mechanisms of precipitation that would be necessary to accumulate enough fissile material to produce a critical assemblage. The second major concern is that this depositional process will operate over geologic time and ^{239}Pu will have sufficient time to decay to ^{235}U. In this section the transport and deposition of plutonium is not evaluated.

6.2.2 Abstraction of Yucca Mountain Geology to Natural Analog Geology

The geology/geomorphology of the Yucca Mountain region includes block-faulted hills consisting of easterly dipping units from the Miocene (Tertiary) age Timber Mountain Tuff, the Paintbrush Group, the Calico Hills Formation, and the Crater Flat Group (Ref. 57, Ref. 40, and Ref. 41), and fault-angle depressions (valleys) filled with alluvial fan and other surficial deposits consisting of Holocene, Pleistocene, Pliocene and Late Miocene age alluvium, colluvium, and eolian deposits. The surficial deposits, including fill in gullies and washes, consist of poorly sorted boulders, gravels, cobbles, and sands that are partially cemented with pedogenic carbonates (Ref. 42). Soil development is relatively thin, consists of various soil and paleosol horizons, and is typical of an arid climate (Ref. 43).

Outcropping bedrock, generally classified as quartz latite and rhyolite tuff, was deposited via multiple ash fall (non-welded, bedded and/or reworked tuffs) and ashflow (welded tuffs) volcanic deposition events (Ref. 57, Ref. 44). At depth in the subsurface, the Tertiary volcanogenic materials are deposited unconformably on Paleozoic carbonates of the Roberts Mountains Dolomite and Lone Mountain Dolomite (Silurian in age; Ref. 33). The multiple

eruptive events have deposited the various units of the Tertiary ash fall and ash flow tuffs. Between these events there have been relatively long periods of quiescence that have produced erosional surfaces and paleosols that are subsequently interbedded between the multiple ash fall and ashflow events (Ref. 40 and Ref. 41).

The Paleozoic carbonates and the Tertiary volcanics tend to change facies somewhat along a traverse away from the proposed repository, but the overall rock types (e.g., tuff, alluvium and carbonate sequences) remain the same. In the direction of regional groundwater flow, the Quaternary sediments thicken to several hundreds of meters of alluvial sediment due to subsidence and range flank erosion. These basin fill sequences such as Frenchman Flat, Yucca Flat, Mid Valley, and Crater Flat basin include not only the debris flow, colluvium, and fan sheet gravels described above, but also lakebed-playa deposits that include siliceous clays, marls, and evaporites (Ref. 42).

The structural control of the bedrock is dominated by basin and range faulting and folding including the typical uplifted horst and downthrown graben blocks that make up the general topography of Nevada. Some of the major north-south striking faults that cross the proposed repository site include Windy Wash, Fatigue Wash, Solitario Canyon, Ghost Dance, Bow Ridge, and Paintbrush Canyon faults. These faults dip steeply towards the west. Several smaller northwest-southeast striking faults also exist including the Drill Hole Wash fault (Ref. 46).

The bulk mineralogy of the Tertiary tuffs includes cristobalite and alkali feldspars through much of the Topopah Spring formation with smectite and glass appearing in the basal vitrophyre. In the Calico Hills and Prow Pass formations, the bulk mineralogy consists of alkali feldspars, opal-CT or cristobalite, and smectite, as well as major abundances of two zeolites; clinoptilolite and mordenite. Deeper, in the Bullfrog formation, the zeolite analcime begins to appear. Fracture lining minerals throughout the tuff formations seem to consist of calcite, smectite, various zeolites (mainly stellerite, heulandite, mordenite, and clinoptilolite), hematite and various manganese oxides including rancieite, lithiophorite, and cryptomelane (Ref. 47).

Uranium deposits normally are classified based on one of the following criteria: host rock type, structural setting, mineralogy, deposit form, or geochemistry; however, for this report, the classification scheme is kept simple based on the review of the available literature. Ore body type descriptions found in Nash et al (Ref. 11) include 11 different types which are based on depositional environment. They are as follows: quartz-pebble conglomerate, unconformity, ultrametamorphic, classical vein, alkalic plutons, contact, volcanogenic, sandstone, calcrete, black shale, and phosphorite. Three of these depositional environments can be associated with the local geology at Yucca Mountain and form the basis for this study; namely unconformity, sandstone, and calcrete deposits. The possible depositional environments that apply to both Yucca Mountain and the three classifications described above are discussed below and in Appendix A.

Unconformity:

There are abundant unconformities and faults present in the far-field at Yucca Mountain. Within the Tertiary volcanic deposits present beneath the potential repository horizon there are at a minimum, five unconformable contacts (others exist including the contact

between the Tertiary volcanics and the Silurian carbonates) commonly classified as bedded tuffs. These bedded tuffs commonly consist not only of reworked ash-fall and ash-flow deposits but contain sandstone, breccia, and paleosols. These bedded tuffs are sandwiched between units of both welded and nonwelded tuff (Ref. 41 and Ref. 44).

Within the welded tuff, highly fractured and brecciated zones are present that could be used as void space/porosity for ore deposition. According to Barr et al (Ref. 48), the maximum fracture frequency in exploratory studies facility (ESF) tunnel occurred between station 4200 and 5250. This is based on a maximum fracture density of mapped fractures (minimal length of 1 meter) in the ESF tunnel. The average fracture density in this interval was around 8/m. According to Steve Beason (Ref. 49), the ESF Geologic Mapping Lead, there are more fractures that were not mapped; these unmapped fractures fell outside the criteria for mapping (i.e. not greater than a meter in length). If these fractures are included, the worst case fracture density would be on the order of 19/m within several locations in the ESF (Ref. 49). This information, coupled with average fracture porosity values of 0.001 for repository host rock (Ref. 46) and aperture values on the order of 200 m. (Ref. 13), indicates that there could be sufficient void space to precipitate mineral phases in the fractures.

The above factors fulfill the geological requirements for advection of mineralizing solutions that are common to unconformity type ore deposition (i.e. an unconformity; a source fluid that could enter a higher porosity sandstone, breccia, or paleosol; and sufficient porosity and/or fracturing and brecciation along faults or fractures).

Sandstone:

The analog to sandstone deposits can be made in three locations. First, as described above, there are sandstone and bedded tuff layers that are or could be the more permeable aquifer units within two semi-confining welded tuff units. An example is shown in Appendix A, Figure A-4.

Second, at some location down gradient of the proposed repository, the tuff aquifer pinches out and becomes an alluvial aquifer. There are fluvial and/or eolian sediments, debris flows, etc., which could provide a preferential flow path within the alluvial aquifer that could be semi-confined within cemented paleosols overbank sediments, or other less permeable alluvium (example is shown in Appendix A, Figure A-5). Because these deposits dip away from the repository and uranium charged groundwater could be flowing down dip in a semi-confined state, or there exist within the alluvium deposits themselves preferential flow channels that follow paleostreams, the geologic advection conditions are present for uranium deposition in the alluvium.

Third, there are sufficient sorbing sites on or in: a) the smectite clays associated with the basal vitrophyre of the Topopah Spring formation, b) significant zeolite facies in the Calico Hills, Prow Pass, and Bullfrog formations, and c) the zeolites, smectite clays, hematite, and manganese oxide minerals lining the fractures.

Calcrete:

Calcrete uranium ore deposits are very similar to the sandstone deposits except for the uranium reconcentration mechanism (example was shown in Appendix A, Figure A-6). Here, there is an evaporitic mechanism. In the arid environment and with known deposits of pedogenic carbonate in the alluvium deposited near Yucca Mountain and the presence of playa lake deposits at Franklin lakes the geologic conditions are present, but the possibility for this type of ore deposit to form is unlikely due to the fact that there is no known source of vanadium in the area that is required to precipitate carnotite. However, due to the fact that Franklin Lakes playa is the currently expected location for surficial discharge of groundwaters flowing beneath Yucca Mountain (Ref. 13),one could expect some accumulation of uranium mineralization via the same evaporative mechanisms that have formed the playa.

6.2.3 Abstraction of Evaluated Scenarios from the TSPA Criticality Workshop to Natural Analogs

The general geology of the Yucca Mountain area provides background for the abstraction to the three potential types of mineral deposits. Most of the far-field scenarios discussed in a previous section fall within or are somewhat analogous to one of the three previously described ore deposit classifications. These include both the I and M branches of the Features, Events, and Processes (FEP) diagram produced as a result of the TSPA criticality abstraction workshop (Ref. 61) and given in Figures 6.2-1 and 6.2-2, respectively.

Table 6.2-1 below shows the correlation between the scenarios on the FEP diagram and the natural analogs described in this section.

Table 6.2-1 TSPA FEP Scenarios and Their Associated Natural Analogs

Analog	Unconformity	Sandstone	Calcrete
Scenario	FF-3a, 3b	FF-3c, 3d, 3e, 1a,1b, 1c, 1d	FF-3f, 3g

FEPs FF-1a and FF-1c (Figure 6.2-1) are somewhat analogous to the sandstone or calcrete type deposits. Although the scenarios are somewhat different, the mechanisms for uranium precipitation do not differ from the standard saturated zone geochemical processes. By definition scenarios FF-1a and 1c (Figure 6.2-1) need either a roll-front/geochemical cell or a sorption mechanism in order to precipitate the uranium minerals.

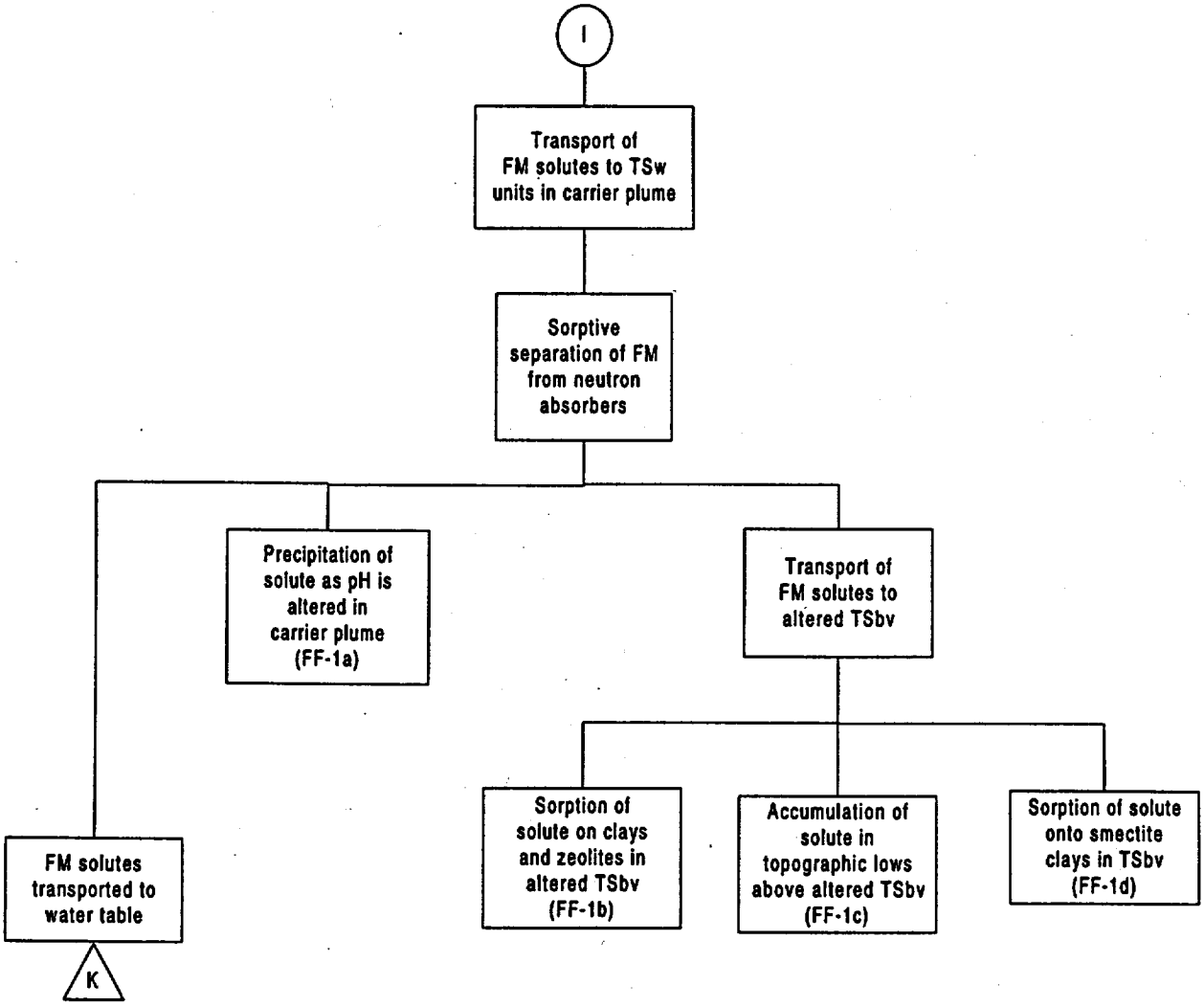

Figure 6.2-1 I Portion of the FEP Diagram Created from the TSPA Criticality Abstraction Workshop

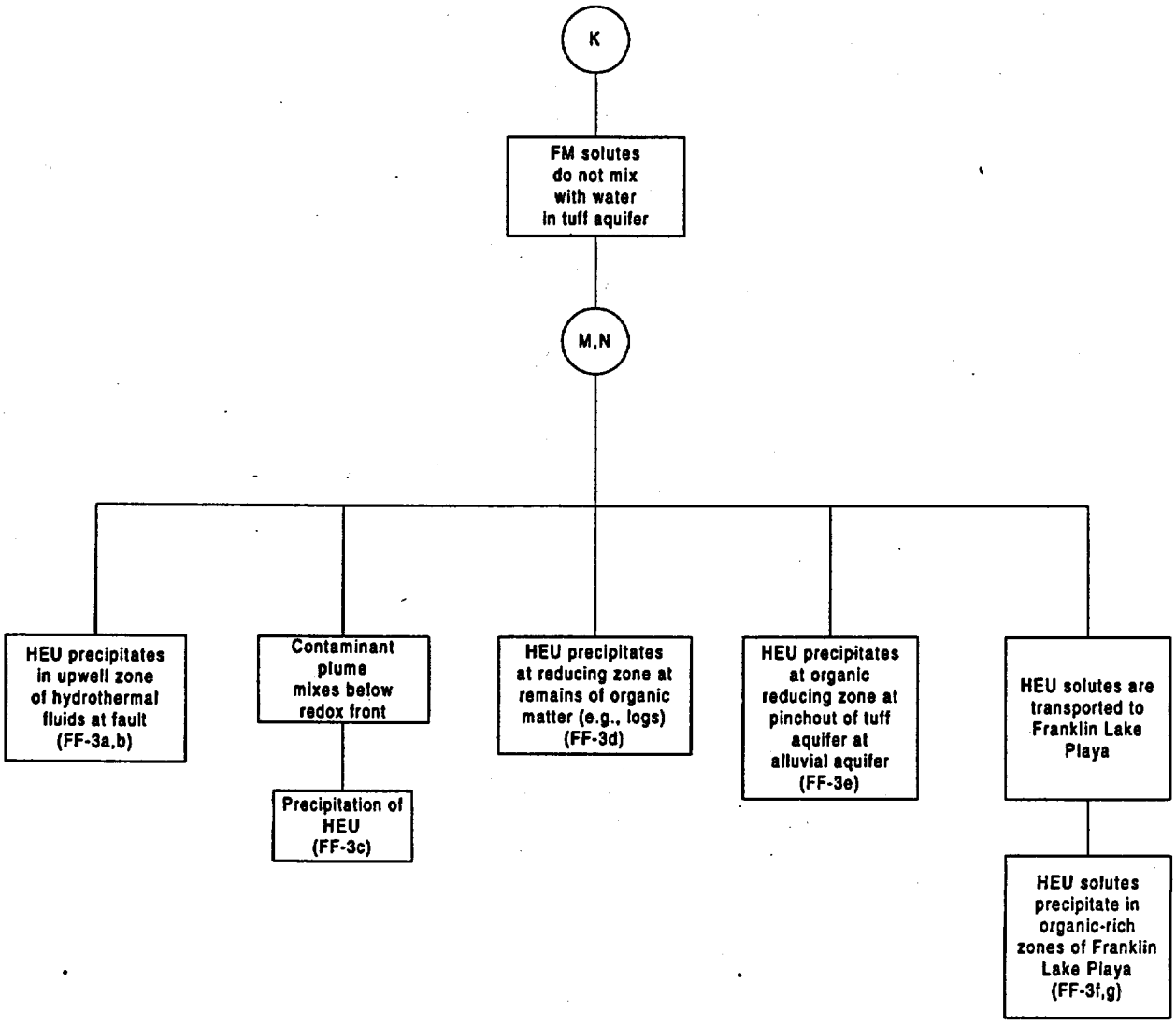

Figure 6.2-2. K,M,N Portion of the FEP Diagram Created from the TSPA Criticality Abstraction Workshop

Analogous to the scenarios represented in Figures 6.2-1 and 6.2-2 are those possibilities which involve transport and precipitation of the fissile material in the form of colloids. Such scenarios are primarily applicable to plutonium, which is known to form colloids readily. They are not easily defined, mainly because they do not deal with saturated groundwater flow systems and colloidal transport and agglomeration is less well known. It is uncertain, at this time, how the Pu colloids behave in the far-field environment. Therefore, this discussion of geologic analogs does not address their effects. Colloids are discussed from the geochemical viewpoint in section 6.4.

6.2.4 Results of Natural Analog Study

The key factor in this study (as with all epigenetic uranium ore deposition) is the need for either a sufficient localized reducing capacity or a source of vanadium within the Yucca Mountain regional geology and aquifer system to precipitate sufficient quantities of ore grade uranium. Without a mechanism or source to either reduce the oxidized uranium species in the groundwater or the vanadium to precipitate oxidized uranium minerals there can be no substantial accumulation of uranium minerals, thus no possible way for a critical assemblage to form. If the required reducing capacity (or presence of vanadium) in the natural system at Yucca Mountain (which is yet unknown or uncharacterized) does not exceed the reducing capacity (or presence of vanadium) that has produced the accumulated known quantities of epigenetic uranium ore in the past, the potential uranium precipitation at Yucca Mountain over geologic time is bounded to that found in ores that occur in similar settings. The three natural analogs are discussed below in this light.

6.2.4.1 Unconformity

A deposit at or near Yucca Mountain resembling an unconformity analog has the highest potential for developing a criticality. On average, ore grade is much higher for the unconformity type than either the sandstone or the calcrete type deposits. The average ore grade for an unconformity type deposit can be 2% (Table 6.2-1) whereas the other analogs have a much lower grade, usually no greater than 0.35% (Table 6.2-2). The percentage of U_3O_8 in these high grade ores seems to dwarf those in the other two analogs. The high grade ores reported in the Athabasca region (Collins Bay, Rabbit Lake, Cluff Lake, Midwest Lake, and Key Lake) have produced localized mineralizations that have high grade ores ranging between 30 and 80% U_3O_8. These high grades are persistent over several meters of the orebody. Certainly these types of deposits, if formed at Yucca Mountain, could potentially result in a criticality. However, the reducing conditions necessary to produce such large concentrated masses of fissile material are evidently absent (Ref. 4, p. 73, 74).

Indications of the fluid geochemistry that was migrating up the faults and reacting with the uranium charged oxidized waters above the unconformity in the Athabasca region, give bounding conditions of what type of fluid is needed to react with the potential uranium rich oxidized waters at Yucca Mountain (see Appendix A, Figure A-2). Gas samples associated with a characteristic odor at Collins bay were analyzed and found to contain short chain aliphatic hydrocarbon gases, hydrogen, and carbon dioxide. Also associated with the ore

Table 6.2-1 Collected Information on Selected Unconformity Type Deposits
Global Average Ore Grade (% U_3O_8) runs between 0.2 to 2.0%

Deposit	High Grade (% U_3O_8)	Average Ore Grade (% U_3O_8)	Ore Body Dimensions	Ore Deposition Age (m.y.)
Collins	80[a]	0.6	3000 ft x 300 x 100 ft	1238[e]
Rabbit	NA	0.4	215 m x 540 m x 200 m	1075[e]
Cluff	29.3[b]	1.9	1200 m x 200 m x 150	1050[e]
Key Lake	35[c]	2.0	3.6 km x 100 m x NA	1160[e]
Midwest	NA	3.4	2 km x 200 m x NA	NA
East	2.47	0.4	NA	NA
Jabiluka	NA	0.39	1500 m x 500 m x 150	NA
Nabarlek	5 to 72[d]	NA	NA	1770 to 800

[a]High grade ore: 7 ft. Section (along fault or breccia zone) of 80% U_3O_8, 30 ft section of 60% U_3O_8; [b]D zone ores have an average grade of 7% with a high grade of 29.3% U_3O_8; [c]high grade ore reported in one case at 35% U_3O_8 over 2 m; [d]Within a 10 meter wide crush zone; [e]General time interval of mineralization for all of the Athabasca deposits runs about 250 m.y. Table compiled using information from Nash et al. (Ref. 11), Hoeve and Sibbald (Ref. 28 and 29), Jones (Ref. 14), Harper (Ref. 30), Clark et al. (Ref. 31) and Clark and Burrill (Ref. 35). NA means not readily available in the literature.

Table 6.2-2 Collected Information on Selected Sandstone and Calcrete Type Deposits

Deposit	High Grade (% U_3O_8)	Average Ore Grade (% U_3O_8)	Ore Body Dimensions	Ore Deposition Age (m. y.)
Sandstone Type	Global Ave. 2.0%	Global Ave. 0.10 to 0.35%		
Olympic Dam	NA	0.05 to 0.1	NA	NA
Fieberbaunn	2.3	NA	A few m x 11 km x	NA
Montezuma	b	0.25	80 ft x several 1000 ft[e]	NA
Happy Jack[a]	1.3[b]	0.39	20 ft x 500 ft x 3500 ft	65 m. y.
Temple	15[c]	NA	NA	84 m. y.
Calcrete Deposits		Global Avg 0.1 to 0.3%		
Yeelirrie	0.36[d]	0.15	8 m x 6 km x 0.05 km	NA

[a]Colorado Plateau deposits average an ore grade of about 0.25% U_3O_8. [b]Colorado Plateau deposits have an average high grade ore of about 2.0% U_3O_8. [c]Temple Mountain has an unique ore chemistry as uranium ore is directly associated with petroleum products such as tar and is not directly associated with the normal uranium ore deposits on the Colorado Plateau. [d]Half of the ore at Yeelirrie grades better than 0.36% U_3O_8; no high grade numbers are given. Table compiled using information from Kerr (Ref. 15), Huff and Lesure (Ref. 16), Kimberly (Ref. 17), Fisher (Ref. 18), Dodd (Ref. 19), Kelley and Kerr (Ref.25), and Nash et al. (Ref. 11). [e]Covers a broad area, of several thousand feet dimension. NA means not readily available in the literature.

deposits are hard glassy hydrocarbon buttons (Ref. 14). With these indications, the waters that were migrating up the fault were certainly charged with methane and carbon dioxide. For other unconformity type deposits, some sort of hydrothermal fluid, which often has gas, is cited as the reductant. These two gases (methane and HAS) are very reducing (Ref. 12) and can potentially promote the formation of very high grade ore deposits.

One potential source of very reducing fluids could be hydrothermal activity. A volcanogenic hazard analysis done on Yucca Mountain suggests that the probability is extremely low for having a volcanic event (Ref. 21). Thus, because of the necessary physical and temporal correlation between hydrothermal activity and volcanism, a hydrothermal event is unlikely (Ref. 21). This low probability rules out a hydrothermal event as a likely source of reducing fluids.

Another potential source of very reducing fluids is associated with petroleum. However, there are no known petroleum deposits at Yucca Mountain (Ref. 22). This does not preclude mineralization from this mechanism at Yucca Mountain. A big uncertainty with current site characterization data lies in the saturated zone geochemistry at Yucca Mountain. There is a lack of measured data from the carbonate aquifer, but with the data that are available, a known chemical gradient exists between the composition of the Paleozoic aquifer and the Tuff aquifer (Table 6.2-3). The measurements found on Table 6.2-3 are not sufficiently reducing; however, there is neither a measurement for Eh nor are there measurements for $_{CH}$ and HAS in these waters.

The information presented above seems to indicate that the only geochemical mechanism that could potentially create an unconformity type of deposit at Yucca Mountain is a nonhydrothermal source of methane (or other hydrocarbon) migrating up a fracture zone or fault plane to react with an oxidized uranium-rich fluid. Without a water chemistry sampling from the Paleozoic aquifer that could yield information on potential petroleum or methane migration from depth, this type of ore deposit cannot be entirely ruled out, although a nonhydrothermal unconformity type deposit due to petroleum migration seems very unlikely in view of the current geochemical understanding of the site.

Table 6.2-3. Water Chemistry for Well UE-25 P#1 (Paleozoic Aquifer) and Average J-13 (Tuff Aquifer) Compositions

Source	*LA-101188-MS*	*OFR-84-450*	*OFR-94-305*	*AVG*	*J-13*
Si	30	41	44	38.3	28.5
Al	0.1				
Fe	<0.1				
Mn	<0.1				
Mg	32	39	31	34.0	2.01
Ca	88	100	94	94.0	13.0
Na	171	150	150	157.0	45.8
K	13.4	7.2	12	10.9	5.0
Li	0.32	0.59	0.31	0.4	0.048
HCO_3^-	698	710	890	766.0	129
F^-	3.5	4.7	4.9	4.4	2.18
Cl^-	37	28	26	30.3	7.1
$SO_4^{=}$	129	160	78	122.3	18.4
$1NO_3^-$	0.1				8.8
pH (field)	6.7	6.6	6.7	6.7	7.4
Temp °C		56	57	56.5	31.0

Values found on this table are taken from References 7, 32, 33, and 34.

6.2.4.2 Sandstone

Sandstone type deposits in the U.S. comprise about one third of all the known minable uranium reserves in the world of which the majority are located on the Colorado Plateau (Ref. 11). Under normal occurrence the high grade ores in sandstone deposits seldom exceed 2% U_3O_8 (Table 6.2-2). The average ore grade for a typical sandstone deposit seems to range somewhere between 0.1 and 0.35% U_3O_8 with the deposits on the Colorado Plateau averaging about 0.25% (Table 6.2-2). However, there are known occurrences of high grade ore that are directly associated with either petroleum (tar and asphalt type materials) or buried logs. The Table Mountain deposit is associated with tar and asphalt like substances as the reducing agent. This deposit has a maximum ore grade of 15% (Ref. 20). Other uranium deposits on the Colorado Plateau have occurrences of petrified logs that have been replaced with uranium minerals. These localized log deposits average around 1.88% uranium with maximum concentrations in individual logs of reaching 16.5 to 20% uranium (Refs. 22, 23, and 24).

Without the presence of either logs or petroleum, no other mechanism is known wherein a sandstone type deposit can precipitate mineral grades much greater than 2% (Ref. 39). Therefore, basic sandstone type deposits, without the reducing capacity of either buried logs or petroleum, will not accumulate enough fissile material to go critical. However, as demonstrated above, uranium deposition in the presence of logs or petroleum products could accumulate enough high grade mineralization wherein sufficient fissile material could precipitate to go critical.

Within the bedded Tuff (ash-fall or reworked) deposits at Yucca Mountain, where there are known sandstone and paleosol deposits, there is the possibility of buried logs. As an example, a study done at Mount St. Helens (Ref. 25) looked at dating ash fall deposits from eruptive events using buried logs within associated lahar and debris flow deposits. Logs tended to be highly disseminated within each deposit; however, within some of the sampled debris flows and lahar deposits, between 17-30 logs were sampled for dating. These logs date from 1355 AD to 1885 AD. Although Yamaguchi and Hoblitt (Ref. 25) do not give a distribution nor the abundance of buried logs in the Mount St. Helens deposits, their study documents the presence of buried logs within volcanic deposits. The possible occurrence of logs within ashfall type deposits cannot be discredited at Yucca Mountain. In Ref. 5, a probabilistic analysis done for far-field criticality suggested that the likelihood a criticality event would occur as a result of uranium mineral precipitation with buried logs is very small. Unless there is either a petroleum deposit or migration event, such as is needed in the unconformity case described above, the likelihood of criticality occurring in a sandstone type mineral deposit is small.

In conjunction with the burial of logs within or in close proximity to volcanic deposits, it should be borne in mind that they tend to become petrified in a geologically short time. For example, about 20 petrified forests have been identified in Specimen Ridge in Yellowstone National Park (Ref. 27, pp. 313-314). This is closely related to the release of silica from the weathering of volcanic glass giving rise to waters supersaturated in quartz, chalcedony, and other silica minerals, which may then precipitate within the cells of the wood. Thus, it is quite likely that any wood buried in the volcanic pile at Yucca Mountain, or in the soils between ash falls, may be petrified, thereby severely limiting its capacity to provide a reducing environment.

6.2.4.3 Calcrete

Calcrete type deposits have similar ore grades as the sandstone type deposits. The average ore grade ranges between 0.1 and 0.3% U_3O_8 (Table 6.2-2). The arguments described above that exclude the sandstone deposits from consideration are the same in this case (i.e., an insufficient amount of vanadium in this environment to precipitate high grade quantities of uranium ore); thus, the likelihood of a critical assemblage is small. Other potential arguments that help in this case include both the potential accumulation of known nuclear fuel poisons and the evaporitic loss of moderating water. The most likely location in the vicinity of Yucca Mountain for this type of deposit is at or near Franklin Lake playa (believed to be a groundwater discharge location for the groundwater flowing beneath Yucca Mountain, Ref. 13). Playa deposits are known to accumulate borates as evaporite deposits (Ref. 26). Boron is a known reactor fuel poison and will be a constituent of the high level waste planned to be disposed at Yucca Mountain. Last of all, due to evaporation, there may be insufficient water to act as a moderator for criticality.

6.2.5 Summary of Analog Evaluations of Criticality Potential

The above discussion indicates that significant uranium mineralizations will only occur if there is either a persistent reducing agent (one strong enough to resist the invasion of oxidizing solutions) or a source of vanadium within the host rock for the uranium to accumulate. If these conditions are not persistent, there can be no more than short term accumulation followed by remobilization. The potential for Yucca Mountain to have the required persistent reducing capacity seems minimal given the current site characterization data. Some of the currently accepted

characterization data are as follows: a) there are no known petroleum deposits in the vicinity of Yucca Mountain (Ref. 22); b) the probability of a hydrothermal event has been determined to be very small (Ref. 21); and c) the probability of uranium ore deposits from log replacement has been determined to be very unlikely (Ref. 5). The three items discussed above cover the main areas of concern for potential criticality in the far-field. The considerations are summarized in Table 6.2-4.

Table 6.2-4 Summary of Geologic Reducing Zone Occurrence Requirements, and Likelihood at Yucca Mountain

Analog type	Reducing media	Occurrence at Yucca Mountain
Unconformity	Hydrothermal fluid	Requires volcanic activity; highly unlikely
	Other methane source	Incredibly low probability
Sandstone	Organic logs	Very unlikely*
	Petroleum	None observed, nor likely to be
Calcrete	Vanadium	None observed

* This case has been shown to have incredibly low probability for low enriched uranium (LEU) commercial SNF with the log occurrence frequency of the Colorado Plateau (Ref. 5).

Although the potential for far-field criticality seems small, one cannot fully rule out the possibility of any of the FEP scenarios (Figures 6.2-1 through 6.2-4) occurring, because of the nature of the geologic environment and the infeasibility to characterize the entire geologic system at Yucca Mountain deterministically. Further site characterizations could identify zones where either reducing capacity (HAS gas, methane, organic logs, etc.) or source of vanadium in the host rock is sufficiently high over extended periods of geologic time to accumulate a high percentage of U_3O_8. However, within the tuffaceous rocks near the repository such formations would be inconsistent with the current geologic observations at Yucca Mountain and the interpretation of its history. For example, it is conceivable that some small amount of organic material could have been deposited in the paleosols developed on the bedded tuffs during intervals between periods of volcanic activity; however, most such organic material would have been oxidized (burned) by the ashfall of subsequent volcanic activity, and what little might be left would be either petrified by silica released during weathering of the volcanics or be of such small quantities as to pose little threat to large accumulations of fissile material. It is, therefore, extremely unlikely that evidence of reducing formations will be uncovered by any future geologic investigations within the tuffs at Yucca Mountain.

6.3 Sorption

6.3.1 Methodology and General Observations

Best practices for geochemical analyses would use a computer code that couples the type of geochemical calculations done in EQ3/6 with sorption and ion exchange. However, these latter capabilities have not been incorporated into the most recently released version of that code package.

To obtain an approximate answer, the so-called Kd approach has been used. This method has often been employed in hydrological flow and transport codes to provide a simple approximation to sorption along flow paths. Nevertheless, it suffers from serious drawbacks in some cases because it does not place an upper bound on the amount adsorbed, whereas in fact no more can be adsorbed than can fit onto adsorption sites on the solid surface (substrate). It also does not take into account changes in solution chemistry, such as whether or not the dissolved element becomes incorporated into complexes, or surface chemistry, such as competition with other ions. Application of available data to cases of interest in evaluating criticality external to waste packages shows that in some cases the calculated amount of adsorption using Kds is unrealistic.

A good example of the complexity of modeling sorption appears in Ref. 54, which deals with the adsorption of uranyl ion onto smectite, but in the absence of carbonates. This paper utilized equations for 34 chemical equilibria in order to model the observed sorption reasonably well. Unfortunately, because of the lack of consideration of carbonate complexes, this paper has little value for the present application except to confirm in a qualitative way the general order of magnitude for the sorption relevant for conditions likely to be present within or near a repository at Yucca Mountain. In particular it is clear that the adsorption of UO_2^{++} is significantly reduced by the presence of moderate to high concentrations of Na^+ and by complexation in solution. Carbonate species in solution were rigorously excluded from the experiments described in this paper in order to avoid this effect. Thus, low values of adsorption for UO_2^{++} are appropriate for the present application.

Data from Los Alamos National Laboratory (Ref. 55), the NEA sorption data base (Ref. 56), a Swedish data set (Ref. 58), a Canadian set (Ref. 59), and TSPA 95 (Ref. 60) were used for obtaining data. For conservatism maximum values were chosen. Table 6.3-1 documents the calculations.

Data chosen are for

(1) goethite (FeOOH), which represents the degradation products of steel,

(2) zeolite, both a value for clinoptilolite from Ref. 55 and one for a zeolite of the heulandite-clinoptilolite family from Ref. 53, and smectite, which represent degradation products of glass waste forms as well as degradation products of tuff and aggregate in concrete,

(3) tuff from Yucca Mountain, and

(4) marl, which resembles the degradation products of the cement in concrete.

Adsorption onto other materials, e.g., quartz and feldspar, is significantly less than on these solids (Ref. 55), or otherwise similar to that for tuff, and has not been included in the analyses. The geometric relationships among these solids as they may lie in the repository, i.e. a mix of two or more of them, or segregation of one into a separate pocket, has not been considered. In effect the analyses conducted assume that each occupies the entire region of the invert below a waste package. Because none of these individually gives rise to a condition in which a criticality could arise, none could arise from any mixture of them. The use of mixtures as a first approximation would require a weighted average of the various constituents. Thus, a mixture of solids will have a lower criticality potential than 100% of the most strongly absorbing species.

The analysis covers a full range of anticipated pH and materials. In no case was a critical condition approached. Below the repository only tuff, sometimes altered to zeolite and/or smectite, together with minor amounts of other materials is present. In view of the analysis here it is apparent that a criticality could not arise there as a consequence of adsorption unless some mechanism could occur that would greatly increase the concentration in the solution. In this connection it should be borne in mind that at least an approximate equilibrium between the concentration in solution and that in or on the solids will prevail. Thus, a solution with a low concentration of fissile material moving through the rock for a long time cannot increase the amount adsorbed. Conversely, if a solution with a low concentration of UO_2^{++} percolates through a region which had previously been enriched in uranium by adsorption from a solution with a higher uranium concentration, the adsorbed uranium will be at least partially desorbed and flushed out. These relations differ in principle from possibilities that might arise through precipitation of uranium or plutonium.

The only circumstance recognized to date in which the Kd approach is clearly inappropriate for the present application is during the relatively brief time span (Section 6.1) that highly alkaline solution is expected to exit the "can-in-can" glass waste package, i.e. immobilized plutonium cans embedded in HLW glass canisters. This case can be evaluated independently, as is done below. The amount of adsorbed fissile material in all other cases is too low to lead to a criticality.

Table 6.3-1 Calculations of Uranium and Plutonium Sorption

This table provides basic relations (estimates) for input to specific configurations. The data are very uncertain. This sheet uses European and Canadian data. The estimations will be based on a simple Kd approach. Concentration units for solutions are mg/kg; densities chosen to be unity, which will be low and conservative. For solids are g element/kg adsorbing substrate. Kd is in ml/g, i.e. solid conc.*1000/soln. conc. The Kd approach used here has limitations. Specifically, at sufficiently high concentrations in solution all adsorption sites on the solid may be occupied. This means that the concentration in the solid is in fact limited, but that this simple model is incapable of showing that.

			Plutonium				Uranium			
Solid	Kd, Pu	Kd, U	Pu gls. effluent, pH 8.01		Comm.SNF pkg effluent		Pu gls. effluent, pH 8.01		Comm.SNF pkg effluent	
			Soln. conc	Solid conc	Soln. conc	Solid conc	Soln. conc	Solid conc	Soln. conc	Solid conc
FeOOH	70000	4000	5.34E-08	3.74E-06			4.78E-03	1.91E-02		
Clinoptilolite	800	30	5.34E-08	4.27E-08			4.78E-03	1.43E-04		
Zeolite		700					4.78E-03	3.35E-03		
Smectite	3000	50	5.34E-08	1.60E-07			4.78E-03	2.39E-04		
Vitric Tuff	80	4	5.34E-08	4.27E-09			4.78E-03	1.91E-05		
Marl	5000	1000	5.34E-08	2.67E-07			4.78E-03	4.78E-03		
			Pu gls. effl., pH 7.01				Pu gls. effl., pH 7.01			
FeOOH	70000	4000	1.56E-07	1.09E-05			1.93E-03	7.72E-03		
Clinoptilolite	800	30	1.56E-07	1.25E-07			1.93E-03	5.79E-05		
Zeolite		700					1.93E-03	1.35E-03		
Smectite	3000	50	1.56E-07	4.68E-07			1.93E-03	9.65E-05		
Tuff	80	4	1.56E-07	1.25E-08			1.93E-03	7.72E-06		
Marl	5000	1000	1.56E-07	7.80E-07			1.93E-03	1.93E-03		
			Pu gls. effl., pH 6				Pu gls. effl., pH 6			
FeOOH	70000	4000	1.48E-06	1.04E-04			2.31E-03	9.24E-03		
Clinoptilolite	800	30	1.48E-06	1.18E-06			2.31E-03	6.93E-05		
Zeolite		700					2.31E-03	1.62E-03		
Smectite	3000	50	1.48E-06	4.44E-06			2.31E-03	1.16E-04		
Tuff	80	4	1.48E-06	1.18E-07			2.31E-03	9.24E-06		
Marl	5000	1000	1.48E-06	7.40E-06			2.31E-03	2.31E-03		
			Pu gls. effl., pH 5.5		Comm.SNF pkg pH 6		Pu gls. effl., pH 5.5		Comm.SNF pkg pH 6	
FeOOH	70000	4000	6.15E-06	4.31E-04	1.87E-06	1.31E-04	4.71E-03	1.88E-02	2.19	8.76E+00
Clinoptilolite	800	30	6.15E-06	4.92E-06	1.87E-06	1.50E-06	4.71E-03	1.41E-04	2.19	6.57E-02
Zeolite		700					4.71E-03	3.30E-03	2.19	1.53E+00
Smectite	3000	50	6.15E-06	1.85E-05	1.87E-06	5.61E-06	4.71E-03	2.36E-04	2.19	1.10E-01
Tuff	80	4	6.15E-06	4.92E-07	1.87E-06	1.50E-07	4.71E-03	1.88E-05	2.19	8.76E-03
Marl	5000	1000	6.15E-06	3.08E-05	1.87E-06	9.35E-06	4.71E-03	4.71E-03	2.19	2.19E+00

Data for FeOOH, clinoptilolite, and vitric tuff taken from Ref. 55.

Data for zeolite taken from Ref. 53.

Data for smectite taken from Ref. 58.

Data for marl taken from Ref. 56.

6.3.2 Analysis for zeolites and clays

Under highly alkaline conditions both Pu and U will be dissolved primarily as tricarbonate complexes, $PuO_2(CO_3)_3^{---}$, and $UO_2(CO_3)_3^{---}$. The large negative charge on these ions is of special importance because the silicate crystalline structure of clays and zeolites carries a net negative charge. This arises from the substitution of Al^{+++} for Si^{++++} in the silicate lattice; within the crystal structure this is compensated by the presence of other metal ions, such as Na^+ and Ca^{++}. On the surface, however, this negative charge isn't balanced by firmly held ions, but by adsorbed positive ions. Negative ions will be repelled. This will effectively prevent the adsorption of the tricarbonate complexes of plutonyl or uranyl ions onto zeolites or clays. These tricarbonate ions are also very large and cannot penetrate into the crystal structures, i.e. into the channels in zeolite or between layers in smectite. Even if they could, they would be repelled because of the net negative charge which limits the ionic exchange to positive ions (cations), not negative ones (anions).

6.3.3 Analysis for goethite and calcite

The nature of adsorption onto goethite and calcite differs markedly from that on the clays. For these minerals the crystal lattice itself does not incorporate a charge imbalance that intrinsically creates a net surface charge. Instead the nature of the surface chemistry changes with pH. This is conveniently viewed in terms of major structural cations, e.g., Fe^{+++}, just below the surface firmly bonded to a surface oxide ion. This can be represented as $\equiv FeO^-$, where the triple equal sign represents bonding to the rest of the structure. The $\equiv FeO^-$ then signifies an active surface chemical group, which interacts with the solution. At low pH hydrogen ions from the solution will become bound to it, producing the group $\equiv FeOH_2^+$. In other words at low pH ferric oxides and hydroxides, such as goethite, will have a net positive charge, and will readily adsorb anions. At an intermediate pH the surface group changes to $\equiv FeOH$, and at high pH to $\equiv FeO^-$, which adsorbs cations. The transition between the first and last of these groups is known as the zero point of charge. For hematite this occurs in the pH range 4.2 to 6.9; for goethite in the range 5.9 to 6.7, and for amorphous $Fe(OH)_3$ in the range 8.5 to 8.8 (Ref. 71, p. 351). Thus in any case the ferric oxyhydroxides will tend to repel the plutonyl and uranyl tricarbonate complexes, which are of importance only at still higher values of pH. It is not yet clear whether calcite will similarly not adsorb Pu and U at high pH; Ref. 71, p. 351 lists two values for the zero point of charge, 8.5 and 10.8. If the latter applies to the situation for Yucca Mountain, potentially large concentrations of these elements could be adsorbed in a concrete invert. Literature searches conducted to date have not found any experimental measurements of adsorption of Pu or U on calcite under highly alkaline oxidizing conditions. (Clay minerals can also exhibit the phenomena of zero point of charge, e.g., for montmorillonite it occurs over a range of ≤ 2 to 3, Ref. 71, p. 351.) It should be kept in mind that the high pH condition applies only to waste packages containing alkali rich borosilicate glasses.

6.3.4 Limits of uranium/plutonium accumulation

In contrast to the implications of the preceding paragraph, large quantities of fissile material will not be available because of the limited duration (Section 6.1) of the high pH phase of waste package degradation. This brevity would arise either because of acid production within the waste package through the potential oxidation of Cr to chromate, or simply because of flushing of the contents of the waste package by infiltrating water. Depending upon these

factors the pH might remain high for periods ranging from 300 to several hundred years (Ref. 2) at an infiltration rate of 1 mm/Yr. Higher infiltration rates will, of course, shorten the length of the high pH period. The maximum mass of fissile material that could be released during 1000 years will be about 1500 grams per waste package. If this is all adsorbed uniformly in the invert immediately below the package, the maximum concentration could reach only 0.05 wt%. For higher infiltration rates the time during which the pH will remain high will be proportionately reduced. Table 6.3-2 shows the results of calculations for several infiltration rates and times. Other distributions of the fissile material in the invert would produce variations in the concentration, e.g., 0.5% fissile material distributed uniformly in the top 10 % of the invert. These are very conservative values because a very high dissolution rate (Ref. 4, p. 11-12) was chosen for the HLW glass.

Table 6.3-2 Calculation of Maximum Amount of Fissile Material Exiting an Immobilized Plutonium Waste Package at pH 10

Dimensions and Transport Characteristics		
Flow Width	171 cm	"shadow" of waste package
Flow Length	323 cm	"shadow" of waste package
Flow Cross Section	55200 sq cm	same as slab deposit area
Water density	1 g/cm^3	estimated same as pure water
Porosity of Invert	0.3	
Depth of Invert	700 mm	
Solid vol. of invert	1160000 ^{0}	
Density of invert	2.65 g/cm^2	
Mass of invert	3070000	
Pu conc. in effluent	78.3 ppm	
U conc. in effluent	6110 ppm	

Infiltration rate, mm/yr	Vol./Yr ^{0}	Transport g/yr,	Time, yr	Fissile mass, g	Conc. in invert, %
1	5520	1.49	300	446.37	0.01
1	5520	1.49	1000	1487.90	0.05
5	27600	7.44	200	1487.90	0.05
10	55201	14.88	100	1487.90	0.05

The results presented above differ markedly from some of those presented in Ref. 53. The experimental results were interpreted to mean that up to about 1 wt% uranium may be adsorbed and/or ion-exchanged by zeolites of the heulandite-clinoptilolite group. The experimental work is described only briefly. The Kd derived from the adsorption experiments is surprisingly high, about 700 ml/g. Some idea of how high the Kd might be can be obtained by utilizing data from a table in Ref. 71, p 351. In this table the cation exchange capacity of smectite-montmorillonite is given as ranging from 80 to 150 meq/100g, and that of zeolites from 100 to 400 meq/100g. Evidently this table includes the combined effects of adsorption and cation exchange within the crystal structure. From these data one may conclude that the capacity of zeolites may be up to about 2 times that for smectite-montmorillonite. This implies that, believing that the data in Table 6.3-1 are reasonable, one may expect the maximum Kd for zeolites to be about 125 ml/g. It is evident from statements made by the authors of Ref. 53 that they understand the need to perform reversed experiments; however,

they made determinations of the Kd only from adding a uranyl containing solution to the zeolite, but not from taking a zeolite previously charged with uranium from a reasonably concentrated solution and reequilibrating the zeolite with a solution with a lower uranium concentration. This casts some doubt on the reliability of the results. Nevertheless, the value of 700 ml/g is also included in Table 6.3-1. The concentrations of U in the aqueous solutions in these experiments are of interest. Calculations performed with the code, EQ6, indicate solubilities in the pH range from 5.5 to 6 or 0.005 to 0.002 ppm (Ref. 2), are far less than those used in the experiments. This article makes no mention of the possibility of precipitation of an insoluble U solid during the course of the experiments. On the other hand the experiments reported in Ref. 55 used similar concentrations and times of reaction, but obtained much smaller values for the distribution coefficient. In summary the results reported in Ref. 53 are questionable. So far as can be determined, Ref. 53 does not properly take into account the principles recommended by the Nuclear Regulatory Commission (NRC) (Ref. 72).

The paper (Ref. 53 also includes a plot comparing the "adsorption ratio" as a function of pH, evidently the percentage of the uranium adsorbed, and "the ratio of residual uranium in H-C zeolite" against pH. (H-C refers to heulandite-clinoptilolite.) This latter ratio refers to results after leaching tests, for which no details are provided. Points from the second determination fall very close to the curved line drawn through the first set. Nevertheless, percent adsorbed does not permit a calculation of the Kd unless the solution concentration is also given, which is not done. Thus, this graph does not correlate directly with the one from which the Kd was estimated and the significance of the comparison is lost. This plot is compatible with the interpretation that uranyl ion is displaced from the zeolite at low pH by hydrogen ion, and that it is prevented from adsorbing, or is removed from the solid, by complexation with carbonate at high pH. However, over the range of pH from about 4 to about 8, where 100% of the U is "adsorbed", it is not possible to tell from the data presented whether it is truly adsorbed or is precipitated. In any case the high percentage of about 0.9% found in the zeolite would be relevant to the issues in this report only for the brief initial period of high pH, and even then only a small percentage of the uranium would consist of ^{235}U.

The highest concentration of uranium in zeolite reported in the geologic literature is 0.166 wt% in the Tono mine in Japan (Ref. 73). Since this is larger than the highest values calculated here, it is likely that the responsible deposition process was enhanced from that described here, with the method of enhancement being inapplicable to the repository source term. In particular, the Tono mine zeolites are found in close association with reducing material (pyrites and organics) which could have enhanced the uranium deposition in a way which could not be distinguished from adsorpion in the zeolite.

6.4 Colloidal Transport and Deposition

The strongest evidence against significant colloidal transport of Pu from a waste package has been observations at the Oklo site, where there was a natural nuclear reactor nearly 2 billion years ago. The relevant observations at Oklo have been summarized in several articles, of which the most directly relevant is Ref. 77. Recent measurements at the Nevada Test Site (Ref. 78) have suggested that Pu could migrate in colloidal form for distances greater than 1 km in times less than 25 years. To assess the potential for colloidal transport and deposition, this section will summarize the conditions for colloidal transport of fissile material and the possibility of formation of fissile deposits to critical mass levels outside the waste package.

Generally, colloids will form by peptization where a previously precipitated solid is resuspended as an extremely small (< 10 angstrom) particle. Such a suspension behaves like a solution in many respects. If Pu or U form such a colloid in the water, then the concentration of Pu and/or U in mobile form could greatly exceed that of the dissolved species. This would allow more rapid transport of fissile material out of the package. Colloids can be filtered from solution by very fine beds of solids (unlike dissolved ions which pass through filters owing to their much smaller size). Transport followed by filtration outside the package thus sets up the potential for a critical mass outside the package.

The fissile species do not have a unique tendency for colloid formation when compared with the many other species present. The dissolution of materials in the waste package gives rise to a variety of clay and other minerals which are prone to form colloids. This is especially true of clay minerals which form from the breakdown of glass waste forms and oxides that are formed during metal corrosion. To obtain an approximation to the likely proportions of different types of colloids one may look at EQ6 simulations. For example, during the dissolution of the immobilized plutonium waste package, the solids at pH 10.003 include 30 g $Na_4UO_2(CO_3)_3$ and 4.7 g PuO_2 in 895 g of other material including 448 g smectite (a material with large tendency to form colloids) (see EQ6 output file" j13awp50.6o" in Section 9.2 of Ref. 4). The same package exhibits similarly diluted material at pH = 7 with 51 g soddyite and 25.6 g PuO_2 in 2098 g of other solids which tend to form colloids, (EQ6 output file "j13avwp45.6o" in Section 9.2 of Ref. 4). At pH 5 the immobilized plutonium package will contain 55.8 g soddyite and 51.3 g PuO_2 in 3970 g of other solids including over 1 kg of smectite (EQ6 output file "j13avwpsoly40.6o" in Section 9.2 of Ref. 4). The commercial SNF package at pH 4 will contain 83.9 g of soddyite and 2450 g of UO_3:$2H_2O$ which appears to be a large percentage of the 4340 g of other solids. However, the U only include 4% fissile material (see EQ6 output file j13avaugfa1.6o in Section 9.2 of Ref. 4).

The MOX SNF package at pH 4 contains only 35.7 g PuO_2 and 82.6 g of soddyite, but it does contain 1330 g of UO_3:$2H_2O$. However, the low U enrichment (0.1675%) means that the total fissile material is very small compared to the 3230 g of other colloid forming solids (see EQ6 output file "j13avmoxa1.60" in Section 9.2 of Ref. 4). More importantly, the presence of so much ^{238}U will absorb a major fraction of any neutrons produced, thereby strongly lowering the criticality potential of such a configuration. Thus it would be expected that any colloids formed will be a mixture typical of all the minerals formed in the waste package - not pure suspensions of only fissile material. Subsequent filtration would result in a solid deposit of very low fissile content - probably similar to degradation products described in the altered rock products from the reaction of solutions with rocks (in Section 6.1, above). Characteristically such materials consist of large amount of dilutent minerals compared to the amount of U or Pu minerals.

Colloids of Pu polymer are well known both as a safety concern and as a useful form for preparing very precise particulates for nuclear fuels (Ref. 50). The sol-gel processes have been used to prepare colloidal solutions of Pu which can be used for a variety of purposes. At the same time Pu polymer has been cited as a safety concern. Precipitates from concentrated acid (such as nitric) solutions when exposed to water can peptize into colloidal suspensions of material which can then transport to process equipment and possibly accumulate in critical geometries. Pu polymer forms from Pu(IV). This polymeric form of Pu(IV) is a hydrolytic form of Pu(IV) that is characterized by a bright green color and distinctive absorption spectrum which differs markedly from the ionic Pu(IV) (Ref. 50). One type of sol-gel process involves

preparation of "high-nitrate" sols from solutions of $Pu(NO_3)_4$ in HNO_3. The HNO_3 is removed from solution either by adding NH_4OH and washing the precipitate to remove NH_3 and nitrate or by solvent extraction of the HNO_3 with n-hexanol. In either case the solids are then peptized by digestion with dilute nitric acid. Highly stable solutions can be prepared with NO_3/Pu ratios of about 1.0. The resultant particles are typically 10 to 20 angstroms in size and can exist in amorphous or crystalline form (Ref. 50). An essential step in the process was found to be an aging process where the washed crystalline material was heated in water for an hour at 100 °C prior to peptization. Without such a step, depolymerization occurred in a significant amount of the material. Significant peptization does not occur unless the initial solution has a NO_3/Pu ratio of at least 0.8. Similar effects can be obtained in sulfuric acid (Ref. 51). As dissolution proceeds in the immobilized plutonium package, an initial acid solution resulting from chromate formation is made alkaline as the glass degrades. This might conceivably replicate the precipitate formation step of the sol-gel process, but the levels of acidity are not appropriate. Further, there is no scenario for the aging step. The continued flushing by J-13 water might supply an appropriate washing step and possibly produce peptization. As mentioned above, while Pu polymer is somewhat unique, peptization of clay precipitates is just as likely to occur. A pure form of a fissile colloid is not envisioned.

Data are not available to indicate whether U could form colloids. One unique aspect of ^{239}Pu is that it decays with a 5.15 MeV alpha which has been found to foster the disproportionation of Pu(V) into Pu(VI) and Pu(IV) enabling colloid formation (Ref. 52). Uranium does not have a corresponding mechanism. It is conceivable that oxides of U in the precipitates formed during degradation could be peptized in some similar manner to form U colloids. In any case there is no reason to believe such colloids would be exclusive of other diluting colloidal material.

Clearly more investigation of this issue is desirable, but there is currently no evidence that this could be a significant driver for the formation of a critical mass external to the waste package.

7. CRITICALITY EVALUATIONS

This section discusses the criticality evaluation of accumulations of fissile material in a fracture network within the thermally altered tuff, reflecting fissile deposition through the invert within the drift and into the first 50 centimeters of rock. The accumulations required for criticality are calculated for the uranium minerals (soddyite), plutonium oxide (PuO_2), and a 50/50 combination of these materials. Because of the uncertainty inherent in modeling the deposition process, the criticality calculations were performed over a range of percentages for filling the fractures with fissile material, to identify the minimum critical filling fraction, or minimal critical mass over the assumed deposition volume, which is described in the following section. The amount of fissile material in the fractures (and total fissile mass) required to cause criticality are significantly larger than the largest values found from the EQ6 calculations for the maximum accumulation of fissile material in the near-field from a source term released from a waste package containing immobilized Pu (Section 6.1.3.1); in fact the difference can be considered a margin of error which the analysis can tolerate or a defense in depth. Only the principle fissile isotopes, ^{235}U and ^{239}Pu are considered in the composition of the accumulation due to the scoping nature of this evaluation.

7.1 MCNP Model Description

The MCNP model is intended to represent the highest density and largest aperture fracture network which could be found immediately beneath a waste package. Extensive mapping of the ESF has been conducted by M&O Scientific Programs, but the results are not yet available in a suitable statistical summary which would suggest an appropriate worst case network. Therefore, the authors made a personal inspection of much of the ESF on July 23, 1997, finding the highest degree of fracturing near the Ghost Dance fault in alcove 6 and in alcove 5 (near the area being prepared for the drift scale heater test) which suggested that the worst case fracture density in the walls of an emplacement drift might be the equivalent of parallel plane spacings of ~3 cm in three dimensions. This fracture scenario is approximated with a three-dimensional array of nested cubes, 3 cm on a side. The inner cube (a minimum of 2.99 cm on a side) is filled with porous tuff. The outer cubic shell represents the fracture filled with an aqueous mixture of soddyite, PuO_2, or a 50/50 mixture of soddyite and PuO_2. The entire model volume is taken as one meter cube for the following reasons:

- The 1 meter square surface area was the largest observed, in the region of the ESF we examined, to have a high density of fractures. This is very conservative, however, because a fracture density as high as 1/3 cm was never observed over an area larger than a 20 cm square.

- A depth of 1 meter is a conservative shrinking from the depth of several meters suggested by the EQ6 analysis. While the calculations of Section 6.1 indicate that the fissile mass would be spread to a depth of several meters; a depth of 1 meter was used because the cube is the most conservative of the rectangular geometries.

When the fracture mapping statistics become available, they will be used for modeling such networks in the future. The chosen 1 meter cube containing the fissile material is surrounded by a one meter thick, cubic shell reflector of tuff with the same porosity and water content as the inner fractured tuff. A conceptual sketch of this arrangement is shown in Figure 7.1-1.

The details of the MCNP model of this geometry and the chemistry of the components are given in Ref. 83.

The evaluation examines material composition effects related to the moderator fraction in both the tuff and the fissile material. The evaluation also determines the effects of the size of the fracture aperture which range from 0.001 to 0.1 cm thick.

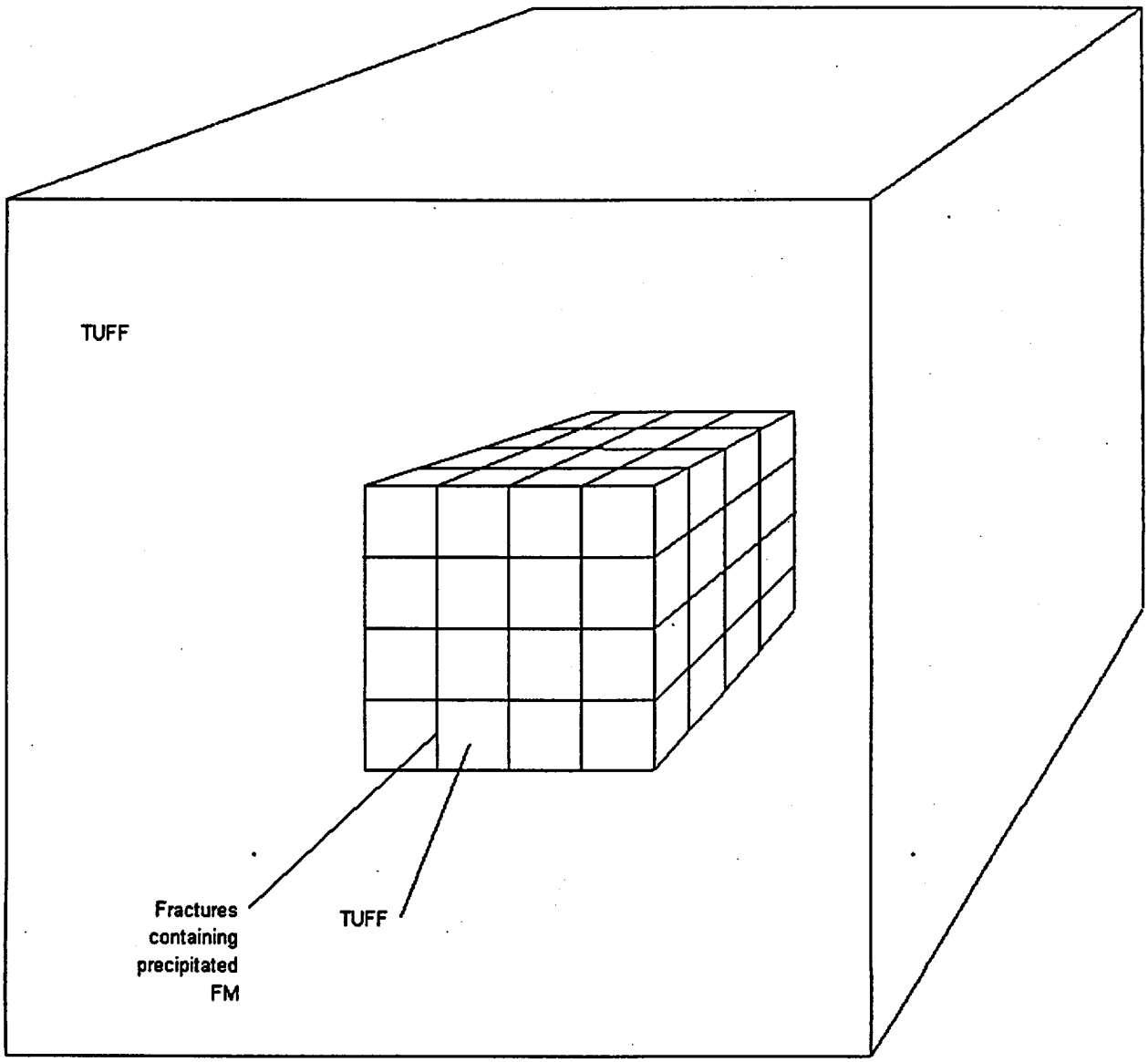

Figure 7.1-1. Illustration of Fracture Matrix Model

7.2 MCNP Results for 0.1 cm Fracture Width

The results for various fracture contents and widths are provided in this section. The results are categorized by fracture width and fracture content. Note that the fissile masses were derived from the volume fractions varied to determine subcritical concentration limits. These values are at least an order of magnitude larger than the maximum deposits obtained from the geochemistry simulation analyses.

Tables 7.2-1, 7.2-2, and 7.2-3 list the results for soddyite, plutonium oxide, and a 50/50 mixture of soddyite and plutonium oxide for fracture widths of 1 mm. The tables cover a range of fissile mass/water mixtures and interstitial water fractions in the tuff matrix. Interstitial water fractions in the tuff averaged about 4% up to a maximum of 13% (Ref. 82) which is the maximum porosity of the rock. Plots of the results are provided in Figures 7.2-1, 7.2-2, and 7.2-3.

The results for soddyite, Table 7.2-1, show a range of k_{eff} values from about 0.92 to 1.03 as the volume fraction of soddyite in the 1 mm fracture increases from 3% to 4% for a tuff water volume fraction of 13%. A similar range is seen for 8% water in the tuff, with k_{eff} values that are generally slightly lower than the 13% cases. For 4% water in the tuff, the reactivities are lower still. To obtain a value of k_{eff} of 0.93, soddyite volume fractions about 0.31, 0.32, and 0.35 are required for tuff with 13%, 8%, and 4% water by volume, respectively. The reason that there is relatively little sensitivity to variations in the amount of water in the tuff is that there is approximately the same amount of water in the fractures, since they are more than 90% filled with water. The trends of the results are illustrated in Figure 7.2-1.

Table 7.2-1 Soddyite in 1 mm Wide Fracture

Vol Frac. Soddyite	^{235}U Mass, Kg	MCNP Case ID	k_{eff}	σ
13 Volume Percent Interstitial Water in Tuff				
0.03	9.68	p87s03.o	0.9164	0.0021
0.031	10.0	p87s031.o	0.9270	0.0014
0.0312	**10.07**	**linear interpolation**	**0.93**	-
0.032	10.33	p87s032.o	0.9398	0.0018
0.04	12.91	p87s04.o	1.0266	0.0015
8 Volume Percent Interstitial Water in Tuff				
0.030	9.68	p92s03.o	0.9023	0.0020
0.0322	**10.39**	**linear interpolation**	**0.93**	-
0.034	10.97	p92s034.o	0.9536	0.0020
0.035	11.29	p92s035.o	0.9571	0.0020
0.040	12.91	p92s04.o	1.0089	0.0017
4 Volume Percent Interstitial Water in Tuff				
0.030	9.68	p96s03.o	0.8817	0.0019
0.0347	**11.2**	**linear interpolation**	**0.93**	-
0.035	11.29	p96s035.o	0.9322	0.0018
0.040	12.91	p96s04.o	0.9818	0.0026
0.050	16.13	p96s05.o	1.0592	0.0026

The general trend for plutonium oxide is the same as shown in Table 7.2-2, however the values of k_{eff} are significantly higher. They range from about 0.88 to 1.14 for 13% water and 0.87 to 1.12 for 8% water. Again, for no water in the tuff, the results are significantly lower. Volume fractions of about 0.0057, 0.0058 and 0.00604 are required to produce a k_{eff} of about 0.93 for tuff/water volume fractions of 13, 8, and 4%, respectively. Figure 7.2-2 illustrates the trend in the plutonium oxide data.

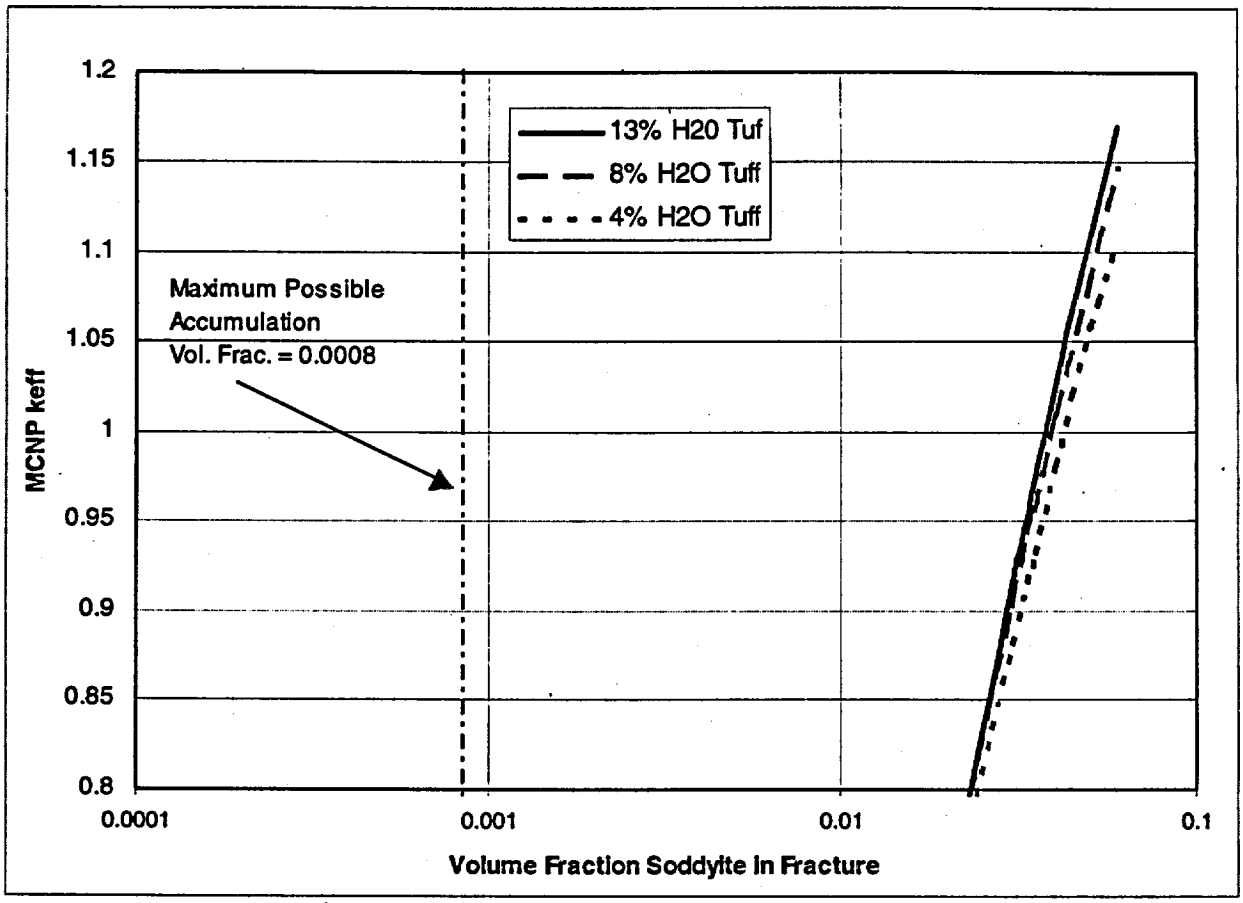

Figure 7.2-1. 1 mm Fracture Width - Soddyite Near-Field Results

Table 7.2-2 Plutonium Oxide in 1 mm Wide Fracture				
Vol Frac. PuO_2	^{239}Pu Mass, Kg	MCNP Case ID	k_{eff}	σ
13 Volume Percent Interstitial Water in Tuff				
0.005	4.89	p87p005.o	0.8783	0.0016
0.0057	**5.57**	**linear interpolation**	**0.93**	-
0.006	5.86	p87p006.o	0.9522	0.0020
0.010	9.77	p87p01.o	1.1388	0.0018
8 Volume Percent Interstitial Water in Tuff				
0.005	4.89	p92p005.o	0.8719	0.0020
0.0058	**5.67**	**linear interpolation**	**0.93**	-
0.006	5.86	p92p006.o	0.9434	0.0019
0.010	9.77	p92p01.o	1.1184	0.0020
4 Volume Percent Interstitial Water in Tuff				
0.005	4.89	p96p005.o	0.8631	0.0018
0.006	5.86	p96p006.o	0.9279	0.0023
0.00604	**5.9**	**linear interpolation**	**0.93**	-
0.007	6.84	p96p007.o	0.9793	0.0025
0.010	9.77	p96p01.o	1.0927	0.0020

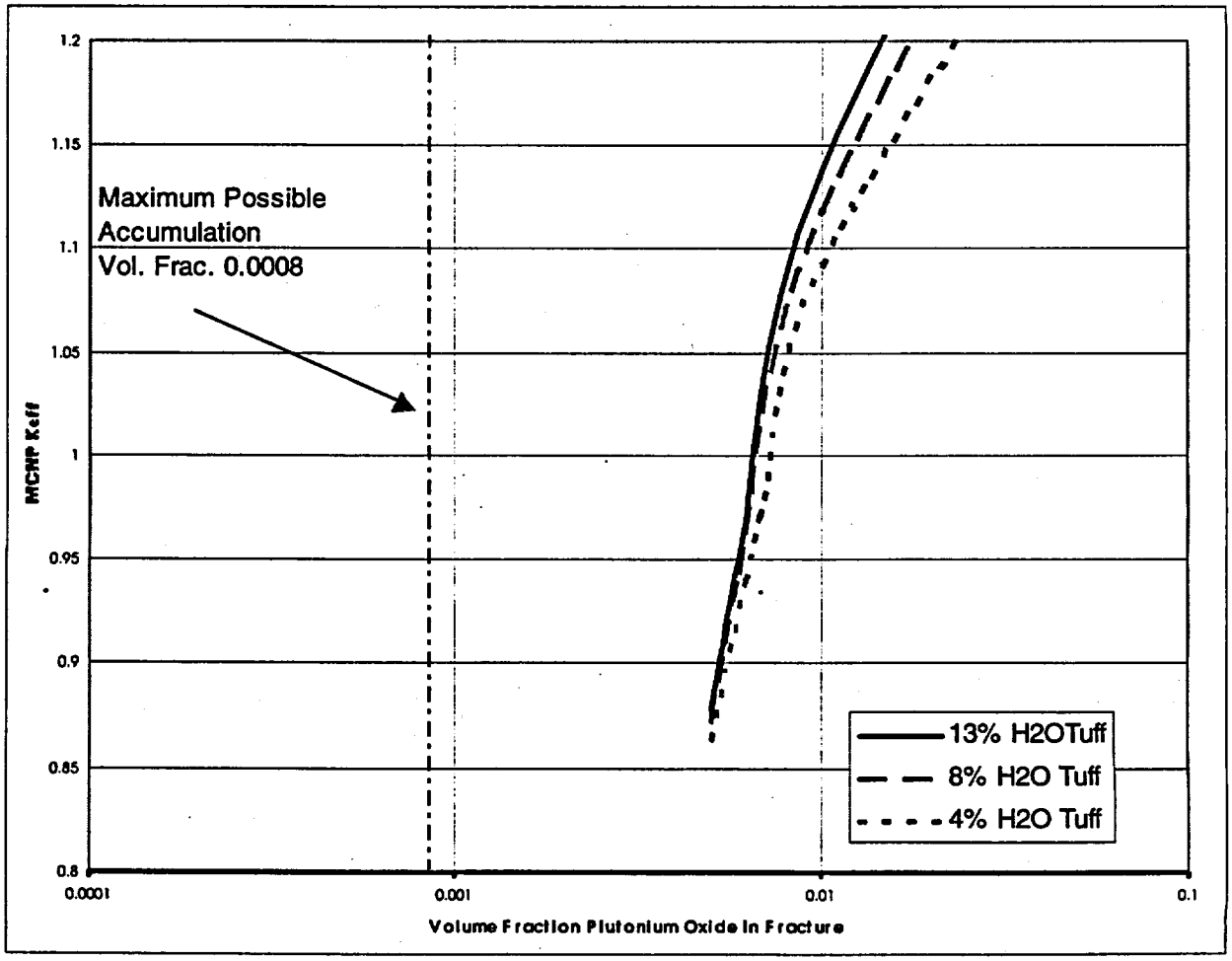

Figure 7.2-2. 1 mm Fracture Width - Plutonium Oxide Near-Field Results

The evaluation of the 50/50 mixture of soddyite and plutonium oxide in water provides results bracketed by those of soddyite and plutonium oxide, see Table 7.2-3. The k_{eff} values range from about 0.91 to 1.19 for a tuff interstitial water volume percent of 13% with slightly smaller values for 8%. The fissile mixture volume percents required for a 0.93 k_{eff} are about 0.0096, 0.0099 and 0.01 for 13%, 8% and 4% tuff water, respectively. Figure 7.2.1-3 illustrates the data trend.

Table 7.2-3 50/50 Mixture of Plutonium Oxide and Soddyite in 1 mm Wide Fracture

Vol Frac. Mixture	$^{235}U+^{239}Pu$ Mass. Kg	MCNP Case ID	k_{eff}	σ
13 Volume Percent Interstitial Water in Tuff				
0.009	5.85	p87sp009.o	0.9061	0.0025
0.0096	**6.24**	**linear interpolation**	**0.93**	-
0.010	6.50	p87sp01.o	0.9483	0.0013
0.020	13.00	p87sp02.o	1.1945	0.0024
8 Volume Percent Interstitial Water in Tuff				
0.009	5.85	P92sp009.o	0.8989	0.0020
0.0099	**6.44**	**linear interpolation**	**0.93**	-
0.010	6.50	p92sp01.o	0.9329	0.0018
0.020	13.00	p92sp02.o	1.1641	0.0015
4 Volume Percent Interstitial Water in Tuff				
0.010	6.50	p96sp01.o	0.9207	0.0022
0.0102	**6.63**	**linear interpolation**	**0.93**	-
0.011	7.15	p96sp011.o	0.9590	0.0019
0.012	7.80	p96sp012.o	0.9856	0.0018
0.020	13.00	p96sp02.o	1.1336	0.0017

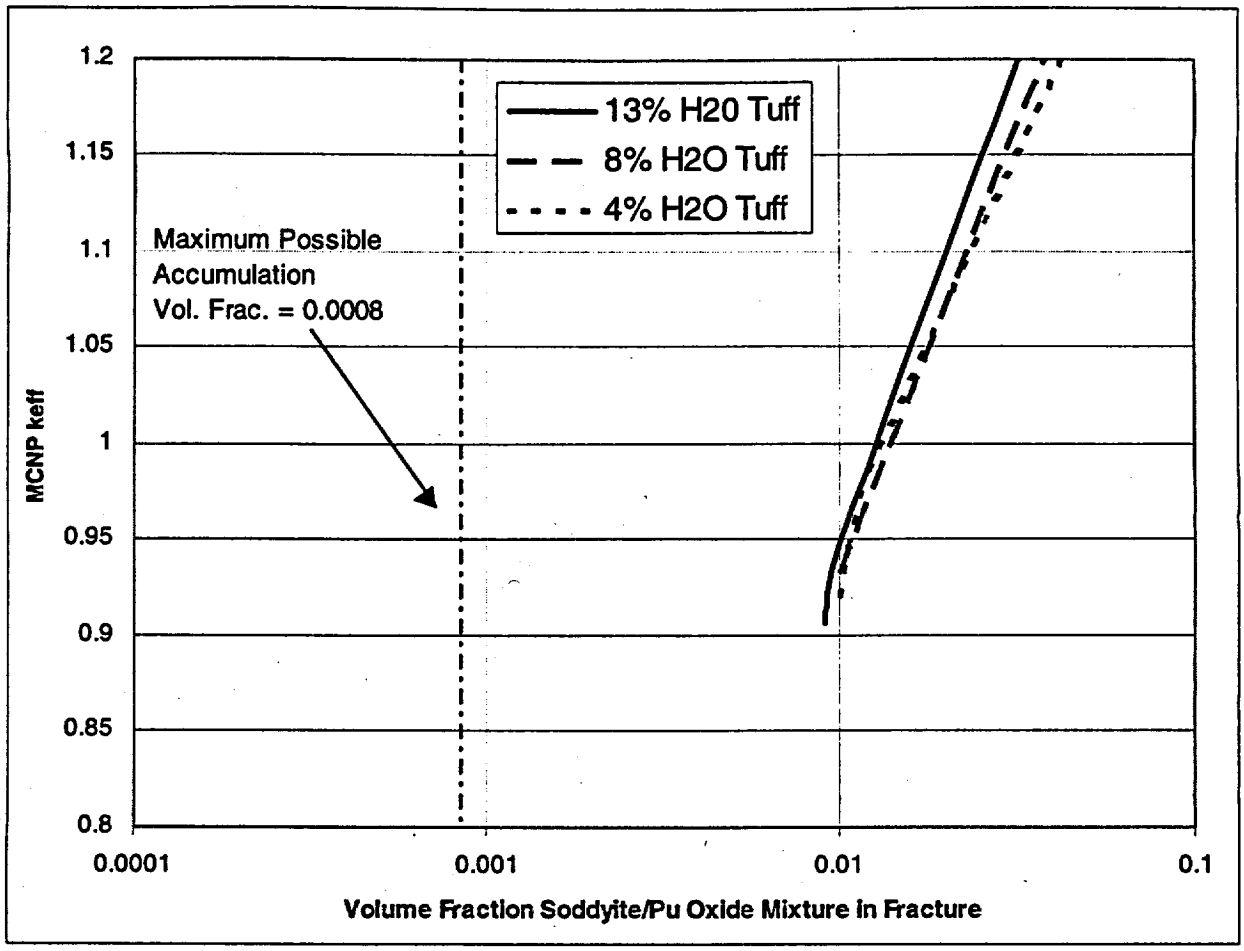

Figure 7.2-3. 1 mm Fractiure Width - 50/50 soddyite/Pu Oxide Mixture Near-Field Results

As shown in the above figures, the fissile mass required to achieve criticality exceeds by an order of magnitude the maximum accumulation resulting from the geochemical simulation analyses. This is based on the results reported in Table 6.1-4, which showed the highest fissile accumulation of all the waste forms and scenarios evaluated in Tables 6.1-1 to 6.1-9 (note that the insignificantly small accumulation with the slightly higher volume fraction that is shown in Table 6.1-6 has been ignored for this comparison). An additional conservatism is that the maximum accumulations reported in Tables 6.1-1 to 6.1-9 typically occurred only over a very small portion of the fracture, with lesser accumulations occurring throughout the majority of the fracture. The criticality calculations, on the other hand, modeled a uniform accumulation throughout the entire fracture network.

8. SENSITIVITY TO UNCERTAIN PARAMETERS

8.1 Sensitivity to Fracture Thickness

The criticality safety criterion can be satisfied with a maximum k_{eff} from MCNP of about 0.93. An evaluation of the fissile masses that produce this k_{eff} is presented in this section. A further evaluation determines the reactivity of fissile masses of both plutonium oxide and soddyite/plutonium oxide mixtures for a total fissile mass equal to the mass of soddyite that produces a k_{eff} of 0.93. As noted in the previous section, the fissile mass required to achieve criticality exceeds by an order of magnitude the maximum accumulation resulting from the geochemical simulation analyses.

The tables in the previous sections provide the reactivity results for the fissile material as a function of fracture width or fissile concentration. In addition, an estimate of the fissile volume fraction and weight that would produce a k_{eff} of 0.93 is tabulated base on linear interpolation. These interpolated values are gathered and listed in Table 8.1-1 as a function of spacing and material. Plots of the data are presented in Figures 8.1-1 and 8.1-2. The trend of the data, see Table 8.1-1 and Figure 8.1-1, indicates that the volume fraction of fissile material is inversely proportional to the fracture width by almost a constant factor, i.e. the volume fraction approximately doubles for a reduction in the width by a factor of 2. Stated another way, and illustrated by Figure 8.1-2, the fissile mass to produce a k_{eff} of 0.93 essentially remains constant for a given material. For uranium, the required weight seems almost constant with small deviations probably due to the statistical nature of the results and linear interpolation. However, for the materials containing plutonium, there seems to be a slight increase in mass as the fissile volume fraction increases. This may also be due to statistics and interpolation. However, since the trend is followed for four sets of data, it is probably related to either the fissile mass increase or the decrease in the hydrogen content of the fissile material.

Table 8.1-1 0.93 Keff Fissile Volume Fractions and Weights

Fracture Width, cm	13% Water VF in Tuff			8% Water VF in Tuff		
	soddyite	PuO_2	Mixture	soddyite	PuO_2	Mixture
	Fissile Volume Fraction			Fissile Volume Fraction		
0.100	0.031	0.006	0.010	0.032	0.006	0.01
0.010	0.355	0.062	0.105	0.438	0.074	0.125
0.005	0.714	0.125	0.214	0.899	0.152	0.258
0.002	-	0.317	0.541	-	0.388	0.662
0.001	-	0.638	-	-	0.784	-
	Fissile Weight, Kg			Fissile Weight, Kg		
0.100	10.07	5.57	6.24	10.39	5.67	6.44
0.010	11.81	6.25	7.03	14.57	7.45	8.37
0.005	11.89	6.31	7.18	14.97	7.67	8.66
0.002	-	6.40	7.27	-	7.84	8.89
0.001	-	6.45	-	-	7.92	-

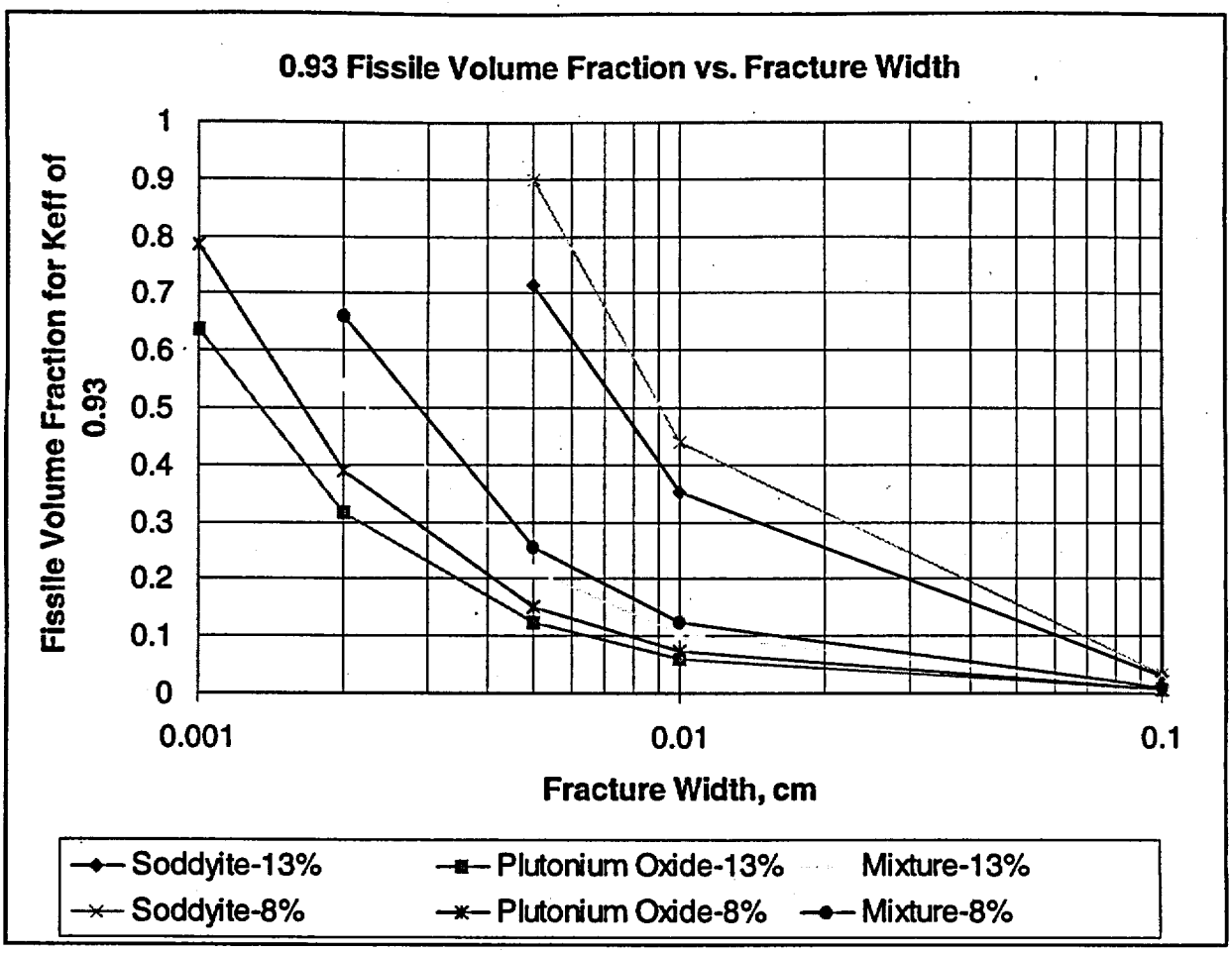

Figure 8.1-1. Trend of Critical Fissile Volume Fraction with Tuff Fracture Width

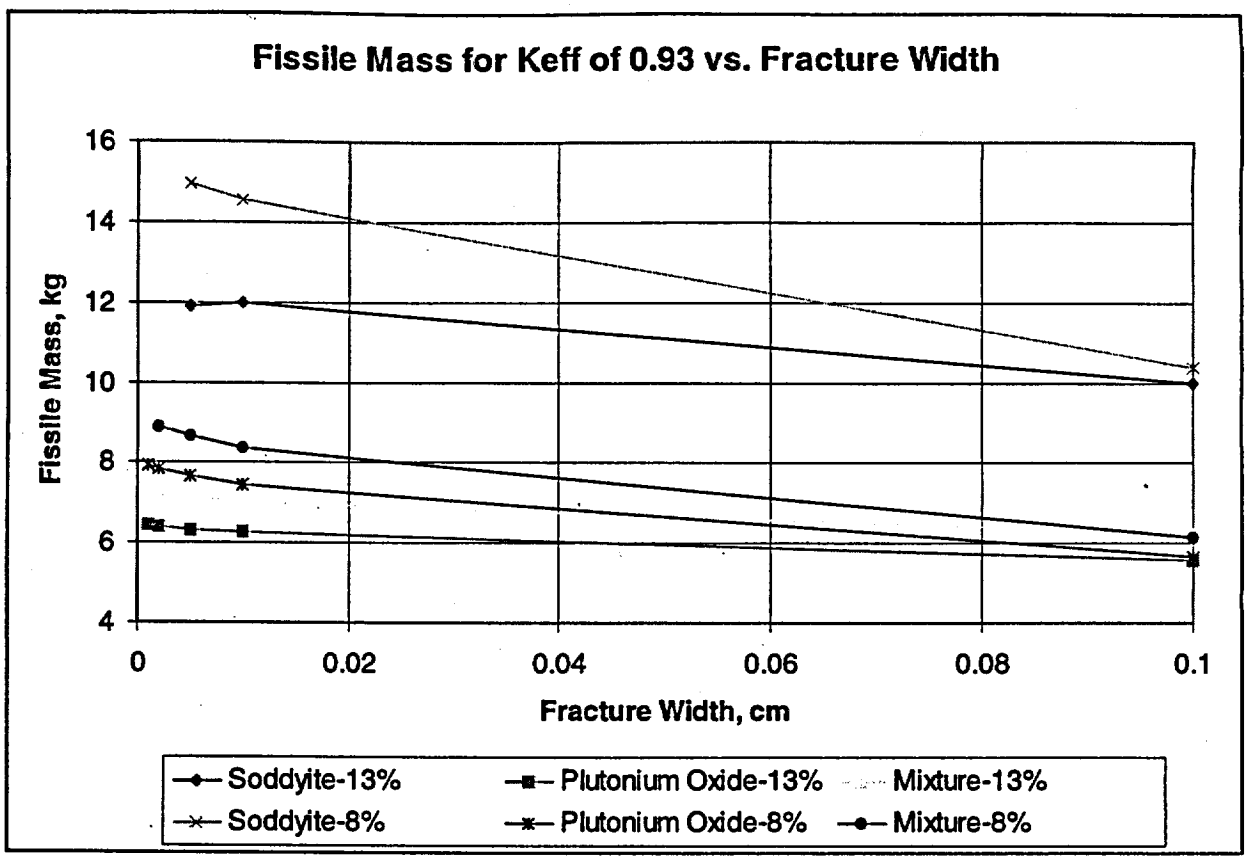

Figure 8.1-2. Trend of Critical Fissile Mass with Tuff Fracture Width

8.2 Sensitivity to Volume of Deposition

The near-field volume over which the fissile material might be deposited could be no greater than the footprint of the waste package (cross sectional area) multiplied by the maximum depth of penetration of the high fissile concentration (3.35 meters, as shown in cell 3 of Table 6.1-3). It is possible that the outflow from the waste package could be concentrated over a much smaller area than the entire package footprint. Therefore the criticality calculations in Section 7, conservatively, used the much smaller volume of a 1 meter cube. The fact that this is conservative with respect to the maximum volume is demonstrated by calculations of k_{eff} for a sequence of volumes ranging from the 1 meter cube to the full volume of the 3.35 meter depth multiplied by the horizontal cross sectional area of the waste package interior (length multiplied by the inside diameter), with the results shown in Table 8.2-1. For these cases, a fixed mass of fissile material, (10.07 kg of ^{239}Pu corresponding to the total amount of Pu deposited in the fractures of the 1x1x1 m cube at a density of 10 wt% PuO_2 and 90 wt% water), is distributed homogeneously throughout the increasing volumes. It was also assumed, conservatively, that the tuff in the homogeneous cases contained 13 wt% interstitial water. Note that the geochemical simulation analyses indicate that these fissile accumulations cannot be achieved.

Table 8.2-1. Comparison of k_{eff} as a function of volume for a fixed fissile mass homogeneously distributed

Dimensions (cm)	k_{eff}	sigma
100x100x100	1.098	0.002
150x150x150	0.773	0.001
250x150x250	0.419	0.001
340x150x334	0.259	0.0002

From the results of Table 8.2-1, it can be concluded that spreading a fixed amount of plutonium over an increasing volume will decrease the k_{eff}. Therefore, the 1 meter cube used for most of the criticality calculations of this study is seen to be conservative with respect to the larger volume which could be occupied by the fissile material.

It should be noted that the k_{eff} for the homogeneous 1 meter cube case, the first row of Table 8.2-1, can be compared with the k_{eff} for the heterogeneous case, given in Table 7.2-2, which consisted of a 1 meter cube divided into 3 orthogonal sets of 33 fracture planes which contain the PuO_2. The k_{eff} for this heterogeneous case is 1.0807 ± 0.0024. Thus the homogenization provides only a slight increase in k_{eff}. This very slight increase is to be expected, since the 3 cm fracture spacing is approximately the same as the mean free path of neutrons in tuff, so that neutrons in the heterogeneous case can typically reach neighboring planes of fissile material by the time they have their first collision. This is in contrast to published work describing homogenization of systems with larger spaced fractures filled with fissile material, which showed a 20% increase on homogenization (Ref. 74). In that case the fracture spacing was at least 10 cm, which is much greater than the mean free path.

8.3 Sensitivity to Dissolution Rates of the Immobilized Plutonium Waste Form

For the immobilized plutonium waste form, the only significant fissile deposits in the near field occurred under conditions of high pH in the source term. As indicated in the discussion of scenarios in Section 4, this high pH will only contain significant fissile material if the HLW glass is not completely degraded by the time the fissile is released from the immobilized plutonium waste form. Since the waste form is developed so that it will be much more resistant to aqueous corrosion than the ordinary HLW glass, the only way in which the release of significant amounts of fissile material could precede the complete degradation of the HLW glass is for the corrosion of the latter to be stretched out in time by delayed, or intermittent, contact of water with some of the HLW canisters.

The most likely way for this delay to occur is for water to fill, or flow through, only the lower part of the horizontal waste package. The canisters which happen to be above the level of significant water contact will not be degraded until the lower canisters have degraded to such an extent that they can no longer support the upper canisters, which will ultimately fall to the bottom of the waste package where they will be able to contact the water and be degraded. Thus all the HLW canisters should be degraded in at most 10x the time it could take for one canister to fully degrade. Therefore, if the immobilized plutonium waste form can be

guaranteed to degrade at less than 1/10 of the rate for the HLW glass, there will be no significant concentration of fissile mass in the near-field, and certainly no criticality.

9. CONSEQUENCES OF A STEADY STATE EXTERNAL CRITICALITY

The purpose of this section is to provide an estimate of the consequences, in terms of increased radionuclide inventory, of a criticality event in fissile material deposited in the fracture network in the tuff external to a WP under the assumption that such an unlikely event does occur. For this purpose, a steady state criticality is used; it has been shown, in Section 8 of Reference 86, that the steady state criticality gives a larger increase in radionuclide inventory than does a transient criticality.

Criticality evaluations have been made for several fracture and fissile material combinations modeled as a 1 m cube (Ref. 83), as discussed in Section 7. The consequences of such a criticality event will be evaluated with respect to changes in the radionuclide inventory of the waste package material. The assumptions required in the models to achieve a critical configuration are sufficiently extreme that a representative calculation is sufficient to provide an estimate of criticality consequences. Thus, the MCNP analyses for a 0.0001 m fracture width was selected as a representative geometry for the consequence analysis. The parameters in this scenario are assumed to provide an upper bound on conditions supporting criticality (high infiltration, water content of tuff material, sufficient fissile material).

9.1 Estimated Power Level

The criticality scenarios discussed in Section 7 depict a situation where fissile material from a degraded and breached WP gradually infiltrates and collects into rock fractures gradually approaching concentrations where criticality (k_{eff}=1) may be possible, particularly if water entrapment in the tuff material increases after deposition of fissile material. As shown in Figure 7.2-4, the criticality of a given fissile mass is sensitive to both the water content of the fractures and the tuff material. Once criticality is reached, power levels can be expected to rise until the water loss from vaporization balances the inflow rate. Additional water loss will reduce the overall water volume fraction, introducing a negative reactivity acting to terminate the criticality event. The maximum steady state power will then be a value sufficient to raise the inflow water to the core temperature, maintain the temperature against conduction losses at the core boundaries, and evaporate the inflow water mass.

Since the analysis is for near field locations and significant fracturing is assumed in the tuff material, the system pressure was assumed to be atmospheric (1013.25 kPa) and water vapor exits the power producing volume at the ambient pressure. The ambient temperature was assumed to be 323.15 K (50.0 °C) (Ref. MGDS-RD 3.7.3.3.B). A conservatively high 50 mm/year rate of water inflow (focused flow) was assumed to maximize the estimated power level and, hence, the burnup. The power level was estimated from the equation

$$P = W*C_p*(T-T_0) + W*h_{fg} + k*S*(T-T_0) \qquad \text{(Equation 9.1)}$$

where

P = Power (J/sec)
W = Flowrate (kg/sec) = Inflow (m/sec)*Surface area (m^2)*Density (kg/m^3)
C_p = Heat Capacity (4.174e3 J/kg-K Ref. 37)
$h_{fg}(T)$ = Heat of vaporization (Water) (J/kg)
k = Thermal Conductivity (Tuff) (1.38 J/sec-m-K Ref. 79)
S = Conduction shape factor for cubes (8.24*L Ref. 80)
L = Length (cube edge) (m).

Equation 9.1 was evaluated and results shown in Table 9.1-1 for temperatures between ambient and 373.15 K to estimate the maximum sustainable power level.

Table 9.1-1. Power from Equation 9.1

Temperature K	Temperature °C	h_{fg} (J/kg)	Inflow Heating (watts)	Vaporization (watts)	Conduction (Watts)	Power (watts)
323.15	50.0	2.426e+06	0	22.8	0	22.8
343.15	70.0	2.329e+06	7.84e-07	21.9	227.4	249
373.15	100.0	2.252e+06	1.96e-06	21.2	568.6	590

The above power represents a conservative ideal condition since, in reality, several mechanisms will act to disrupt equilibrium. Some of these mechanisms include decreases in the drift flow rate resulting from climatic cycles, non-uniform distribution of water in fractures, and non-uniform distributions of interstitial water in the tuff. The combined effect of these mechanisms will likely limit any single near-field criticality event to a relatively short duration, with periodic recurrences as conditions such as above permit. Therefore, use of a steady state power of 0.59 kW (Table 9.1-1) to estimate the total burnup resulting from a long term postclosure near-field criticality should provide a reasonable upper bound to the cumulative effect of periodic events.

The MCNP case used as a basis for the criticality consequence analysis was Case t87p10.o (10.1 Kg ^{239}Pu in a 1 m^3 volume, 0.1 volume percent PuO_2 in 0.0001 m fractures) from Table 7.3-5 in Ref. 83, which was the critical case with the lowest PuO_2 volume fraction in the rock fractures for 0.0001 m fractures. This case, with an initial k_{eff} of 1.081, represents a conservatively high initial ^{239}Pu loading in the rock fractures. However, as shown in Section 7, the critical mass for material in the fractures declines with increasing interstitial water content in the adjacent rock. While water inflow was assumed to continue, deposition of additional fissile material during the steady state criticality was not included in the burnup evaluation. The termination of the criticality event was defined by sufficient loss of fissile material and buildup of fission products to reduce the k_{eff} below 1.0. This occurred at about 4,000 years where the criticality event was terminated and the radionuclide inventory decay followed for an additional 60,000 years.

9.2 Effects of a Steady State Criticality on Radionuclide Inventory

To evaluate long term effects on the radionuclide inventory at the WP location, the computer code SAS2H was run using the MCNP case t87p10.o from Table 7.3-5 in Ref. 83 (summarized above) as the basis. Since the SAS2H code requires the neutronic system to be represented in a 1-dimensional sense, it was necessary to convert the three-dimensional MCNP model (an array of 0.03 m cubes) to an equivalent 1-dimensional model consisting of an infinite array of unit cells which determine the shape and dimensions for cross-section processing. The unit cell specified for the SAS2H model was a symmetric slab cell consisting of a sheet of the PuO_2-H_2O fuel mixture between moderator layers of the tuff-water composition. A finite fuel volume was specified for the input power and nuclide inventory tracking. Equivalence was defined for this analysis where the SAS2H k_{eff} matched the MCNP value. For the MCNP case, fuel sheets were 0.0001 m thick surrounding 0.0299 m cubes. The initial cell width for the SAS2H model was reduced by a factor of 3 from the MCNP model to convert from 3-D to 1-D. The fuel sheet thickness and cell width were varied in the SAS2H model to obtain a initial k_{eff} matching the MCNP value. This resulted in an initial k_{eff} of 1.083 for a fuel thickness of 0.00012 m and a cell width of 0.008 m compared to the MCNP value of 1.081. Burnup steps of 1,000 years were taken at a power level of 0.59 kW until the k_{eff} reached sub-critical ($k_{eff} < 1.0$) which occurred after 4,000 years.

The total activity of the radionuclides from the criticality event in curies and the fraction due to ^{239}Pu following the criticality is given in Table 9.2-2 for cooling increments of 10,000 years up to 60,000 years following termination of the criticality event. As shown, most of the activity results from the plutonium decay. The Pu mass after the 60,000 Yr cooling period was 3.7 Kg (initial mass - 10.1 Kg).

Table 9.2-2. Radioactivity in Curies Following a Criticality Event

Isotope	0 years	10,000 years	20,000 years	30,000 years	40,000 years	50,000 years	60,000 years
^{239}Pu	479	359	269	202	152	114	85.3
Total	560	387	279	206	153	115	85.6
^{239}Pu fraction	0.86	0.93	0.97	0.98	0.99	0.995	0.996

Input data and selected output data including the complete radionuclide activity data from the SAS2H case are listed in Appendix B.

10. MAJOR FINDINGS

- The principal opportunity for accumulation of fissile material in the near-field, and the host rock immediately below the waste package, occurs when the pH of the source term solution is greater than 10; under such circumstances the solubility of U will be at its highest, and the reaction with neutral pH invert material will be the strongest. This establishes a strong data need for accurate waste form dissolution rate. If this rate is sufficiently slower than the DHLW glass dissolution rate there will be very little fissile material released during the high pH period. See Section 6.1.3.

- The maximum accumulation of uranium possible in the invert and the host rock immediately below a single waste package, under physically realistic conditions, is less than 2 kg. The maximum accumulation of plutonium is two orders of magnitude smaller.

- Since most of the near-field fracture/void space will fill with non-fissile precipitate from the source flow, the only possibility of accumulation of a critical mass in the near field is if the fracture aperture is greater than 1mm. This is based on the critical masses of 6 kg for plutonium and 12 kg for uranium, which were calculated for a very conservative fracture network filled to approximately 0.3% with fissile material. The critical mass for uranium is more than 6 times the maximum which could be accumulated under the worst case physical conditions as indicated in the previous item. See Section 8.1.

- The range of fracture apertures considered in this study (0.01 mm to 1 mm), and fracture spacing, is based on direct observation by the authors. The USGS has been preparing a comprehensive study of the ESF fractures which should give more definitive data on the subject. See Section 7.1.

- Review of geologic literature and field data strongly suggests that there are no formations at Yucca Mountain which would be capable of hosting the types of uranium deposits which could lead to a critical mass of highly enriched uranium. There should be some survey of broader geologic opinion on the subject and concurrence with the conclusions expressed here. See Section 6.2.

- Zeolites, smectities, and other naturally adsorbing materials present in the host rock beneath the repository can accumulate amounts of uranium which are significantly larger than the natural background, but are not within an order of magnitude of the amount which would be necessary to cause criticality. See Section 6.3.

- For the immobilized plutonium waste package the primary determinant of the concentrations in the source term, is the HLW chemistry, rather than the much smaller amount of immobilized Pu waste form. See Sections 5.2 and 5.3.

- The external criticality potential from a MOX waste package source term is much less than from the immobilized Pu waste form because the effective enrichment is much smaller, and there is no unique MOX chemistry which would cause it to accumulate in

the external environment any more readily than the fissile elements from the immobilized Pu source term. See Section 6.1.5.

- Cumulative effects from multiple waste packages have been considered and shown to not significantly effect the above findings because the *worst case* accumulation in local geologic features could saturate the accumulation capability of the invert and the immediately adjacent rock with the contents of a single waste package, and such a worst case has already been reflected in the above findings. See Section 6.1.3.5.

- In the extremely unlikely event that an external criticality does occur, the effects will be minimal, even for the high effective enrichment of the immobilized Pu waste form. It is estimated that the maximum power would be no more than 500 Watts and the maximum duration would be no more than 4000 years. The increased radionuclide inventory at termination from such a criticality would be less than 14% of the radioactivity present from Pu (< 480 curies). See Section 9.

11. REFERENCES

1. *Report on Evaluation of Plutonium Waste Forms for Repository Disposal, Rev 01,* DI#: A00000000-01717-5705-00009 REV 01, CRWMS M&O, March 1996.

2. *Degraded Mode Criticality Analysis of Immobilized Plutonium Waste Forms in a Geologic Repository, Rev 01,* DI#: A000000000-01717-5705-00014 REV 01, CRWMS M&O, March 1997

3. *Report on Evaluation of MOX Spent Fuel from Existing Reactors for Repository Disposal, Rev. 01,* DI#: A00000000-01717-5705-00012 REV01, CRWMS M&O, October 1996.

4. *Evaluation of the Potential for Deposition of Uranium/Plutonium from Repository Waste Packages,* DI#: BBA0000000-01717-020-00050 REV 00, CRWMS M&O, September 1997.

5. *Probabilistic External Criticality Evaluation,* DI#: BB0000000-01717-2200-00037 REV 00, CRWMS M&O, May 1996.

6. *Standard Specification for Concrete Aggregates,* ASTM Designation C33-93, American Society for Testing and Materials, Philadelphia, PA.

7. Harrar, J. E., Carley, J. F., Isherwood, W. F., and Raber, E., *Report of the Committee to Review the Use of J-13 Well Water in Nevada Nuclear Waste Storage Investigations,* UCID-21867, Lawrence Livermore National Laboratory (LLNL), Livermore, CA, 1990.

8. Lichtner, P. C., *Continuum Model for Simultaneous Chemical Reactions and Mass Transport in Hydrothermal Systems,* Geochemica et Cosmochimica Acta, Vol. 49, pp. 779-800, 1985.

9. Lichtner, P. C., *The Quasi-stationary state Approximation to Coupled Mass Transport and Fluid-Rock Interaction in a Porous Medium,* Geochimica et Cosmochimica Acta, vol. 52, pp. 143-165, 1988.

10. Knapp, R. B., *A Lagrangian Reactive Transport Simulator with Successive Paths and Stationary-States: Concepts, Implementation and Verification,* UCRL-100952 Rev 1, Preprint, LLNL, 1989.

11. Nash, J. T., Granger, H. C., and Adams, S. S., *Geology and Concepts of Genesis of Important Types of Uranium Deposits,* Economic Geology, 75th Anniversary Volume, pp. 63-116, 1981.

12. Gruner, J. W., *Concentration of Uranium in Sediments by Multiple Migration-Accretion,* Economic Geology, Vol. 51, pp. 495-519, 1956.

13. Bodvardson, G. S., and Bandurraga, T. M., *Development and Calibration of the Three-Dimensional Site-Scale Unsaturated Zone Model of Yucca Mountain, Nevada*, Lawrence Berkeley National Laboratory report, 1996.

14. Jones, B. E., *The Geology of Collins Bay Deposit, Saskatchewan, Canada*, CIM Bulletin, Vol. 73, pp. 84-90, 1980.

15. Kerr, P. F., *Uranium Emplacement in the Colorado Plateau*, Geological Society of America Bulletin, Vol. 69, pp. 1075-1111, 1958.

16. Huff, L. C., and Lesure, F. G., *Diffusion Features of Uranium-Vanadium Deposits in Montezuma Canyon, Utah*, Economic Geology, Vol. 57, pp. 226-237, 1962.

17. Kimberley, M. M., *Short Course in Uranium Deposits, Their Mineralogy and Origin*, Mineralogical Association of Canada, Short Course Handbook 3, p. 521, 1978.

18. Fischer, R. P., *The Uranium and Vanadium Deposits of the Colorado Plateau Region*, Ore Deposits of the United States 1933/1967, Graton-Sales Vols. New York: AIME, pp. 735-746, 1968.

19. Dodd, P. H., *Happy Jack Mine, White Canyon Utah*, RMO-660, U. S. Atomic Energy Commission, p. 23, 1950.

20. Kelley, D. R., and Kerr, P. F., *Urano-organic Ore at Temple Mountain Utah*, Geological Society of America Bulletin, Vol. 69, pp. 701-756, 1958.

21. Geomatrix Consultants, *Probabilistic Volcanic Hazard Analysis for Yucca Mountain, Nevada,* Volume I of II, Draft Report, prepared for CRWMS M&O, Vienna, VA, 1996.

22. Berger, I. A., *The role of Organic Matter in the Accumulation of Uranium, in Formation of Uranium Ore Deposits*, IAEA-SM-183/19, International Atomic Energy Agency, 1974.

23. Hess, F. L., *Uranium, Vanadium, Radium, Gold, Silver, and Molybdenum Sedimentary Deposits*, Ore Deposits of the Western States, Lindgren Volume of the American Institute of Mining and Metallurgical Engineers, New York, 1933.

24. Chenoweth, W. L., *The Uranium-Vanadium Deposits of the Uravan Mineral Belt and Adjacent Areas, Colorado and Utah*, New Mexico Geological Society Guidebook, 32nd Field Conference, Western Slope Colorado, pp. 165-170, 1981.

25. Yamaguchi, D. K., and Hoblitt, R. P., *Tree-Ring Dating of Pre-1980 Volcanic Flowage Deposits at Mount St. Helens, Washington*, Geological Society of America Bulletin, Vol. 107, pp. 1077-1093, 1995.

26. Klein, C., and Hurlbut Jr., C. S., *Manual of Mineralogy*, John Wiley and Sons, New York, p. 596, 1985.

27. Harris, Ann, and Tuttle, Esther, *Geology of National Parks, 3rd Edition*, Kendall-Hunt Publishing Company, Dubuque, IA, 1983.

28. Hoeve, J. and Sibbald, T. I. I., *Rabbit Lake Uranium Deposit*, Uranium in Saskatchewan, Geological Society of Saskatchewan Special Publication 3, pp. 331-354, 1977.

29. Hoeve, J. and Sibbald, T. I. I., *On the Geneses of Rabbit Lake and Other Uncomformity-Type Uranium Deposits in Northern Saskatchewan Canada*, Economic Geology, Vol 73, pp. 1450-1473, 1978.

30. Harper, C. T., *The Geology of the Cluff Lake Uranium Deposits, Northern Saskatchewan*, CIM Bulletin, Vol. 71, pp. 65-78, 1978.

31. Clark, R. J. McH., Homeniuk, L. A., and Bonner, R., *Uranium Geology in the Athabasca and a Comparison with Other Canadian Proterozoic Basins*, CIM Bulletin, Vol. 75, pp. 91-98, 1982.

32. Perfect, D. L., Faunt, C. C., Steinkampf, W. C., and Turner, A. K., *Hydrochemical Data Base for the Death Valley Region, California and Nevada,* Open-File Report 94-305, U.S. Geological Survey, 1995.

33. Craig, R. W., and Johnson, K. A., *Geohydrologic Data for Test Well UE-25p#1, Yucca Mountain Area, Nye County, Nevada*, Open-File Report 84-450, U.S. Geological Survey.

34. Triay, I., Degueldre, C., Wistrom A., Cotter, C., and Lemons, W., *Progress Report on Colloid-Facilitated Transport at Yucca Mountain*, Los Alamos National Laboratory Yucca Mountain Milestone #3383, 1996.

35. Clark, L. A., and Burrill, G. H. R., *Unconformity-related Uranium Deposits Athabasca Area, Saskatchewan, and East Alligator Rivers Area, Northern Territory, Australia,* CIM Bulletin, Vol 74, No. 831, pp. 63-72, 1981.

36. Katayama, N., Kubo, K., and Hirono, S., *Geneses of Uranium Deposits of the Tono Mine, Japan*, Formation of Uranium Ore Deposits, IAEA-SM-183/19, International Atomic Energy Agency, pp. 437-452, 1974.

37. *Criticality Consequence Analysis Involving Intact PWR SNF in a Degraded 21 PWR Assembly Waste Package*, DI#: BBA000000-01717-0200-00057 REV 00, CRWMS M&O.

38. Grow, J. A., Barker, C. E., and Harris, A. G., *Oil and Gas Exploration Near Yucca Mountain, Southern Nevada*, Proceedings of the Fifth Annual High Level Radioactive Waste Management Conference, Volume 3, American Nuclear Society, La Grange Park, IL, pp. 1298-1315, 1994.

39. Rackley, R. I., *Origin of Western-States Type Uranium Mineralization*, Handbook of Strata-Bound and Stratiform Ore Deposits, II, Regional Studies and Specific Deposits, Volume 7, Au, U, Fe, Mn, Hg, Sb, W, and P Deposits, Elsevier Scientific Publishing Company, New York, pp. 89-156, 1976.

40. Buesch, D. C., Spengler, R. W., Moyer, T. C., and Geslin, J. K., *Proposed Stratigraphic Nomenclature and Macroscopic Identification of Lithostatigraphic Units of the Paintbrush Group Exposed at Yucca Mountain, Nevada*, Open-File Report 94-469, U.S. Geological Survey, p. 45, 1996.

41. Moyer, T. C. and Geslin, J. K., *Lithostatigraphy of the Calico Hills Formation and Prow Pass Tuff (Crater Flat Group) at Yucca Mountain, Nevada,* Open-File Report 94-460, U. S. Geological Survey, p. 59, 1995.

42. Hoover, D. L., Swadley, W. C., and Gordon, A. J., *Correlation Characteristics of Surficial Deposits with a Description of Surficial Stratigraphy in the Nevada Test Site Region*, Open File Report 81-512, U. S. Geological Survey, p. 27, 1981.

43. Taylor, E. M., *Impact of Time and Climate on Quaternary Soils in the Yucca Mountain Area of the Nevada Test Site*, Unpublished Masters Thesis, University of Colorado, Boulder CO, p. 217, 1986.

44. Diehl, S. F., and Chornack, M. P., *Stratigraphic Correlation and Petrography of the Bedded Tuffs, Yucca Mountain, Nye County, Nevada,* Open File Report 89-3, U.S. Geological Survey, p. 152, 1990.

45. Bredehoeft, J. D., King, M. J., and Tangborn, W., *An Evaluation of the Hydrology at Yucca Mountain; The Lower Carbonate Aquifer and Amargosa River*, Yucca Mountain Project Oversight report for Inyo County California and Esmeralda County Nevada, P.O. Box 352 (234 Scenic Drive), LaHonda, CA, p. 28, 1996.

46. Shenker, A. R., Robey, T. M., Rautman, C. A., and Barnard, R. W., *Stochastic Hydrologic Units and Hydrologic Properties Development for Total-System Performance Assessments,* SAND94-0244, Sandia National Laboratory, 1995.

47. Vaniman, D. T., Bish, D. L., Chipera, S. J., Carlos, B. A., and Guthrie, Jr. G. D., *Summary and Synthesis Report on Mineralogy and Petrology Studies for the Yucca Mountain Site Characterization Project, Volume 1, Chemistry and Mineralogy of the Transport Environment at Yucca Mountain*, Yucca Mountain Milestone report #3665, Los Alamos National Laboratory, 1996.

48. Barr, et al., *Geology of the Main Drift, Station 28-55, ESF,* YMP, Yucca Mountain, Nevada, 1997.

49. Beason, S., *Personal Communication*, 2 e-mail memos, subject Re: Fracture Information, from Steven Beason to Darren Jolley dated 8/19/1997 and 8/20/1997.

50. Lloyd, M. H.,and Haire, R. G., *The Chemistry of Plutonium in Sol-Gel Processes,* Radiochimica Acta, Vol 25, pp. 139-148, 1978.

51. Brunstad, A., *Polymerization and Precipitation of Plutonium(IV) in Nitric Acid,* Industrial and Engineering Chemistry, Vol 51, No. 1, pp. 38-40, January 1959.

52. Newton, T. W., Hobart, D. E., and Palmer, P. D., *The Formation of Pu(IV) Colloid by the Alpha-reduction of Pu(V) or Pu(VI) in Aqueous Solutions,* Radiochimica Acta, Vol 39, pp. 139-147, 1986.

53. Katayama, N., Kubo, K., and Hirono, S., *Genesis of Uranium Deposits of the Tono Mine, Japan*, Formation of Uranium Ore Deposits, IAEA-SM-183/19, International Atomic Energy Agency, pp. 437-452, 1974.

54. Turner, G. D., Zachara, J. M., McKinley, J. P., and Smith, S. C., *Surface-charge Properties and UO_2^{2+} Adsorption of a Subsurface Smectite*, Geochimica et Cosmochimica Acta, Vol. 60, pp. 3399-3414, 1996.

55. Triay, I. R., Cotter, C. R., Kraus, S. M., Huddleston, M. H., Chipera, S. J., and Bish, D. L., *Radionuclide Sorption in Yucca Mountain Tuffs with J-13 Well Water: Neptunium, Uranium, and Plutonium*, Los Alamos National Laboratory, LA-12956-MS, 1996.

56. McKinley, I. G., and Scholtis, A., *Compilation and Comparison of Radionuclide Sorption Databases Used in Recent Performance Assessments*, Radionuclide Sorption from the Safety Evaluation Perspective, Proceedings of an NEA Workshop, Interlaken Switzerland, pp. 21-55, October 16-18, 1991, Nuclear Energy Agency, Organization for Economic Co-operation and Development, Publications Service, OECD, 2, rue André-Pascal, Paris, CEDEX, France.

57. Scott, R. B.,and Bonk, J., *Preliminary Geologic Map of Yucca Mountain, Nye County Nevada, with Geologic Sections,* Open File Report 84-494, U.S. Geological Survey, 1984.

58. Brandberg, F., and Skagius, K., *Porosity, Sorption and Diffusivity Data Compiled for the SKB 91 Study*, SKB Technical Report 91-16, Swedish Nuclear Fuel and Waste Management Co., Stockholm.

59. Vandergraaf, T. T., Ticknor, K. V., and Melnyk, T. W., *The Selection and Use of Sorption Database for the Geosphere Model in the Canadian Nuclear Fuel Waste Management Program*, Radionuclide Sorption from the Safety Evaluation Perspective, Proceedings of an NEA Workshop, Interlaken Switzerland, pp. 81-120, October 16-18, 1991, Nuclear Energy Agency, Organisation for Economic Co-operation and Development, Publications Service, OECD, 2, rue André-Pascal, Paris, CEDEX, France.

60. *Total System Performance Assessment - 1995: An Evaluation of the Potential Yucca Mountain Repository*, DI#: B00000000-01717-2200-000136 REV 01, CRWMS M&O.

61. *Construction of Scenarios for Nuclear Criticality at the Potential Repository at Yucca Mountain, Nevada*, DI#: B00000000-01717-2200-00194, CRWMS M&O, September 1997.

62. Guilbert, J. M., and Park, C. F. Jr., *The Geology of Ore Deposits*, W. H. Freeman and Company, New York, p. 985, 1986.

63. Langmuir, D., *Uranium Solution-Mineral Equilibria at Low Temperatures with Applications to Sedimentary Ore Deposits*, Uranium Deposits, Their Mineralogy and Origin, Mineralogical Association of Canada, Short Course Handbook, Volume 3, University of Toronto Press, Toronto, Canada, pp. 17-55, 1978.

64. McKelvey, V. E., Everhart, D. L., and Garrels, R. M., *Origin of Uranium Deposits*, Economic Geology 50th Anniversary Volume, pp. 464-533, 1955.

65. Gauthier-Lafaye, F., and Weber F., *The Francevillian (Lower Proterozoic) Uranium Ore Deposits of Gabon*, Economic Geology, Vol. 84, pp. 2267-2285, 1989.

66. Pearcy, E. C., Prikryl, J. D., Murphy, W. M., and Leslie, B. W., *Alteration of Uraninite from the Nopal I Deposit, Pe˜na Blanca District, Chihuahua, Mexico, Compared to Degradation of Spent Fuel in the Proposed U. S. Hifh-level Nuclear Waste Repository at Yucca Mountain, Nevada*, Applied Geochemistry, Vol. 9, pp. 713-732, 1994.

67. Devoto, R. H., *Uranium Phanerozoic Sandstone and Volcanic Rocks*, Uranium Deposits, Their Mineralogy and Origin, Mineralogical Association of Canada, Short Course Handbook, Volume 3, University of Toronto Press, Toronto, Canada, pp. 293-305, 1978.

68. Langford, F. F., *Mobility and Concentration of Uranium in Arid Surfical Environments*, Uranium Deposits, Their Mineralogy and Origin, Mineralogical Association of Canada, Short Course Handbook, Volume 3, University of Toronto Press, Toronto, Canada, pp. 383-394, 1978.

69. Broxton, David E., Warren, Richard G., Hagan, Roland C., and Luedemann, *Chemistry of Diagenetically Altered Tuffs at a Potential Nuclear Waste Repository, Yucca Mountain, Nye County, Nevada*, Los Alamos National Laboratory, LA-10802-MS, 1986.

70. Mann, A. W., and Deutscher, R. L., *Genesis Principles for the Precipitation of Carnotite in Calcrete Drainages in Western Australia*, Economic Geology, Vol 73, pp. 1724-1737, 1978.

71. Langmuir, D., *Aqueous Environmental Geochemistry*, Prentice-Hall, Upper Saddle River, NJ, 1996.

72. *Determination of Radionuclide Sorption for High-Level Nuclear Repositories*, Technical Position Paper, U. S. Nuclear Regulatory Commission, 1986.

73. Cato, C., Ochiai, Y., Takeda, S., *Natural Analog Study of Tono Sandstone Type Uranium Deposits in Japan*, Natural Analogs in Radioactive Waste Disposal, Graham & Trotman, 1987.

74. Greenspan, E., Vujic, J., and Burch, J., *Neutronic Analysis of Critical Configurations in Geologic Repositories: I - Weapons Grade Plutonium*, Nuclear Science and Engineering, **127**, pp 262-291 (1997).

75. DOE/SF/19683--6, DOE-AC03-93SF19683, *Plutonium Disposition in Existing Pressurized Water Reactors*, Westinghouse Electic Corporation, Jun3 1, 1994.

76. *Characteristics of Spent Fuel from Plutonium Disposition Reactors, Vol 3: A Westinghouse PWR design,* ORNL-TM-13170/V3, 1996.

77. Oversby, V. M., *Criticality in a High Level Waste Repository,* SKB Technical Report, 96-07, June 1996.

78. Rogers, K., *Plutonium Migration in Yucca Mountain Ground Water,* Las Vegas Review Journal, September 11, 1997.

79. *Emplacement Scale Thermal Evaluations of Large and Small WP Designs,* DI#: BB0000000-01717-0200-00009 REV 00, CRWMS M&O, 1995.

80. *Heat Transfer,* Holman, J.P., 7th Edition, McGraw-Hill Publishing Company, 1990.

81. Bates, J., Strachan, D., Ellison, A., Buck, E., Bibler, N., McGrail, B. P., Bourcier, W., Grambow, B., Sylvester, K., Wenzel, K., and Simonson, S., *Glass Corrosion and Irradiation Damage Performance,* Plutonium Stabilization & Immobilization Workshop, Washington, D. C., December 11-14, 1995.

82. Wilson, M. L., Gauthier, J. H., Barnard, R. W., Barr, G. E., Dockery, H. A., Dunn, E., Eaton, R. R. , Gauerin, D. C., Lu, N., Martinez, M. J., Nilson, R., Rautman, C. A., Robey, T. H., Ross, B., Ryder, E. E., Schenker, A. R., Shannon, S. A., Skiner, L. H., Halsey, W. G., Gansemer, J. D., Lewis, L. C., Lamont, A. D., Triay, I. R., Meijer, I. R., and Morris, D. E., *Total-System Performance Assessment for Yucca Mountain - SNL Second Iteration (TSPA-1993),* Volume 1, SAND93-2675, April, 1994.

83. *Criticality Analysis of Pu and U Accumulations in a Tuff Fracture Network,* DI#: A00000000-01717-0200-00050, REV 00, CRWMS M&O, 1997.

84. *MCNP Evaluations of Laboratory Critical Experiments: Homogeneous Mixture Criticals,* DI#: BBA000000-01717-0200-00045 REV00, CRWMS M&O.

85. Krief, R. A., *Nuclear Criticality Safety, Theory and Practice,* American Nuclear Society, 1993.

86. *Waste Package Probabilistic Criticality Analysis: Summary Report Of Evaluation in 1997,* DI#: BBA0000000-01717-5705-00015 REV 00, CRWMS M&O.

APPENDIX A

SHORT OVERVIEW OF URANIUM GEOCHEMISTRY AND ORE DEPOSITION ENVIRONMENTS AND MECHANISMS

Uranium never occurs naturally as a native element because it would react with water in a geologically short time to form an oxide and elemental hydrogen. Because all uranium minerals contain oxygen, and this marked affinity for oxygen plays a dominant role in determining uranium geochemical properties, uranium occurs only in the oxidation states of U^{+4}, U^{+5} and U^{+6}. Most of the geochemical reactions are adequately described in terms of either the reduced U^{+4} or the oxidized U^{+6} state.

At low temperatures and pressures, uranium in rocks and minerals undergoing weathering and leaching is oxidized from U^{+4} to U^{+6} and becomes soluble in groundwater as UO_2^{2+} ion, as one of the uranyl carbonate complex ions (Figure A-1), or as any of a number of other complexes; among these are complexes with PO_4^{-3}, SO_4^{-2} and AsO_4^{-3} (Ref. 11). As long as groundwaters containing these complexes remain oxidizing, the hexavalent uranium ions will remain mobile; but when they encounter and percolate through reducing environments, the uranyl ions are reduced to tetravalent uranium and are reprecipitated as uraninite, pitchblende, coffinite, or some other reduced uranium mineral. Vanadium may also be deposited by this same sort of reductive mechanism as tetravalent V in montroseite, roscoelite, etc. (Ref. 62). Reduction of mobile uranyl species to U^{+4} with precipitation of highly insoluble uraninite or coffinite normally reflects the concurrent oxidation of proportionate amounts of more abundant species in nature, such as ferrous iron, sulfides, and/or organic carbon (Ref. 63). Reactions for vanadium are similar. Subsequent to this deposition process, the minerals containing reduced vanadium may oxidize along with the minerals with reduced uranium to produce uranyl vanadate minerals such as carnotite and tyuyamunite.

Epigenetic uranium mineral deposits vary in size and grade, depending on geology, but one fact remains: the need for a reducing environment (or vanadium) for the primary mineral(s) to precipitate. Gruner (Ref. 12) stated that the oxidation-reduction potential is so low at pH values expected in nature that only carbonaceous matter or H_2S could reduce uranyl solutions at temperatures below about 100°C. Other authors explicitly state that the precipitation mechanism for epigenetic uranium ore deposits is reduction (Ref. 12, Ref. 62, Ref. 11). To further illustrate the need for reduction as the precipitation mechanism in epigenetic deposits, a pH of 3 or less would be required to provide the acidity necessary to dissolve more than a few parts per million from pitchblende without oxidizing it (Ref. 64).

Therefore, without sufficient reducing potential in the depositional environment, the precipitation of uranium by reduction of uranyl ions cannot occur, and only minor amounts would precipitate in cases of low reducing potentials or small reducing capacity. Once there is sufficient reducing capacity within the host rock, uranium will accumulate in sufficient quantities to form ore grade deposits if other conditions necessary for mineral deposition are present, e.g., sufficient porosity, favorable host rock, stable groundwater flow, etc.

Uranium deposits normally are classified based on one of the following criteria: host rock type, structural setting, mineralogy, deposit form, or geochemistry; however, for this report, the classification scheme is kept simple based on the review of the available literature. Ore body

type descriptions found in Nash et al (Ref. 11) include 11 different types which are based on depositional environment. They are as follows: quartz–pebble conglomerate, unconformity, ultrametamorphic, classical vein, alkalic plutons, contact, volcanogenic, sandstone, calcrete, black shale, and phosphorite. Three of these depositional environments can be associated with the local geology at Yucca Mountain and form the basis for this study; namely unconformity, sandstone, and calcrete deposits. The uranium deposits at Oklo, Gabon and Peña Blanca, Mexico have often been cited as natural analogs to Yucca Mountain. However, these two deposits did not utilize epigenetic processes to accumulate the uranium ore. The Oklo deposit falls under the quartz-pebble-conglomerate type deposit (Ref. 65) and the Peña Blanca deposit is classified as a hydrothermal type deposit (Ref. 66). Therefore, neither of these two deposits apply to this study. Below is a brief description of the three types of deposits that seem to apply to epigenetic ore deposition.

Unconformity:

The key to the formation of these deposits, and thus to their geologic characteristic, is the interplay of dissolved U^{+6} ions reacting with a reducing environment. The general mechanism seems to be a leaching of uranium into oxidizing groundwaters and flowing in a permeable sandstone/conglomerate above an unconformity. The reductant consists of methane or other hydrocarbon charged fluids moving upward along faults from the basement rock and through the unconformable contact boundary (Figure A-2). The criteria for unconformity type deposits consist of the following (Ref. 62, which is based on Ref. 35):

1. The basement rocks (usually metamorphosed) are commonly topped with a weathered soil zone, a regolith or perhaps a paleosol, although the paleosol is not essential.

2. The host rocks above the unconformity are normally fluvial-deltaic sandstones or siltstones, thus providing a high porosity location (relative to rocks below the unconformity) for ore deposition.

3. The deposits occur at or within a few tens to hundreds of meters above the unconformity or a few meters below it and are horizontally elongated, ribbonlike deposits along faults through the unconformity.

4. The deposits are epigenetic, with predominant open space filling textures in faults, breccia zones and fractures. Low pressures and low to moderate temperatures are indicated. Where reported, lead-lead isotopic dates are those of the cover rocks above the unconformity or younger.

5. The uranium mineralogy is simple, generally pitchblende with coffinite or thucolite.

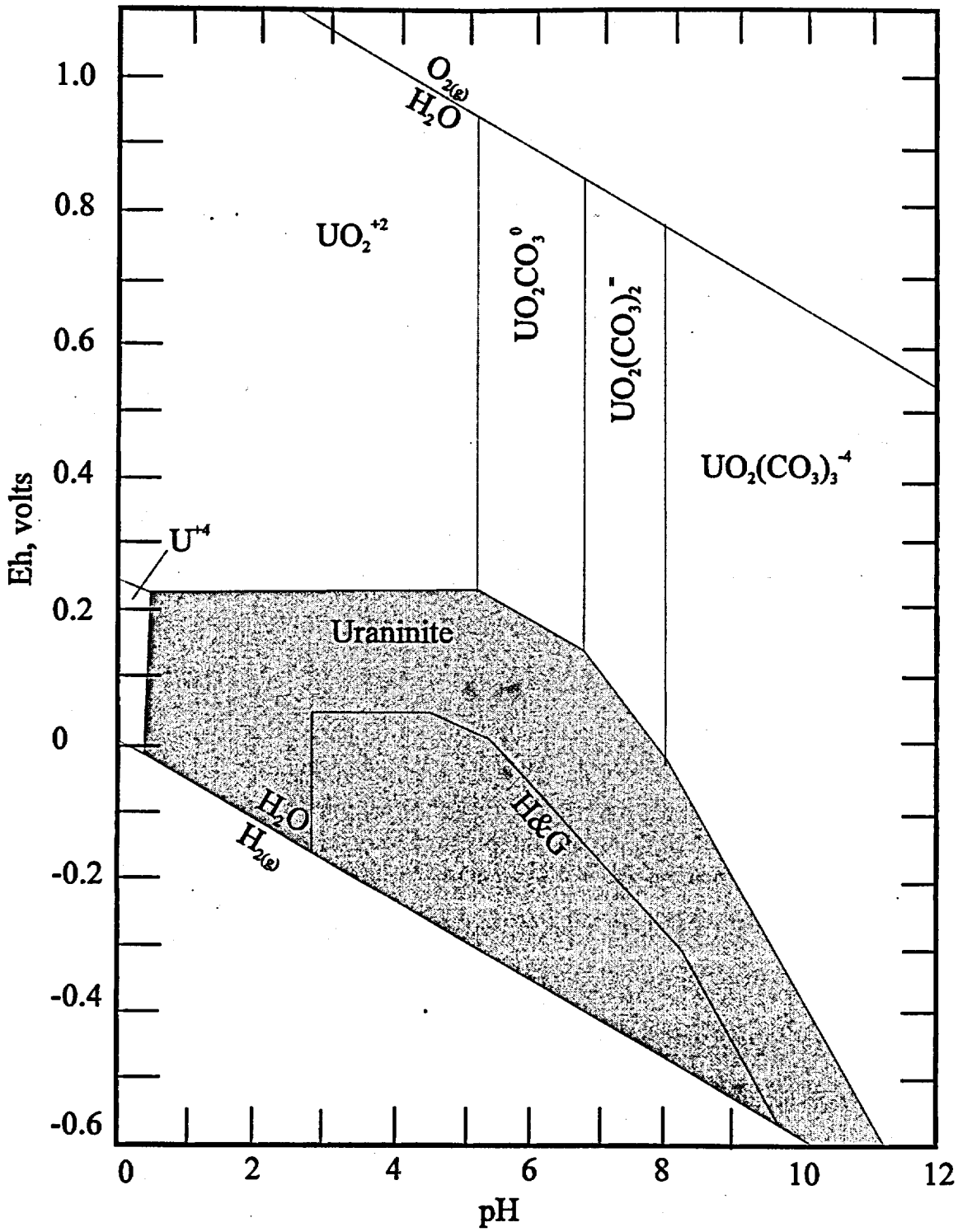

Figure A-1 Eh-pH Diagram of the U-O_2-CO_2-H_2O System at 25°C and $\rho CO_2 = 10^{-2}$ atm

6. The altered wall rocks show fine-grained chloritization, argillization, albitization, hematitizaton, and veinlets of carbonates.

Sandstone:

Generally there are two major types of epigenetic sandstone uranium deposits; those associated with organic material as a reducing agent and those deposited without organic material (includes mineral deposits formed by sorption). However the general mechanisms seem to be similar and the requirements for ore deposition are the same; namely (Figure A-3) (Ref. 62):

1. A source of uranium,

2. Oxidation, mobilization and transportation of the uranium,

3. Sufficient permeability in the host rock,

4. Reducing capacity (or sorptive capacity) in the host rock, and

5. Stable, sustained groundwater flow.

Uranium sources seem to vary, including magmatic and meteoric hydrothermal solutions, leaching of host rocks, and leaching of granitic rocks. Of most interest to the present study case, many of the sandstone ore deposits seem to have their uranium source as devitrified volcanic ash (Figure A-3). In fact, there is a striking correlation between the presence of volcanic ash and ore (Ref. 11, Ref. 62).

The ore is mainly deposited in the sandstones or conglomeratic facies (either in confined or semi-confined aquifers; Figure A-3) where the oxidized uranium bearing fluids interact with a reducing agent or fluid. The ore is normally deposited along what is termed a roll-front (Ref. 67, Ref. 11, Ref. 62) or a geochemical cell (Ref. 39) where the reducing agent or fluid is in contact with the oxidized groundwater (Figure A-4). The reducing agent may or may not be organic, however the result is the same.

Common organic reducing environments seem to be fluvial organic debris and/or buried logs (Figure A-5); however, lignite or petroleum bearing sands or shales can also lead to deposition. Common inorganic redox environments tend to be associated with reduced iron or sulfide based minerals (Figure A-4). An alternate mechanism for formation of a few of these types of deposits can be attributed to sorption onto zeolites and clays (Ref. 11).

Calcrete:

These epigenetic deposits occur in areas of internal drainage where evaporation exceeds rainfall. The general locations for these types of deposits occur along the lower ends of alluvial valleys, at playa lakes, and at desiccated calcrete terraces. One proposed mechanism for precipitation is related to evaporitic processes by which potassium is concentrated, uranyl ion activity is increased, as carbonate complexes are weakened by

common ion effects (i.e., other ions compete for the carbonate), and pH is decreased. The precipitation occurs as groundwater is constricted by barriers and caused to move upward where V^{+4} is oxidized to V^{+5} thus allowing the precipitation of the oxidized uranium mineral carnotite (Ref. 70, Figure A-6). This precipitation mechanism is unlikely to occur at Yucca Mountain because of the low concentrations of vanadium in the environment (less than 10 to about 60 parts per million, Ref. 69, Appendix C). An alternate mechanism of precipitation (one that should operate in the arid environment of the Yucca Mountain region) is that of upward diffusion of uranyl ions into the unsaturated soil were evaporation can concentrate the uranyl complexes, thus allowing precipitation to occur (Ref. 68). The only ore that has been found deposited in this type of depositional environment is carnotite. This mineral requires vanadium to precipitate; the chemical formula for carnotite is $K_2(UO_2)_2(VO_4)\cdot 3H_2O$ and is located in regolith, fluvial detritus, or in fractures and voids in the calcretes. (Ref. 44, Ref. 11, Ref. 68)

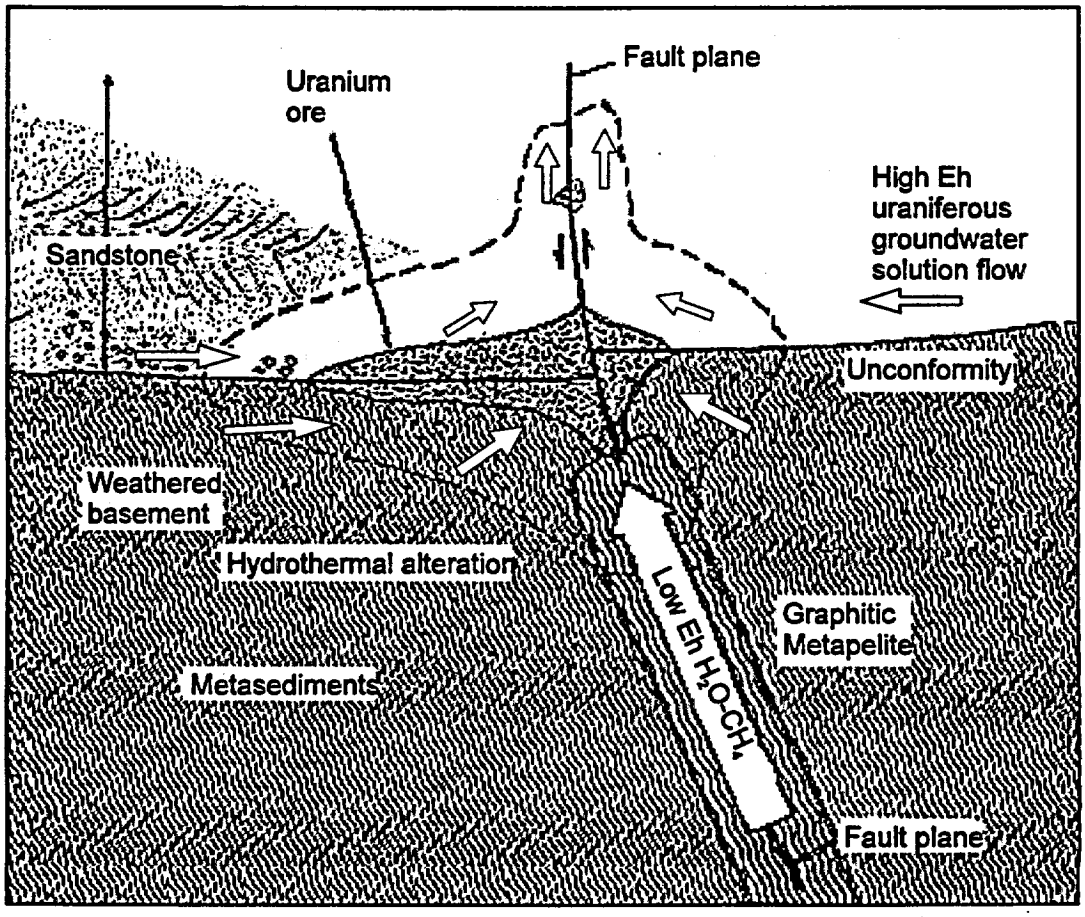

Figure A-2 Schematic Cross Section of the Formative Processes of an Unconformity-type Uranium Deposit.

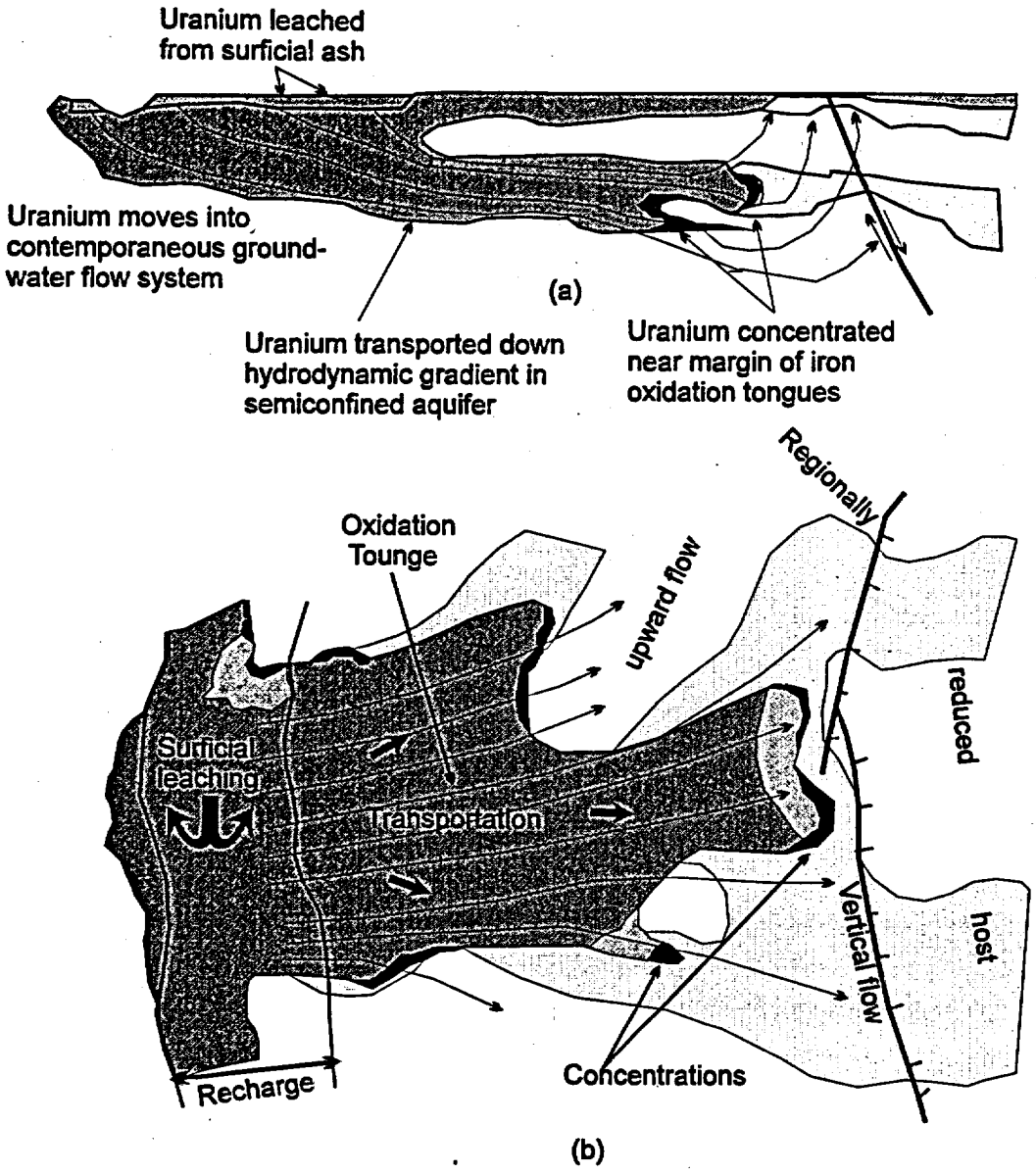

Figure A-3 Conceptual Cross Section and Plan View of a Roll-front Type System

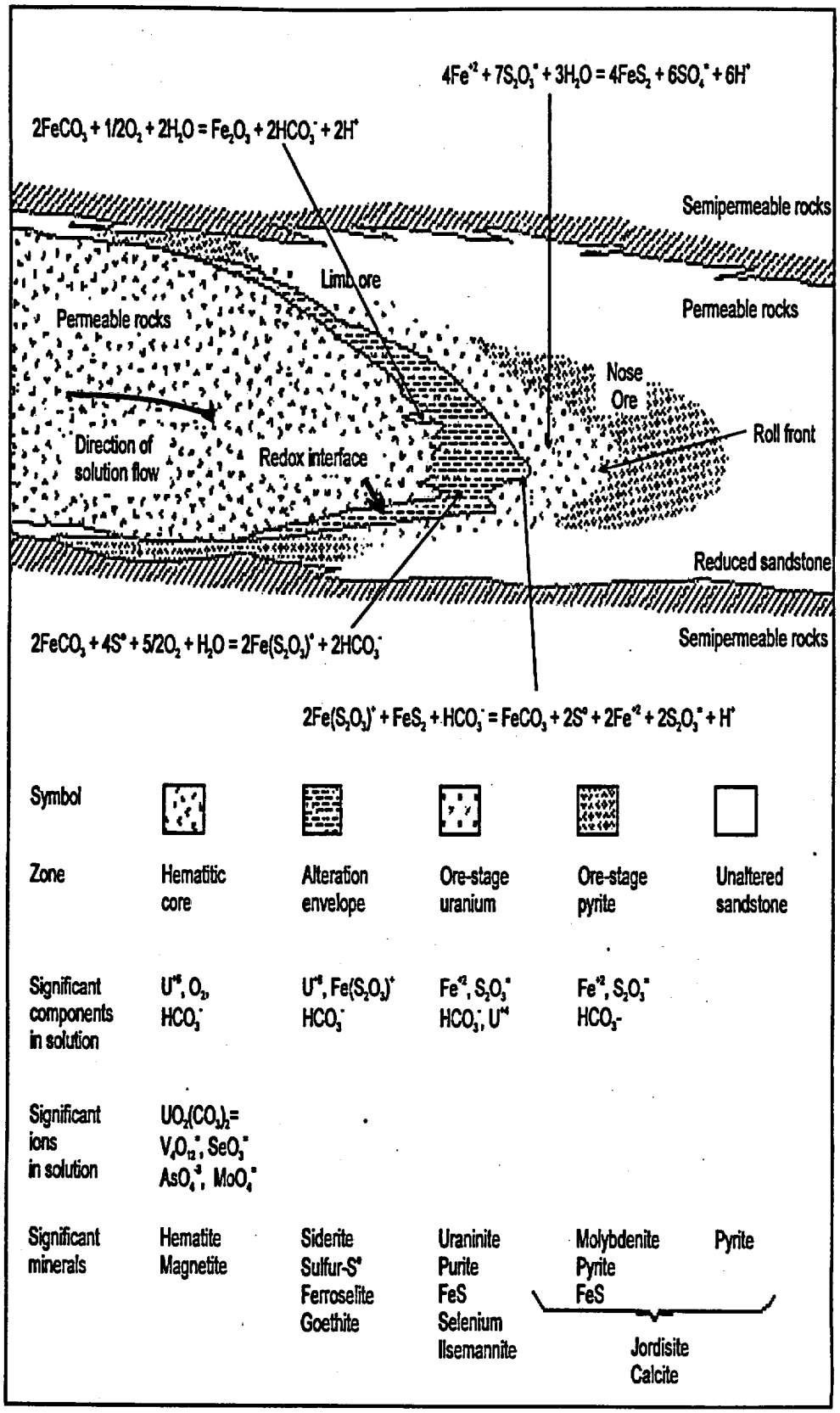

Figure A-4 Diagram of a Roll-front Uranium Deposit Advancing to the Right

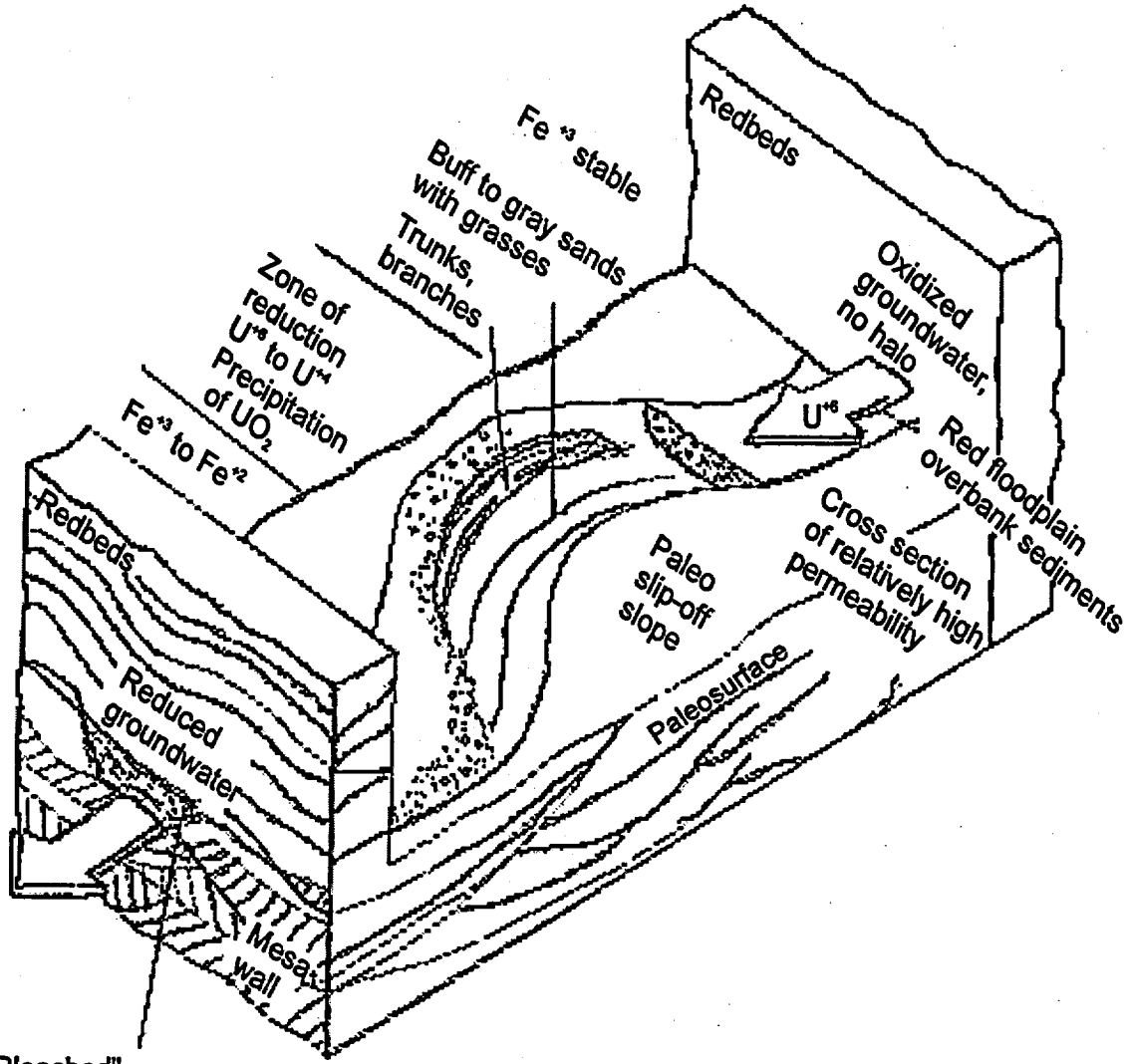

Figure A-5 Oxidation-reduction Dynamics in Sandstone Type Paleostream Channel Mineralization

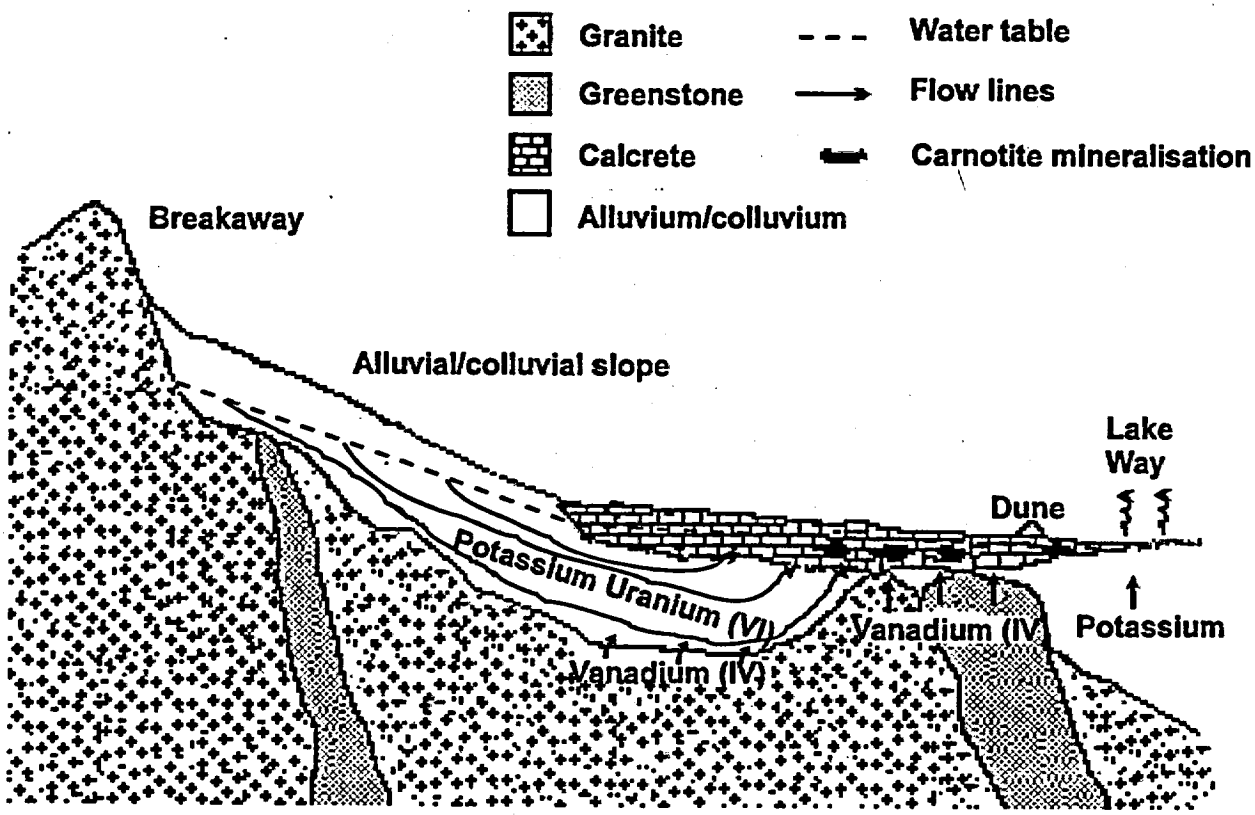

Figure A-6 Idealized Section along a Representative Catchment Showing the Postulated Redox-controlled Genesis of Carnotite in Calcrete. Reducing groundwaters supplying vanadium for precipitation at the redox front can be either localized beneath, or laterally displaced from, the precipitation site. Modified from Mann and Deutscher (Ref. 70).

APPENDIX B

INPUT DATA and PARTIAL OUTPUT LISTING from SAS2H CASE

The SAS2H analysis of criticality consequences for Pu deposition in Yucca Mountain tuff fractures was referenced to the MCNP analysis providing an upper bound on conditions supporting criticality as discussed in Section 9. These conditions are summarized below. The information about the SAS2H case summarizes the method of representing the MCNP 3-D model in an approximate manner by a 1-D model for SAS2A. The input data file for SAS2A case is listed next, followed by a subset of the output file containing the isotopic inventories in grams and activity in curies for 6 decay intervals of 10,000 years each.

MCNP4 case -

13 volume % water in Tuff
10 volume % Pu in fuel matrix
geometry 1m cube of Tuff with 0.01 cm fissures at ~ 3.0 cm intervals in each dimension
fuel volume = 9966 cm^3, Pu mass = 10.1 kg
eigenvalue = 1.08071

SAS2H case

model system as a symmetric slab where fuel planes alternate with Tuff planes.
Pitch = distance between fuel centerlines
Fuel Width = fuel thickness
In the MCNP model, the Tuff/water moderator is always enclosed with fuel. Adjustment of the pitch and fuel width is necessary in the SAS2H slab geometry to get a critical system. Isotopic inventories are to first order dependent upon the fuel atom densities and fuel volume with spectral effects somewhat less important. One method which can be used to define a 1-D simulation of a 3-D model is to balance reaction rates as much as possible or at least for important reactions. This requires a number of iterations. In this case, pitch and fuel thickness were adjusted to achieve an initial eigenvalue close to the MCNP value.

Pitch = 0.08 cm
Fuel thickness = 0.012 cm
eigenvalue (initial) = 1.083
estimated amount of Pu consumed =~ 2.6 Kg over 10,000 years
eigenvalue (4000 yr) = 0.9931
Pu replacement not modeled

```
0*************************************************************************
 *                                                                       *
 *                    SCALE4.3  Bulletin  Board                          *
 *                    --------  --------  -----                          *
 *                                                                       *
 *                      Welcome to SCALE-4.3.                            *
 *                                                                       *
 *                                                                       *
 *************************************************************************
1         primary module access and input record ( scale driver - 95/03/29 - 09:06:37 )
-   module sas2h     will be called
      SAS2H: PuO2-H2O in Tuff matrix (3 cm cubes - 0.01 cm PuO2)
      '
      ' PuO2 + H2O modeled as intrusion into Tuff fractures
      '          array of 3 cm cubes of Tuft surrounded by fissile matl
      '   Far field Criticality Conseq for PuO2
      '
      44group     latticecell
      '
```

```
'  MCNP input mixtures for fuel-pin-cell, assembly-cell, and waste package
'comp      MX VF   atom/bn-cm  temp K
'  mixtures of Puo2 and water in 0.01 cm cracks modeled as infinite slabs:
'     0.062  vol fract Pu 265 deg C
' arbm-puo2  1.64852  3  0 0 0 1001 6.3679007 8016 55.618573 94239  38.013527
'                      1  1.0  538.0  end
'     0.100  vol fract Pu 265 deg C
arbm-puo2  2.046  3  0 0 0 1001 4.92294 8016 45.676137 94239  49.400923
                  1  1.0  538.0  end
'
kr-83       1 0 1-20         538.00 end
kr-85       1 0 1-20         538.00 end
y-89        1 0 1-20         538.00 end
sr-90       1 0 1-20         538.00 end
zr-93       1 0 1-20         538.00 end
zr-94       1 0 1-20         538.00 end
zr-95       1 0 1-20         538.00 end
nb-94       1 0 1-20         538.00 end
ru-106      1 0 1-20         538.00 end
rh-105      1 0 1-20         538.00 end
pd-105      1 0 1-20         538.00 end
pd-108      1 0 1-20         538.00 end
sb-124      1 0 1-20         538.00 end
xe-131      1 0 1-20         538.00 end
xe-132      1 0 1-20         538.00 end
xe-135      1 0 1-20         538.00 end
xe-136      1 0 1-20         538.00 end
cs-134      1 0 1-20         538.00 end
cs-135      1 0 1-20         538.00 end
cs-137      1 0 1-20         538.00 end
ba-136      1 0 1-20         538.00 end
la-139      1 0 1-20         538.00 end
pr-141      1 0 1-20         538.00 end
pr-143      1 0 1-20         538.00 end
nd-147      1 0 1-20         538.00 end
ce-144      1 0 1-20         538.00 end
pm-147      1 0 1-20         538.00 end
pm-148      1 0 1-20         538.00 end
eu-154      1 0 1-20         538.00 end
eu-155      1 0 1-20         538.00 end
'-----------------------------------------
'    moderator material tuff+water 13 % interstial water 265 deg C
'
arbm-tuff2  2.37513 12 0 0 0  1001 0.61255   8016 51.38553  11023  2.52188
                              12000 0.139805 13027  6.379740 14000 33.79764
                              15031 0.006194 19000  3.87208  20000  0.378671
                              22000 0.055589 25055  0.049092 26000  0.619226
                              2 1.0 538.0   end
'
arbm-tuff3  2.37513 12 0 0 0  1001 0.61255   8016 51.38553  11023  2.52188
                              12000 0.139805 13027  6.379740 14000 33.79764
                              15031 0.006194 19000  3.87208  20000  0.378671
                              22000 0.055589 25055  0.049092 26000  0.619226
                              3 1.0 538.0   end
'
' - - - - - - - - - - - - - - - - - - - - - - - - - - - - - - - - - -
end comp
'
' - - - - - - - - - - - - - - - - - - - - - - - - - - - - - - - - - -
'
'  fuel-pin-cell geometry:
'
'  3 cm cells, 0.01 cm fuel pins
' symmslabcell  3.0  0.01  1  3  1.0  2 end
'
'  1 cm cells, 0.01 cm fuel pins - account for 3-D planes
'  symmslabcell  1.0  0.01  1  3  0.5  2 end
'
'  1 cm cells, 0.01 cm fuel pins - account for 3-D planes
'  symmslabcell  1.0  0.015  1  3  0.5  2 end
'
'  0.8 cm cells, 0.01 cm fuel pins - account for 3-D planes
'  symmslabcell  0.8  0.01  1  3  0.5  2 end
'
'  1 cm cells, 0.01 cm fuel pins - account for 3-D planes
'  symmslabcell  1.0  0.012  1  3  0.5  2 end
'
'  0.8 cm cells, 0.012 cm fuel pins - account for 3-D planes
symmslabcell  0.8  0.012  1  3  0.5  2 end
'
' - - - - - - - - - - - - - - - - - - - - - - - - - - - - - - - - - -
'
'  case pul0atuff - fuel length = 100 cm
'  case pul0btuff - fuel length = 200 cm
'  case pul0ctuff - fuel length = 200 cm, temp = 300 K
'  case pul0dtuff - fuel length = 200 cm, temp = 538 K, pitch=1.0 cm,
'                   fuel width=0.015 cm
'  case pul0etuff - fuel length = 200 cm, temp = 538 K, pitch=0.8 cm,
'                   fuel width=0.01 cm
'  case pul0ftuff - fuel length = 200 cm, temp = 538 K, pitch=1.0 cm,
'                   fuel width=0.012 cm
'  case pul0gtuff - fuel length = 200 cm, temp = 538 K, pitch=0.8 cm,
'                   fuel width=0.012 cm
'                   k-eff drops to - 1.0 around 4000 yr
'
'  assembly and cycle parameters:
'  0.59 KW, 1000y/r periods, 4,000 yr total, 60,000 yr cooling
'
npin/assm=1 fuelngth=200.0 ncycles=4 nlib/cyc=1 volfueltot=9966.0
printlevel=6 inplevel=0 end
'
'     Power (MW), burn (days), down (days)
'   power 0.59 KW, Burn time 1000 yr
'
power=0.00059 burn=3.6525e5 down=0.
power=0.00059 burn=3.6525e5 down=0.
power=0.00059 burn=3.6525e5 down=0.
power=0.00059 burn=3.6525e5 down=2.1915e7
   end
```

1

0 sas2h: puo2-h2o in tuff matrix (3 cm cubes - 0.01 cm puo2) light elements page 1
nuclide concentrations, grams
basis =single reactor assembly

	initial	1E-18 d
na 23	5.97E+02	5.97E+02
al 27	1.51E+03	1.51E+03
p 31	1.47E+00	1.47E+00
mn 55	1.16E+01	1.16E+01
total	2.12E+03	2.12E+03

1

0 sas2h: puo2-h2o in tuff matrix (3 cm cubes - 0.01 cm puo2) actinides page 2
nuclide concentrations, grams
basis =single reactor assembly

	initial	1E-18 d
u235	.00E+00	7.72E-22
pu239	1.01E+04	1.01E+04
total	1.01E+04	1.01E+04

1 sas2h: puo2-h2o in tuff matrix (3 cm cubes - 0.01 cm puo2)
power= .00mw, burnup= 215.mwd, flux= 9.82E+08n/cm**2-sec page 3
0 basis =
0 (note, k-infinities, clad and moderator absorptions are correct, only, if correctly weighted cross sections are applied.)

	initial	91313. d	182625. d	273938. d	365250. d	365250. d
productions	5.459718E+04	5.389955E+04	5.320673E+04	5.251866E+04	5.183528E+04	5.183528E+04
absorptions	2.877887E+04	2.857844E+04	2.834791E+04	2.809729E+04	2.783316E+04	2.783316E+04
k infinity	1.897127E+00	1.886022E+00	1.876919E+00	1.869172E+00	1.862357E+00	1.862357E+00

0

	initial	91313. d	182625. d	273938. d	365250. d	365250. d
actinide absorptions	2.876649E+04	2.846361E+04	2.816112E+04	2.785900E+04	2.755726E+04	2.755726E+04
non-actinide abs. fracs.	4.302859E-04	4.017949E-03	6.589293E-03	8.480906E-03	9.912848E-03	9.912848E-03

1 sas2h: puo2-h2o in tuff matrix (3 cm cubes - 0.01 cm puo2)
power= .00mw, burnup= 862.mwd, flux= 1.15E+09n/cm**2-sec page 33
0 basis =
0 (note, k-infinities, clad and moderator absorptions are correct, only, if correctly weighted cross sections are applied.)

	initial	******* d	******* d	******* d	******* d
productions	4.648146E+04	4.584010E+04	4.520320E+04	4.457069E+04	4.394255E+04
absorptions	2.540117E+04	2.510562E+04	2.481075E+04	2.451663E+04	2.422333E+04
k infinity	1.829895E+00	1.825890E+00	1.821920E+00	1.817978E+00	1.814059E+00

0

	initial	******* d	******* d	******* d	******* d
actinide absorptions	2.500652E+04	2.470370E+04	2.440194E+04	2.410125E+04	2.380166E+04
non-actinide abs. fracs.	1.553637E-02	1.600909E-02	1.647717E-02	1.694268E-02	1.740777E-02

1

sas2h: puo2-h2o in tuff matrix (3 cm cubes - 0.01 cm puo2)
decay, following reactor irradiation identified by: power= 5.900E-04mw, burnup=8.6198E+02mwd, flux= 1.06E+09n/cm**2-sec
0 light elements page 43
nuclide concentrations, grams
basis =single reactor assembly

	initial******* d	******* d	******* d	******* d	******* d	******* d	******* d
h 1	1.36E-05	1.36E-05	1.36E-05	1.36E-05	1.36E-05	1.36E-05	1.36E-05
he 4	9.79E-06	9.79E-06	9.79E-06	9.79E-06	9.79E-06	9.79E-06	9.79E-06
ne 20	1.45E-05	1.45E-05	1.45E-05	1.45E-05	1.45E-05	1.45E-05	1.45E-05
na 23	5.97E+02	5.97E+02	5.97E+02	5.97E+02	5.97E+02	5.97E+02	5.97E+02
mg 24	3.03E-02	3.03E-02	3.03E-02	3.03E-02	3.03E-02	3.03E-02	3.03E-02
mg 26	9.28E-07	9.28E-07	9.28E-07	9.28E-07	9.28E-07	9.28E-07	9.28E-07
al 27	1.51E+03	1.51E+03	1.51E+03	1.51E+03	1.51E+03	1.51E+03	1.51E+03
si 28	3.34E-02	3.34E-02	3.34E-02	3.34E-02	3.34E-02	3.34E-02	3.34E-02
p 31	1.47E+00	1.47E+00	1.47E+00	1.47E+00	1.47E+00	1.47E+00	1.47E+00
s 32	2.84E-05	2.84E-05	2.84E-05	2.84E-05	2.84E-05	2.84E-05	2.84E-05
mn 55	1.16E+01	1.16E+01	1.16E+01	1.16E+01	1.16E+01	1.16E+01	1.16E+01
fe 56	1.54E-02	1.54E-02	1.54E-02	1.54E-02	1.54E-02	1.54E-02	1.54E-02
fe 57	1.84E-06	1.84E-06	1.84E-06	1.84E-06	1.84E-06	1.84E-06	1.84E-06
total	2.12E+03	2.12E+03	2.12E+03	2.12E+03	2.12E+03	2.12E+03	2.12E+03

1

sas2h: puo2-h2o in tuff matrix (3 cm cubes - 0.01 cm puo2)
decay, following reactor irradiation identified by: power= 5.900E-04mw, burnup=8.6198E+02mwd, flux= 1.06E+09n/cm**2-sec
0 light elements page 44
element radioactivity, curies
basis =single reactor assembly

	initial******* d	******* d	******* d	******* d	******* d	******* d	******* d
totals	4.67E-01	6.89E-17	2.05E-17	6.12E-18	1.83E-18	5.45E-19	1.62E-19

1

sas2h: puo2-h2o in tuff matrix (3 cm cubes - 0.01 cm puo2)
decay, following reactor irradiation identified by: power= 5.900E-04mw, burnup=8.6198E+02mwd, flux= 1.06E+09n/cm**2-sec
0 light elements page 45
element thermal power, watts
basis =single reactor assembly

	initial******* d	******* d	******* d	******* d	******* d	******* d	******* d
totals	8.82E-03	2.02E-20	6.02E-21	1.80E-21	5.36E-22	1.60E-22	4.76E-23

1

sas2h: puo2-h2o in tuff matrix (3 cm cubes - 0.01 cm puo2)
decay, following reactor irradiation identified by: power= 5.900E-04mw, burnup=8.6198E+02mwd, flux= 1.06E+09n/cm**2-sec
0 light elements page 46
nuclide gamma power, watts
basis =single reactor assembly

	initial******* d	******* d	******* d	******* d	******* d	******* d	******* d
total	6.78E-03	1.35E-34	1.35E-34	1.35E-34	1.35E-34	1.35E-34	1.35E-34

1

sas2h: puo2-h2o in tuff matrix (3 cm cubes - 0.01 cm puo2)
decay, following reactor irradiation identified by: power= 5.900E-04mw, burnup=8.6198E+02mwd, flux= 1.06E+09n/cm**2-sec
0 actinides page 49
nuclide concentrations, grams
basis =single reactor assembly

	initial******* d	******* d	******* d	******* d	******* d	******* d	******* d
he 4	1.87E+01	5.49E+01	8.05E+01	9.91E+01	1.13E+02	1.23E+02	1.31E+02
pb206	1.36E-06	2.94E-04	1.24E-03	2.80E-03	4.89E-03	7.45E-03	1.04E-02
pb207	4.97E-05	1.80E-03	7.93E-03	2.00E-02	3.86E-02	6.38E-02	9.54E-02
pb208	1.38E-05	1.49E-05	1.50E-05	1.51E-05	1.52E-05	1.54E-05	1.57E-05
pb210	6.41E-08	2.04E-06	4.14E-06	6.00E-06	7.63E-06	9.06E-06	1.03E-05
bi209	1.48E-06	4.30E-04	2.46E-03	6.69E-03	1.33E-02	2.22E-02	3.35E-02
ra226	4.95E-06	1.57E-04	3.20E-04	4.63E-04	5.90E-04	7.00E-04	7.96E-04
ac227	1.25E-06	1.24E-05	3.08E-05	5.26E-05	7.56E-05	9.81E-05	1.19E-04
th229	2.45E-05	1.35E-03	3.83E-03	6.72E-03	9.68E-03	1.26E-02	1.54E-02
th230	8.66E-04	9.45E-03	1.70E-02	2.37E-02	2.96E-02	3.47E-02	3.92E-02
th232	3.50E-03	6.74E-02	1.72E-01	2.91E-01	4.15E-01	5.41E-01	6.67E-01

pa231	1.92E-03	1.90E-02	4.71E-02	8.06E-02	1.16E-01	1.50E-01	1.83E-01	
pa233	5.74E-07	7.65E-07	7.62E-07	7.60E-07	7.58E-07	7.55E-07	7.53E-07	
u233	6.56E-03	7.66E-02	1.43E-01	2.07E-01	2.68E-01	3.26E-01	3.81E-01	
u234	3.01E-01	3.22E-01	3.13E-01	3.05E-01	2.96E-01	2.88E-01	2.80E-01	
u235	9.72E+02	2.87E+03	4.29E+03	5.35E+03	6.15E+03	6.75E+03	7.20E+03	
u236	8.62E+01	3.14E+02	3.93E+02	4.20E+02	4.30E+02	4.33E+02	4.34E+02	
u238	1.02E-04	9.43E-04	1.77E-03	2.58E-03	3.38E-03	4.16E-03	4.93E-03	
np237	1.69E+01	2.25E+01	2.24E+01	2.24E+01	2.23E+01	2.22E+01	2.22E+01	
pu239	7.71E+03	5.78E+03	4.34E+03	3.25E+03	2.44E+03	1.83E+03	1.37E+03	
pu240	3.55E+02	1.23E+02	4.29E+01	1.49E+01	5.19E+00	1.81E+00	6.28E-01	
pu242	4.59E-02	4.57E-02	4.49E-02	4.40E-02	4.32E-02	4.24E-02	4.17E-02	
am243	4.66E-04	1.82E-04	7.11E-05	2.78E-05	1.08E-05	4.23E-06	1.65E-06	
total	9.17E+03	9.17E+03	9.17E+03	9.17E+03	9.17E+03	9.17E+03	9.17E+03	

1

sas2h: puo2-h2o in tuff matrix (3 cm cubes - 0.01 cm puo2)
decay, following reactor irradiation identified by: power= 5.900E-04mw, burnup=8.6198E+02mwd, flux= 1.06E+09n/cm**2-sec actinides page 50
element concentrations, grams
basis =single reactor assembly

	initial*******	d *******	d *******	d *******	d *******	d *******	d *******	d
he	1.87E+01	5.49E+01	8.05E+01	9.91E+01	1.13E+02	1.23E+02	1.31E+02	
pb	6.49E-05	2.11E-03	9.19E-03	2.28E-02	4.35E-02	7.13E-02	1.06E-01	
bi	1.48E-06	4.30E-04	2.46E-03	6.69E-03	1.33E-02	2.22E-02	3.35E-02	
ra	4.95E-06	1.57E-04	3.20E-04	4.64E-04	5.90E-04	7.00E-04	7.97E-04	
ac	1.25E-06	1.24E-05	3.08E-05	5.26E-05	7.56E-05	9.81E-05	1.19E-04	
th	4.39E-03	7.82E-02	1.93E-01	3.22E-01	4.54E-01	5.88E-01	7.21E-01	
pa	1.92E-03	1.90E-02	4.71E-02	8.06E-02	1.16E-01	1.50E-01	1.83E-01	
u	1.06E+03	3.18E+03	4.68E+03	5.77E+03	6.58E+03	7.19E+03	7.64E+03	
np	1.69E+01	2.25E+01	2.24E+01	2.24E+01	2.23E+01	2.22E+01	2.22E+01	
pu	8.07E+03	5.91E+03	4.38E+03	3.27E+03	2.45E+03	1.83E+03	1.37E+03	
am	5.59E+00	1.83E-04	7.11E-05	2.78E-05	1.08E-05	4.23E-06	1.65E-06	
totals	9.17E+03	9.17E+03	9.17E+03	9.17E+03	9.17E+03	9.17E+03	9.17E+03	

1

sas2h: puo2-h2o in tuff matrix (3 cm cubes - 0.01 cm puo2)
decay, following reactor irradiation identified by: power= 5.900E-04mw, burnup=8.6198E+02mwd, flux= 1.06E+09n/cm**2-sec actinides page 51
nuclide radioactivity, curies
basis =single reactor assembly

	initial*******	d *******	d *******	d *******	d *******	d *******	d *******	d
tl207	9.05E-05	8.95E-04	2.22E-03	3.80E-03	5.45E-03	7.08E-03	8.61E-03	
tl209	1.02E-07	5.60E-06	1.60E-05	2.80E-05	4.03E-05	5.24E-05	6.41E-05	
pb209	4.85E-06	2.67E-04	7.60E-04	1.33E-03	1.92E-03	2.50E-03	3.05E-03	
pb210	4.89E-06	1.56E-04	3.16E-04	4.58E-04	5.83E-04	6.92E-04	7.87E-04	
pb211	9.07E-05	8.97E-04	2.23E-03	3.81E-03	5.47E-03	7.10E-03	8.63E-03	
pb214	4.89E-06	1.56E-04	3.16E-04	4.58E-04	5.83E-04	6.92E-04	7.88E-04	
bi210	4.89E-06	1.56E-04	3.16E-04	4.58E-04	5.83E-04	6.92E-04	7.87E-04	
bi211	9.07E-05	8.97E-04	2.23E-03	3.81E-03	5.47E-03	7.10E-03	8.63E-03	
bi213	4.85E-06	2.67E-04	7.60E-04	1.33E-03	1.92E-03	2.50E-03	3.05E-03	
bi214	4.89E-06	1.56E-04	3.16E-04	4.58E-04	5.83E-04	6.92E-04	7.88E-04	
po210	4.89E-06	1.56E-04	3.16E-04	4.58E-04	5.83E-04	6.92E-04	7.87E-04	
po211	2.50E-07	2.47E-06	6.12E-06	1.05E-05	1.50E-05	1.95E-05	2.37E-05	
po213	4.75E-06	2.61E-04	7.44E-04	1.30E-03	1.88E-03	2.44E-03	2.99E-03	
po214	4.89E-06	1.56E-04	3.16E-04	4.58E-04	5.83E-04	6.92E-04	7.87E-04	
po215	9.07E-05	8.97E-04	2.23E-03	3.81E-03	5.47E-03	7.10E-03	8.63E-03	
po218	4.89E-06	1.56E-04	3.16E-04	4.58E-04	5.83E-04	6.93E-04	7.88E-04	
at217	4.85E-06	2.67E-04	7.60E-04	1.33E-03	1.92E-03	2.50E-03	3.05E-03	
rn219	9.07E-05	8.97E-04	2.23E-03	3.81E-03	5.47E-03	7.10E-03	8.63E-03	
rn222	4.89E-06	1.56E-04	3.16E-04	4.58E-04	5.83E-04	6.93E-04	7.88E-04	
fr221	4.85E-06	2.67E-04	7.60E-04	1.33E-03	1.92E-03	2.50E-03	3.05E-03	
fr223	1.25E-06	1.24E-05	3.07E-05	5.25E-05	7.55E-05	9.80E-05	1.19E-04	
ra223	9.07E-05	8.97E-04	2.23E-03	3.81E-03	5.47E-03	7.10E-03	8.63E-03	
ra225	4.85E-06	2.67E-04	7.60E-04	1.33E-03	1.92E-03	2.50E-03	3.05E-03	
ra226	4.89E-06	1.56E-04	3.16E-04	4.58E-04	5.83E-04	6.93E-04	7.88E-04	
ac225	4.85E-06	2.67E-04	7.60E-04	1.33E-03	1.92E-03	2.50E-03	3.05E-03	
ac227	9.07E-05	8.97E-04	2.23E-03	3.81E-03	5.47E-03	7.10E-03	8.63E-03	
th227	8.95E-05	8.85E-04	2.19E-03	3.76E-03	5.39E-03	7.00E-03	8.51E-03	
th229	4.85E-06	2.67E-04	7.60E-04	1.33E-03	1.92E-03	2.50E-03	3.05E-03	
th230	1.79E-05	1.95E-04	3.51E-04	4.89E-04	6.10E-04	7.16E-04	8.08E-04	
th231	2.11E-03	6.20E-03	9.27E-03	1.16E-02	1.33E-02	1.46E-02	1.56E-02	
pa231	9.06E-05	8.97E-04	2.23E-03	3.81E-03	5.47E-03	7.10E-03	8.63E-03	
pa233	1.19E-02	1.59E-02	1.58E-02	1.58E-02	1.57E-02	1.57E-02	1.56E-02	
u233	6.32E-05	7.38E-04	1.38E-03	2.00E-03	2.58E-03	3.14E-03	3.68E-03	
u234	1.87E-03	2.00E-03	1.95E-03	1.89E-03	1.84E-03	1.79E-03	1.74E-03	
u235	2.10E-03	6.20E-03	9.27E-03	1.16E-02	1.33E-02	1.46E-02	1.56E-02	
u236	5.58E-03	2.03E-02	2.54E-02	2.72E-02	2.78E-02	2.80E-02	2.81E-02	
np237	1.19E-02	1.59E-02	1.58E-02	1.58E-02	1.57E-02	1.57E-02	1.56E-02	
np239	9.33E-05	3.64E-05	1.42E-05	5.54E-06	2.16E-06	8.45E-07	3.30E-07	
pu239	4.79E+02	3.59E+02	2.69E+02	2.02E+02	1.52E+02	1.14E+02	8.53E+01	
pu240	8.06E+01	2.80E+01	9.75E+00	3.39E+00	1.18E+00	4.10E-01	1.43E-01	
pu242	1.81E-04	1.81E-04	1.77E-04	1.74E-04	1.71E-04	1.68E-04	1.65E-04	
am243	9.31E-05	3.64E-05	1.42E-05	5.54E-06	2.16E-06	8.45E-07	3.30E-07	
total	6.03E+02	3.87E+02	2.79E+02	2.06E+02	1.53E+02	1.14E+02	8.56E+01	

1 * normal termination of execution *